VIETNAM
JOURNAL OF HYDRO - METEOROLOGY

ISSN 2525 - 2208

VIETNAM METEOROLOGICAL AND HYDROLOGICAL ADMINISTRATION

No 12
09-2022

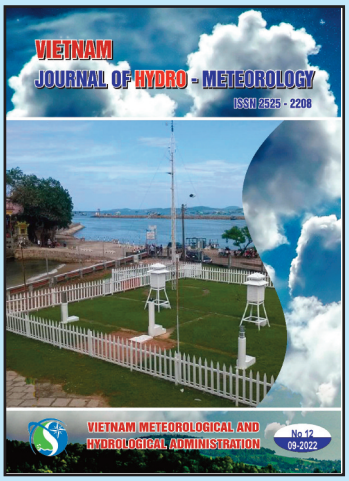

Publishing licence
No: 166/GP-BTTTT - Ministry of Information and Communication dated 17/04/2018

Editorial office
No 8 Phao Dai Lang, Dong Da, Ha Noi
Tel: 024.39364963
Email: tapchikttv@gmail.com

Engraving and printing
Vietnam Agriculture Investment Company Limited
Tel: 0243.5624399

VIETNAM JOURNAL OF HYDROMETEOROLOGY
Volume 12 - 9/2022

TABLE OF CONTENT

VIETNAM JOURNAL OF HYDROMETEOROLOGY

Rerearch Article

Rainfall–triggered landslide warning for Viet Nam using an antecedent rainfall index

Hoang–Minh Nguyen[1*], Tien–Dung Phung[1], Van–Khiem Mai[1], Van–Dai Hoang[1], Nguyen Phuong Nhung[2]

[1] National Centre for Hydro–Meteorological Forecasting, Viet Nam Meteorological and Hydrological Administration; hoangminh281287@gmail.com; ptdung77@gmail.com; maikhiem77@gmail.com; daihydro2003@gmail.com

[2] University of Transport Technology; nguyenphuongnhung0302@gmail.com

*Corresponding author: hoangminh281287@gmail.com; Tel.: +84–967519798

Received: 14 April 2022; Accepted: 16 August 2022; Published: 25 September 2022

Abstract: This study is conducted to perform the rain–induced landslide warning for Viet Nam using an antecedent rainfall index (ARI) integrated with a landslide susceptibility map. The method used ARI 95th quantile as the warning threshold according to the suggestion of several previous studies. The results testing for the 6 historical landslide events indicated that the ARI values at the 95th quantile are more proper for the landslide events that are triggered by rainfall occurring on a small scale, whereas with respect to rain events happening on a large scale, the area under warning is widespread which leads to false alarm a lot. The warning area is reduced significantly when the 99th quantile is used as the warning threshold, which results in a decrease in the false alarm ratio. However, the warnings could not detect the landslide events that are triggered by rainfall occurring on a small scale. These results recommend that the ARI values at the 95th quantile should be used as the threshold for landslide warning with respect to the heavy rainfall events happening on a small scale, meanwhile, for the heavy rainfall events that occur on a large scale, the 99th quantile is a better choice.

Keywords: Rainfall–triggered landslide warning; ARI; Landslide susceptibility map.

1. Introduction

Landslides are dangerous natural disasters occurring frequently and commonly around the world, causing thousands of human losses and the destruction of local infrastructures every year. The threats of landslides go up with the relentless development of the mountain areas. Landslide alerts or early warnings could provide helpful information for disaster managers and emergency planners to make robust decisions in mitigating the landslide damages [1–3].

The landslides could be triggered by several factors, such as rainfall, snowmelt, earthquakes, human activities, and so on. Precipitation is the most common ones among these factors. Landslides triggered by rainfall are usually because of the rise of the negative pore–water pressure which reduces the soil shear strength and causes the slope failures. This kind of landslide often follows a long period of high soil moisture in the lower zone and is then triggered by intense rainfall. Given rainfall is able to demonstrate both the antecedent soil water content and recent rainfall conditions, it is widely used to define the threshold for the occurrence of landslides by applying an empirical method. Most of the previous studies define rainfall threshold as a line that is identified visually [4] or by statistical approaches (e.g Bayesian inference [5–6] and the frequentist method [7] to separates the occurrence or non–occurrence of landslides. The most popular features used to categorize rain events are

precipitation intensity–duration (ID) and accumulated event precipitation–rain duration (ED). Numerous rainfall thresholds were suggested and applied for landslide warning [8–11]. Despite they are the key tool in landslide warning systems, their deficiencies are often realized and discussed. For instance, the antecedent soil moisture or the recent rainfall information in some studies is not obviously taken into account in the threshold identification. For rainfall events happening in short durations, they seem to ignore the antecedent soil moisture information. Meanwhile, with respect to the rainfall event occurring in long durations, in spite of it implicitly contains the antecedent soil moisture information, it could not illustrate the relationship between rainfall events and landslides, because there might be the highest amount of rainfall which trigger landslides, antedated by a rainfall period which is able to lead to the slope to failure [12]. Nevertheless, the intensity computed from such a long period would flatten the intensity peak, neglecting the importance of the rainfall trigger.

To more manifest consider the antecedent soil moisture condition and the recent rainfall, numerous studies were conducted to obtain the rainfall thresholds which consider both the antecedent soil moisture condition and the rainfall trigger. They integrate the antecedent soil moisture condition into the determination of thresholds. In some systems of landslide warning, the antecedent accumulated precipitation over a period is used to simulate soil moisture condition which is associated with the recent rainfall amounts to obtain the landslide–triggered thresholds. For instance, the threshold proposed in [13] is identified by using the recent 3–day rainfall and the antecedent 15–day rainfall, whereas [14] take into account the recent daily rainfall and the antecedent 3–day rainfall information. [15] implemented an Antecedent Rainfall Index (ARI) to express implicitly the antecedent soil moisture condition by using the 7–day recent rainfall.

In Viet Nam, the operational landslide warnings are performed by overlapping precipitation and landslide susceptibility maps. The operational warning method uses the most recent 12 hours of observed rainfall associated with a 6–hour rainfall forecast which is the maximum value among the three numerical weather prediction models being launched in operation to establish a precipitation distribution map. In this way, the rainfall used is determined as the triggering rainfall, whereas the antecedent wetness condition is not under consideration. This could lead to a missing warning because landslide happens occasionally even without heavy rain. Therefore, this study is conducted to test the applicability of a state–of–art method that considers both recent rainfall and antecedent wetness condition for operational landslide warning in Viet Nam.

2. Materials and Methods

2.1. Data collection

Daily precipitation data at 186 meteorological stations over the whole Viet Nam from 1991 to 2020 derived from Viet Nam Meteorological and Hydrological Administration (VNMHA) are collected to calculate ARI values. Due to the landslide susceptibility map (LSM) developed by Viet Nam Institute of Geosciences and Mineral resources (VIGMR) (hereafter referred to as VIGMR–LSM) has been completed for 15 provinces located in mountainous areas of the north of Viet Nam, and Thanh Hoa and Nghe An provinces and not covering the whole Viet Nam yet, another LSM obtained from NASA (https://gpm.nasa.gov/landslides/projects.html) (hereafter referred to as NASA–LSM) is collected to fill up the LSM missing area. The locations of 186 meteorological stations, VIGMR–LSM and NASA–LSM are displayed in Figure 1. The VIGMR–LSM and NASA–LSM are saved in raster format and have different spatial resolutions which are about 22.5 m and 1 km, respectively. Therefore, in order to merge the two maps and in service of landslide warning at the 1km scale, the VIGMR–LSM is converted to the resolution of 1 km. Eventually, a complete LSM map covering the whole Viet Nam is made by overlapping the two layers with the priority for VIGMR–LSM.

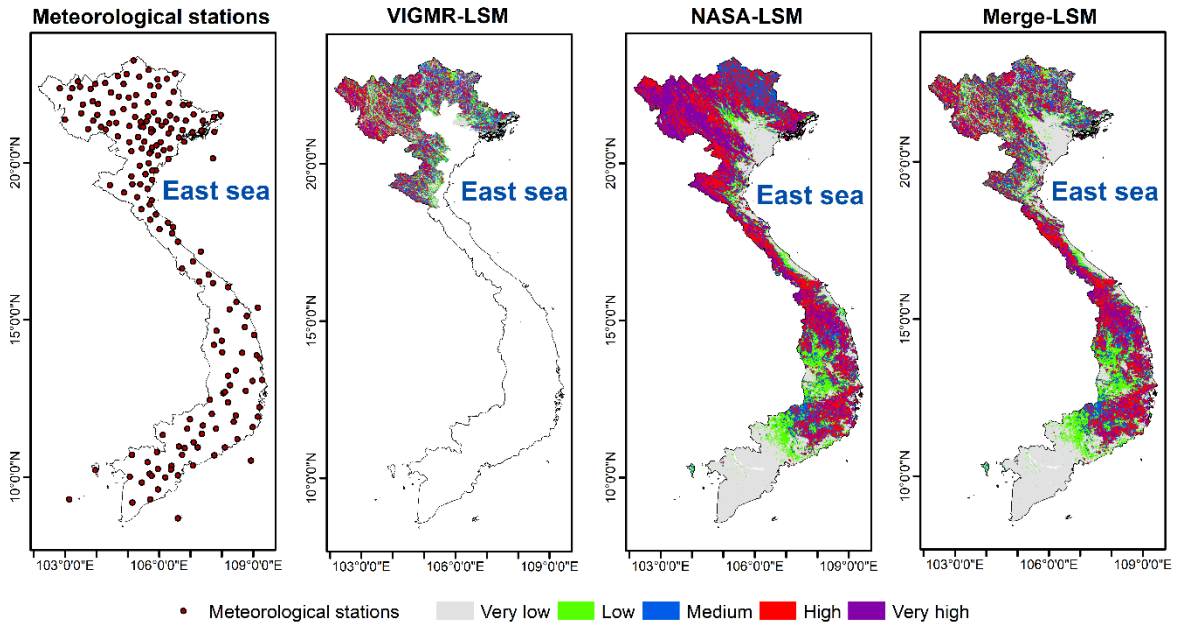

Figure 1. Location of the meteorological stations and landslide susceptibility maps.

2.2. Landslide warning through the integration between ARI and LSM

The ARI calculates a weighted average of the most recent 7 days of rainfall, containing the current date as shown in Eq. (1):

$$ARI = \frac{\sum_{t=0}^{6} w_t P_t}{\sum_{t=0}^{6} w_t} \quad (1)$$

where t is the number of days before the current day, P_t is the rainfall amount at time t, and $w_t=(t+1)^{-2}$ is weight of day t. According to this weighting method, the contribution of rainfall amount to trigger landslide would decrease when t increase.

This study utilizes the 30–year record of continuous daily rainfall at 186 meteorological stations and calculates ARI. In near real–time, the ARI value of the most recent 7 days of rainfall is calculated and then is compared with the ARI threshold which is defined as 95th quantile. It is noted that the 95th ARI quantile is determined based on non–zero rainfall. It means the days that are no rain would be excluded from the calculation. The warning or no warning would be decided based on a decision tree framework which is displayed in Figure 2. It integrates the ARI index with a landslide susceptibility map. The ARI index is calculated every 6 hours at each station sites and then is interpolated to a 1x1 km grid using an inverse distance weighting method (IDW). The grided–ARI is compared against the ARI threshold. If it is lower than this value, no warning is issued but if the ARI value is higher than the threshold, then the landslide susceptibility map is under consideration. No warning is issued if the susceptibility value is very low or low, whereas if susceptibility is medium, high or very high, the nowcasts of caution, warning and danger are issued, respectively.

3. Results and Discussion

The applicability of the method for landslide warning in Viet Nam is tested for 6 landslide events occurring on 05 August 2016 at Bat Xat, Lao Cai, 03 August 2017 at Mu Cang Chai, Yen Bai, 03 August 2018 at Quan Son, Thanh Hoa, 03 October 2020 at Phong Dien, Thua Thien Hue, 18 October 2020 at Huong Hoa, Quang Tri, and 28 October 2020 at Nam Tra My, Quang Nam. In which, the two first events occurred because of the heavy rainfall events on a small scale, whereas the other ones are on a large scale. These are very dangerous landslide events that are responsible for the death of hundreds of persons and the destruction of hundreds of houses and infrastructure. The results of ARI calculation for the

six events are shown in Figure 3, whereas maps of landslide warning using ARI 95th as threshold are indicated in Figure 4. The results show that by using ARI 95th as a warning threshold, the applied method could catch the locations of landslide occurrence of all landslide events and put them under high (warning) or very high (danger) possibility of occurrence. This is because the locations of landslide occurrence are in the high susceptibility areas (Figure 1) and the values of ARI at the 95th quantile are quite low (Figure 5).

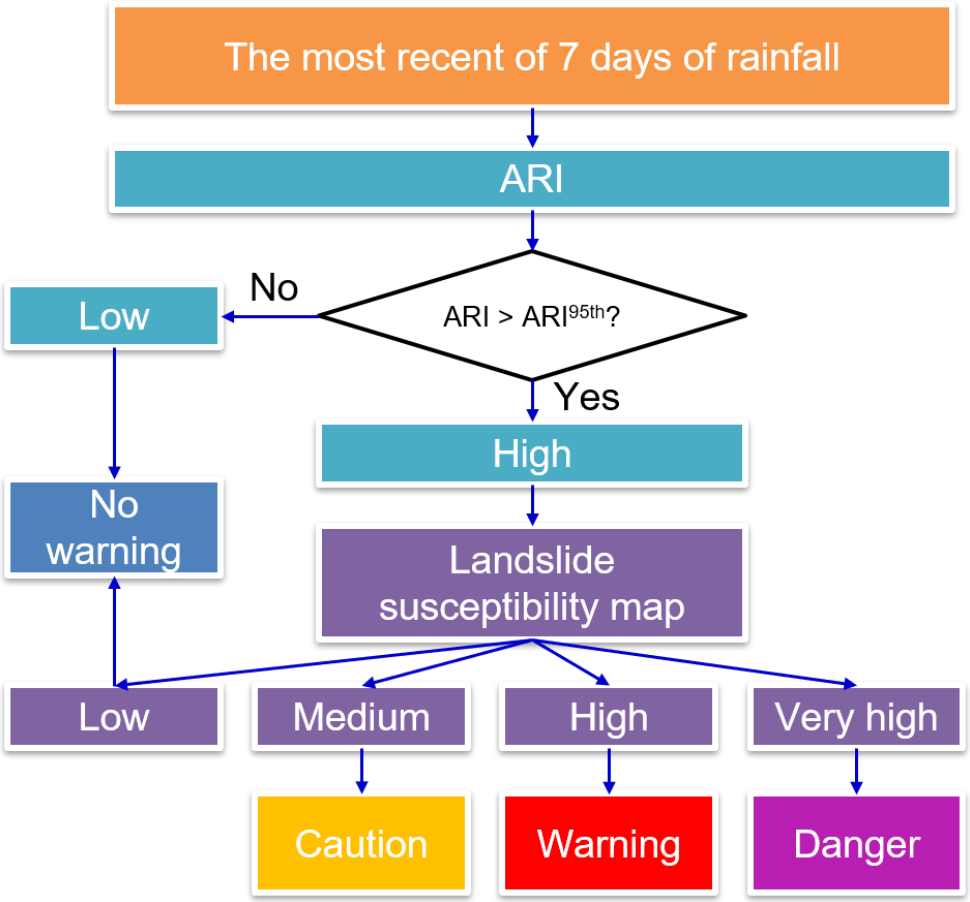

Figure 2. Decision tree structure for generating near real–time landslide nowcasts.

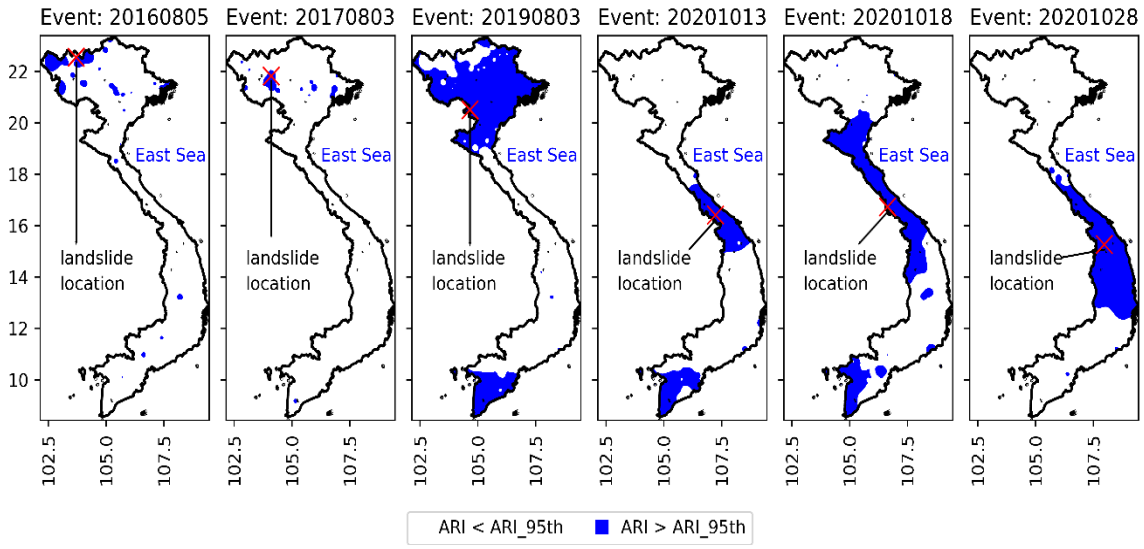

Figure 3. Maps of the ARI higher than ARI 95th for the 6 events.

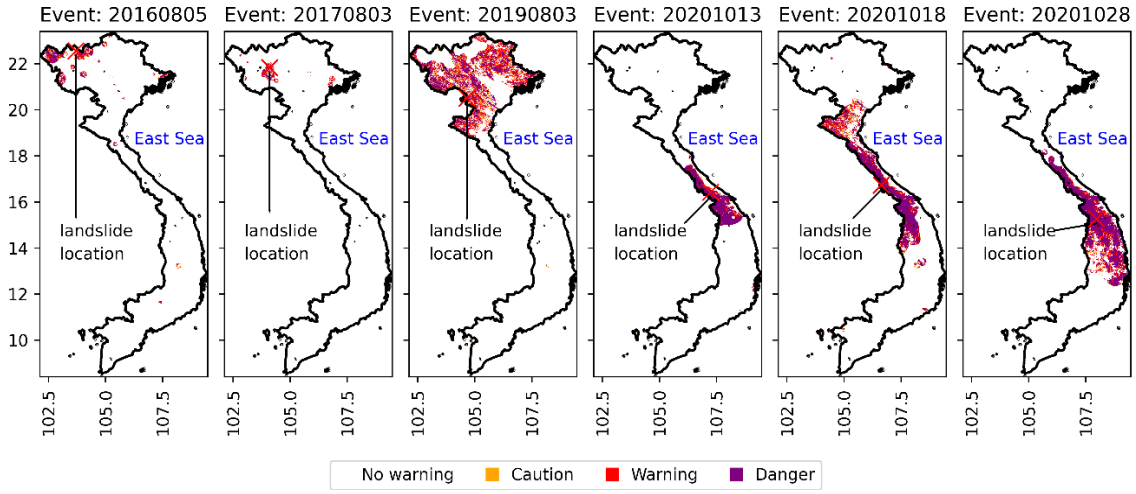

Figure 4. Maps of the regions under landslide warning for the 6 events using ARI 95th as threshold.

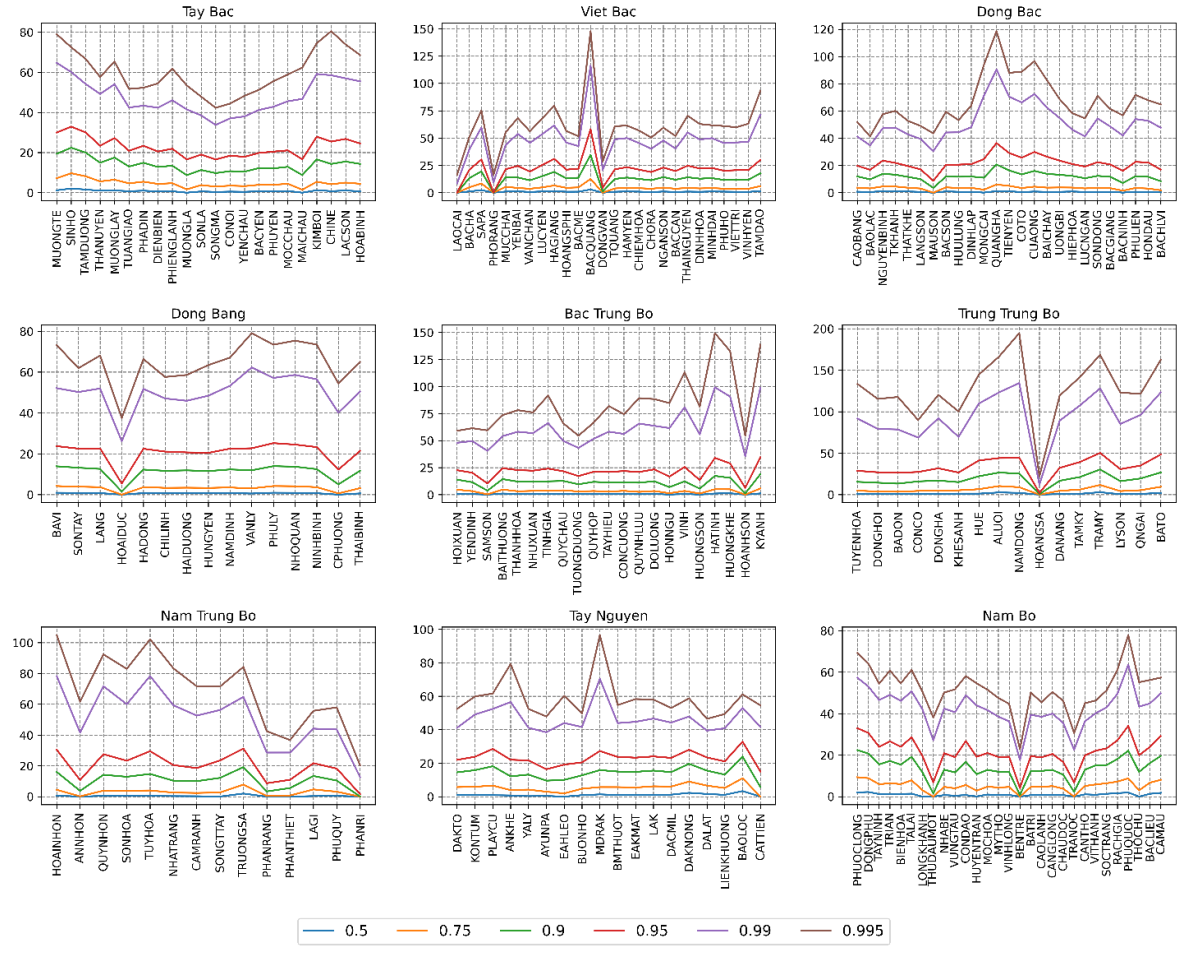

Figure 5. Variation of ARI value according to various quantiles at 186 meteorological stations.

In order to investigate the effect of threshold selection on the result of landslide warning, this study employs analyzing the variation of ARI values according to different quantiles and the warning area corresponding to the quantiles. Figure 5 illustrates the variation of ARI value according to various quantiles at 186 meteorological stations. The 50th, 75th, and 90th ARI values are lower than 20 mm at most of the stations. These values are too small with the landslide situation in Viet Nam, so they should be eliminated in the threshold determination.

Using these quantiles as a warning threshold would cause an increase in false alarms. The ARI values at the 95th quantile fluctuate around 22–25 mm, they are still quite small. This happens due to most of the days in the year have no rain or little rain. On the other hand, the ARI values at the 99th quantile are relatively proper for the condition in Viet Nam, but as shown in Figure 6, the landslide warning using this quantile as the threshold cannot catch the two first events, so it leads to a missing warning. Similarly, there is no point under the warning in the two first events when the 99.5th quantile is chosen. In this case, the warning area for the other events is reduced significantly compared to that of using the 0.95th and 0.99th quantiles. This result could decrease the false alarm ratio; however, it is vulnerable due to the occurrence of landslides containing much uncertainty. Additionally, the ARI values at this quantile are seems to be quite high.

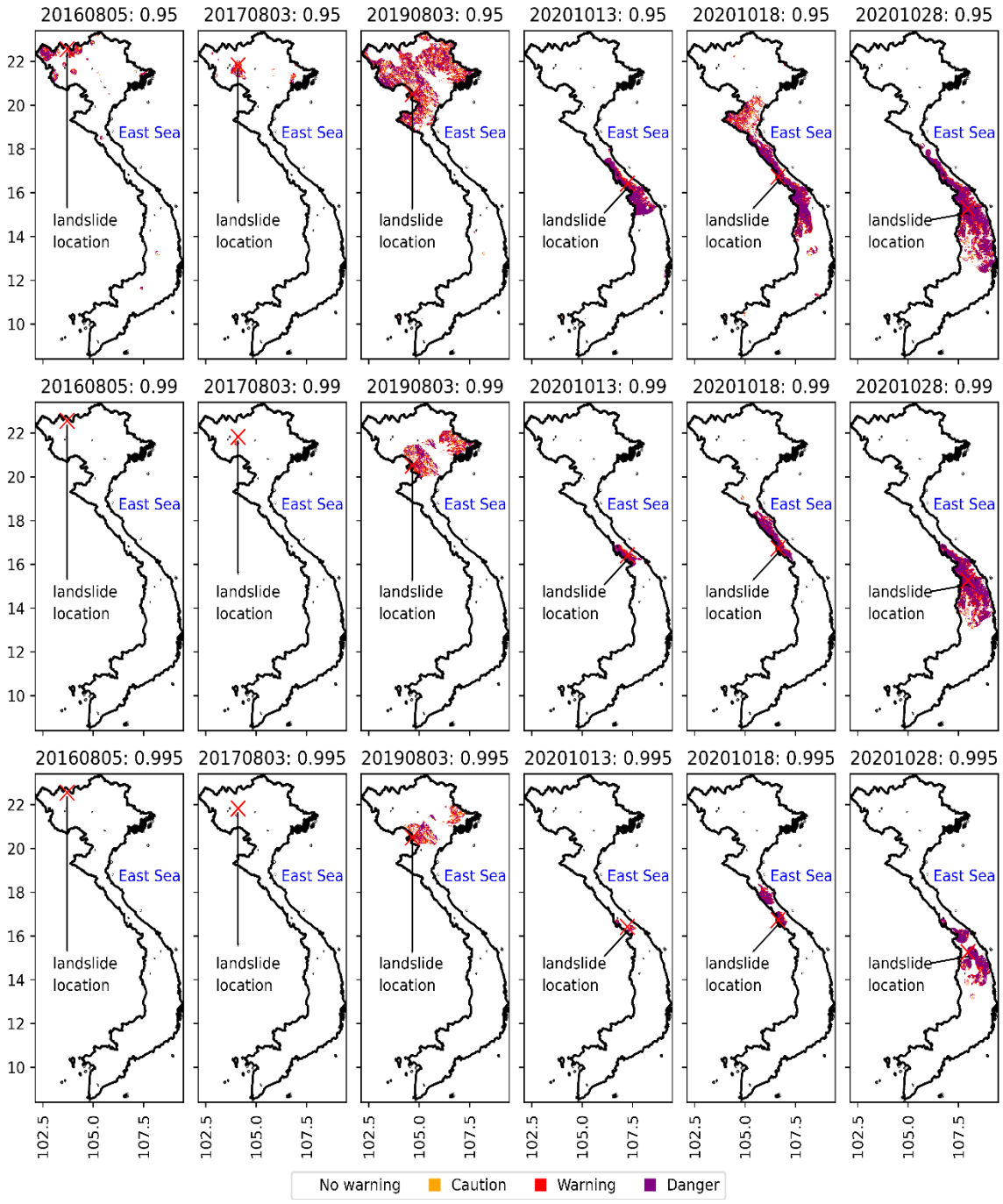

Figure 6. Variations of landslide warning area according to the change of ARI quantiles during the 6 landslide events.

Based on the above analysis, we suggest that for the rain events at a small scale, the ARI value at the 95th quantile should be selected as the warning threshold, whereas the ARI value at the 99th value would be a better choice with respect to the rain events at a large scale. Of course, these recommendations are based on the testing results of the 6 landslide events only. To achieve the best threshold used for landslide warning in Viet Nam, it is very crucial to test the method for a lot of other landslide events in the past and for the upcoming rainy season as well.

4. Conclusion

This study evaluated the applicability of a method which is the integration of an antecedent rainfall index and landslide susceptibility map for landslide warning in Viet Nam. The method used ARI 95th quantile as the warning threshold according to the suggestion of several previous studies. The results testing for the 6 historical landslide events indicated the viability of the method for landslide warning in Viet Nam. It is realized that the ARI values at the 95th quantile are more proper for the landslide events that are triggered by rainfall occurring on a small scale, whereas with respect to rain events happening on a large scale, the area under warning is widespread which leads to false alarm a lot. The warning area is reduced dramatically when the 99th quantile is used as the warning threshold, which results in a decrease in the false alarm ratio. However, the warnings could not detect the landslide events that are triggered by rainfall occurring on a small scale. These results recommend that the ARI values at the 95th quantile should be used as the threshold for landslide warning with respect to the heavy rainfall events happening on a small scale, meanwhile, for the heavy rainfall events that occur on a large scale, the 99th quantile is a better choice.

The results and recommendations above are the consequence of applying the method for only 6 landslide events. It is able to vary when the number of landslide events increases. Hence, it is very essential to include much more events in the selection of rainfall threshold. It is also noted that the LSM used for the provinces from Ha Tinh to the south is extracted from a global landslide susceptibility map that includes much uncertainty. Besides, the number of stations used in this study is quite sparse, which leads to many errors when the rainfall data are interpolated to a 1x1 km grid. Thus, further studies should be conducted to complete the LSM developed by VIGMR and to exploit the rainfall data at automatic stations as well as include much more landslide events.

Author contribution statement: Calculation and coding; manuscript writing and editing: H.M.N.; manuscript editing; methodology; results analysis and discussions: H.M.N., T.D.P., V.K.M., V.D.H.; data processing and analysis: N.P.N.

Acknowledgements: This work was supported by project “Disaster risk classification and warning mapping for flash floods, landslides and land subsidence caused by rain in midland and mountainous areas”, funded by Viet Nam Ministry of Natural Resources and Environment (MONRE).

Competing interest statement: The authors declare no conflict of interest.

References

1. Keefer, D.K.; Wilson, R.C.; Mark, R.K.; Brabb, E.E.; Brown, W.M.; Ellen, S.D.; Harp, E.L.; Wieczorek, G.F.; Alger, C.S.; Zatkin, R.S. Real-time landslide warning during heavy rainfall. *Science* **1987**, *238*, 921–925.
2. Jakob, M.; Holm, K.; Lange, O.; Schwab, J.W. Hydrometeorological thresholds for landslide initiation and forest operation shutdowns on the north coast of British Columbia. *Landslides* **2006**, *3*, 228–238.
3. Mirus, B.B.; Becker, R.E.; Baum, R.L.; Smith, J.B. Integrating real-time subsurface hydrologic monitoring with empirical rainfall thresholds to improve landslide early warning. *Landslides* **2018**, *15*, 1909–1919.

4. Caine, N. The rainfall intensity-duration control of shallow landslides and debris flows. *Geogr. Ann. Ser. A Phys. Geogr.* **1980**, *62*, 23–27.
5. Guzzetti, F.; Peruccacci, S.; Rossi, M.; and Stark, C. P. Rainfall thresholds for the initiation of landslides in central and southern Europe. *Meteorol. Atmos. Phys.* **2007b**, *98*, 239–267.
6. Guzzetti, F.; Peruccacci, S.; Rossi, M.; Stark, C.P. The rainfall intensity–duration control of shallow landslides and debris flows: an update. *Landslides* **2007a**, *5*, 3–17.
7. Brunetti, M.; Peruccacci, S.; Rossi, M.; Luciani, S.; Valigi, D.; Guzzetti, F. Rainfall thresholds for the possible occurrence of landslides in Italy. *Nat. Hazards Earth Syst. Sci.* **2010**, *10*, 447–458.
8. Peruccacci, S.; Brunetti, M. T.; Luciani, S.; Vennari, C.; and Guzzetti, F. Lithological and seasonal control on rainfall thresholds for the possible initiation of landslides in central Italy. *Geomorphology* **2012**, *139–140*, 79–90.
9. Segoni, S.; Rosi, A.; Lagomarsino, D.; Fanti, R.; Casagli, N. Brief communication: Using averaged soil moisture estimates to improve the performances of a regional-scale landslide early warning system. *Nat. Hazards Earth Syst. Sci.* **2018**, *18*, 807–812.
10. Gariano, S.L.; Brunetti, M.T.; Iovine, G.; Melillo, M.; Peruccacci, S.; Terranova, O.; Vennari, C.; Guzzetti, F. Calibration and validation of rainfall thresholds for shallow landslide forecasting in Sicily, southern Italy. *Geomorphology* **2015**, *228*, 653–665.
11. Peruccacci, S.; Brunetti, M.T.; Gariano, S.L.; Melillo, M.; Rossi, M.; Guzzetti, F. Rainfall thresholds for possible landslide occurrence in Italy. *Geomorphology* **2017**, *290*, 39–57.
12. Bogaard, T.; Greco, R. Invited perspectives: Hydrological perspectives on precipitation intensity-duration thresholds for landslide initiation: proposing hydro-meteorological thresholds. *Nat. Hazards Earth Syst. Sci.* **2018**, *18*, 31–39.
13. Chleborad, A.F.; Baum, R.L.; Godt, J.W.; Powers, P.S. A prototype system for forecasting landslides in the Seattle, Washington. *Rev. Eng. Geol.* **2008**, *20*, 103–120.
14. Lee, J.H.; Park, H.J. Assessment of shallow landslide susceptibility using the transient infiltration flow model and GIS-based probabilistic approach. *Landslides* **2015**, *13*, 885–903.
15. Glade, T.; Crozier, M.; Smith, P. Applying probability determination to refine landslide-triggering rainfall thresholds using an empirical "Antecedent Daily Rainfall Model". *Pure Appl. Geophys.* **2000**, *157*, 1059–1079.
16. Tran, V.P.; Ly, H.B.; Phan, T.T.; Prakash, I.; Dao, T.H. Landslide susceptibility mapping using Forest by Penalizing Attributes (FPA) algorithm based machine learning approach. *VN J. Earth Sci.* **2020**, *42(3)*, 237–246.
17. Nhu, V.H.; Bui, T.T.; Nguyen, M.L.; Vuong, H.; Hoang, N.D. A new approach based on integration of random subspace and C4.5 decision tree learning method for spatial prediction of shallow landslides. *VN J. Earth Sci.* **2022**, 1–16.
18. Tran, V.T.; Dao, M.D.; Nguyen, M.T.; Van, D.C. Preliminary assessments of debris flow hazard in relation to geological environment changes in mountainous regions, North Vietnam. *VN J. Earth Sci.* **2016**, *38(3)*, 257–266.
19. Le, D.A. A method for study of rainfall thresholds for landslide warning. *VN J. Earth Sci.* **2012**, *32(2)*, 97–105.
20. Mai, T.T.; Nguyen, V.T. Studying landslides in Thua Thien – Hue province. *VN J. Earth Sci.* **2014**, *36(2)*, 121–130.

VIETNAM JOURNAL OF HYDROMETEOROLOGY

Check for updates

Research Article

Global Land Surface Data Applications in Flood Hydrologic Modeling Using HEC–GeoHMS and HEC–HMS for Three Watersheds in Southeast Asia

Nguyen Thi Thuy Linh[1*], Hoang Thi Nguyet Minh[1]

[1] Hanoi University of Natural Resources and Environment; nttlinh.tnn@hunre.edu.vn; htnminh.tnn@hunre.edu.vn

*Corresponding author: nttlinh.tnn@hunre.edu.vn; Tel.: +84–945014398

Abstract: Flood is one of the most commonly occurring forms of natural disaster which damage to environment and society. Flood events have been increased both in their intensity and frequency associating with increasing average global temperature due to climate change. In order to contribute to the work of mitigating the effect of climate change as well as floods' damage, this study introduces a method to simulate discharge with respect to design storm through hydrological modeling system (HMS). This model is applied for three case studies the Upper Sunter river basin in Indonesia, the Vu Gia–Thu Bon river basin and the Nhat Le River basin in Vietnam in which there were several severe floods occurred, causing severe impacts on social development. Hydrologic simulations were performed using the software of Hydrologic Engineering Center's Hydrologic Modeling System (HEC–HMS). With three different precipitation input data, daily data in the Upper Sunter river basin, 6–hourly data in the Vu Gia–Thu Bon river basin and hourly data in the Nhat Le river basin were used to simulate. The HEC–HMS calibration and validation were conducted to assess the model performance, and the estimation of design floods with respect to design storm was also presented. NSE coefficients are higher than 0.70 in both calibration and validation process through the years which is acceptable for further simulation. With the validated model, seven return periods (2, 5, 10, 25, 50, 100 and 200 years) were used to design seven floods.

Keywords: HEC–HMS; Model; Rainfall–runoff; Simulation.

1. Introduction

Lack of database in many areas of the world is a serious obstacle for the hydrologic model. At the similar time, most of the generating databases on a local and global scale are also making a problem of model that causes an uncertainty source [1–2]. The unsimilar databases were applied for the one river basin making the unlike model results and, consequently, different estimates of water resources ecosystem variables [3–5]. In order to understand and support decisions regarding of water resources management, water pollution, and flood control, the consequences of anthropogenic and natural changes forecasting in the environment are crucial [6–8]. However, using a model to simulate the real river basin has made evidence to be challenging, because of many impossible sources, such as parameter estimation, model structure, forcing data, input data, and using goodness–of–fit criteria [9–11]. The spatial information was used for input data of distributed or semi–distributed hydrological models, such as topography (elevation), LULC (land use/land cover), soils, or (hydro–) geology [12–14]. These categories of data are often possible in different or same

resolutions and can be collected from different sources, with the latter providing some different information [15–17].

Now a day, the technology of satellite and remote sensing is providing extraordinary data on land surface processes, which allow land surface hydrology modeling at large spatial scales, arranging from the river basin to regional, to continental [18–20]. Therefore, we can simulate or forecast some kinds of natural disasters such as typhoons, floods, droughts [21–22]. Due to climate change and the rising of global temperature, the flood tendency and intensity has been increased as well [23–25]. Therefore, in order to minimize the bad effect of climate change, it is needed to provide reliable models for simulating a flood.

Hydrological modeling system (HMS) was created in the nineteenth century when the software systems and technologies have been generally. HMS model was developed by the US Army Corps of Engineers [26]. A part of the major objectives of the model is to support engineers and hydrologists in provided the most reliable evaluation of annual floods [27–28]. The HEC–HMS was applied to simulate flood events and continuous hydrologic modeling [29–30]. This model was proved to perform flood events accurately through several studies. The rainfall–runoff is simulated by separating the river basin into three sub–catchment, and each sub–catchment is simulated with its parameters [31]. The hydrologic modeling article was used new version of HEC–HMS released in April 2006 by the US Army Corps of Engineers. This model contains of two parts: runoff scenarios using IDF curves and event–based hourly simulations. Infiltration loss and baseflow parameters of each sub–catchment is calibrated with hourly simulations [32–33]. Therefore, the simulated run–off results can be applied for flood damage estimation and flood control in another studies.

Simulating the rainfall–runoff by the HEC–HMS model from Probable Maximum Storm (PMS) – a most severe event that can occur in a particular region [34–35]. This simulation was to assess discharge hydrographs combined with the Probable Maximum Flood (PMF) at extraordinary locations in each river basin. These hydrographs were consequently applied for developing flood inundation maps of the study areas and characterizing phenomena of sediment transport in the streams with severe flooding conditions [36]. Moreover, at Tapi river India, HEC–HMS was used for simulation of rainfall–runoff [37]. The peak flow discharges and maximizing the Nash–Sutcliffe is fitted to this study. For better runoff estimation SCS unit hydrograph and Snyder Unit hydrograph methods are analyzed, and the best adapted method for the study area is chosen for the final simulation.

The flood frequency analysis (FFA) and hydrological modeling system (HMS) is used to estimate the peak discharges [38–39]. FFA method was carried out using two distribution functions, i.e., Gumbel's extreme value distribution (Gumbel's) and lognormal (LN) distribution, while HMS was performed using the Hydrologic Engineering Center's Hydrologic Modeling System (HEC–HMS) model [40]. Calibrating and validating processes were using to analyze the applicability of HEC–HMS model to simulate the discharge of Sungai Rinching [38]. These results showed that the model performance is exceptional. Using FFA and HMS to estimate peak discharges for several average recurrence intervals (ARIs), i.e., 2, 5, 10, 20, 50, and 100 years estimated, were also compared.

This study mainly used ArcGIS 10.4 with Geospatial Hydrologic Modeling (HEC–GeoHMS) and HEC–HMS 4.2.1. The ArcGIS used to prepare the spatial datasets for the hydrological and hydraulic model, in HEC–HMS and HEC–RAS respectively. The HEC–GeoHMS extension component delineates and maps river networks for HEC–HMS manipulation [41]. In HEC–HMS, each component in the model performs different purpose of the precipitation–runoff process within a part of the catchment or basin known as a sub–catchment [42]. The result of the modeling process is the figuring of streamflow hydrographs at the catchment outlet or inlet to the reservoir. Finally, the discharge hydrographs with respect to the seven design storms are estimated and presented in the study.

2. Methodology

2.1. Study site

In this research, three different study areas will be selected to simulate the rainfall–runoff and design storm. In order to make the result comparisons, each study area will use different precipitation time steps: daily, 6–hour and hourly for simulation.

The Upper Sunter river basin will be select for daily data time step, as shown in Figure 1. The watershed includes two upstream rivers: Sunter River and Cipinang River that combine into a major river in the downstream area. The maximum watershed length is approximately 37 km; the river basin is calculated 330 km^2 with the annual average temperature is 26°C. Moreover, the average annual rainfall is estimated 1883 mm according to the Cipinang gauge station data from 2001 to 2007 [43]. The Cipinang Gauge roles the streamflow observation. Furthermore, the purpose of water is identifying for agricultural, urban business and hydroelectric power industry sectors [44]. Nevertheless, the stream role is only for domestic purposes nowadays.

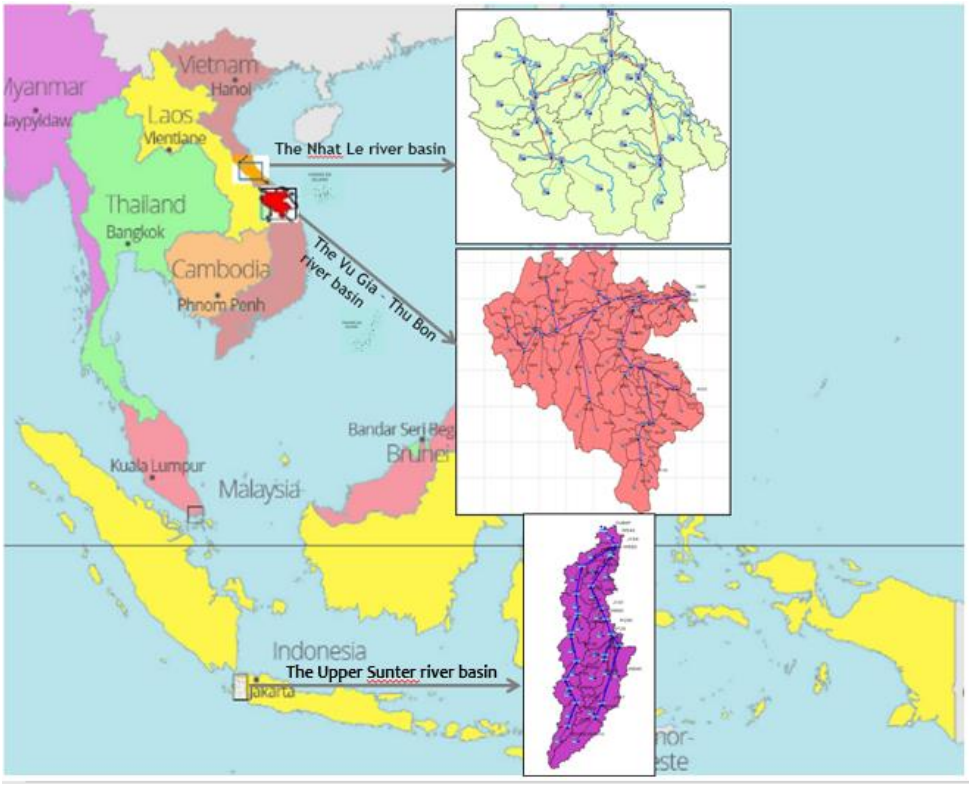

Figure 1. The three river basins in this study.

The Vu Gia–Thu Bon river basin will be used with 6hours data time step, which is the largest river basin in the Vietnam central region. The river basin area is approximately 10,350 km², the basin consists of a part of Kon Tum, Quang Ngai, Quang Nam province, and Da Nang city [45]. Over the past century, floods have appeared more frequently in the Vu Gia–Thu Bon river basin. The historic floods were in 1964, 1996, 1998, 1999, 2007, 2009, 2011 and 2013 [46]. During the period from 1997 to 2009, the floods in Quang Nam province leaded to 589 dead, 33 missing, 1,550 injured, the financial loss of 9,436.5 billion (109) VND [47].

The Nhat Le River basin will be used with hourly data time step, is located in the south Quang Binh Province, Vietnam, with its area of about 2,647 km^2. This basin is the second largest river system in Quang Binh, after the Gianh River system in the north area. Downstream of the river, there are densely populated areas, especially the coastal areas

including Dong Hoi city, in which the population density is six times higher than that of the whole province. Along the banks of the river, the population is also more concentrated; therefore, people living here are strongly affected by severe floods. The topography of the area is mainly mountainous, narrow with short streams and steep slopes from West to East. This characteristic leads to water is rapidly gathered, and the floods quickly rise and flow down to the sea when heavy rains appear. However, unlike other river systems, the amount of water usually drains into the sea through several streams, the Nhat Le river system only has one outlet (Nhat Le estuary). Therefore, floods cannot be released directly to the sea. Moreover, there is a relatively high sand dune (30–40 m) making a natural dike running parallel to the shoreline that also contributes to preventing the floods flush out. Besides, in some areas, the terrain is lower than the sea level (0.8–1 m), so heavy rains combined with high tides cause these areas to flood in a long time and water escape to the sea in days [48].

2.2. Data collection

A proper understanding of the hydrological, topographical and climatic conditions of this study areas and considerable set of data defining them are most essential for analyzing and simulating the realistic hydrologic and hydraulic event. In addition, the exactly of input data for modeling has direct impact to the model results, so the data collection should be analyzed and processed before using them.

Watershed/ Sub–basin Characteristics

Topography in the form of a Digital Elevation Model (DEM) was extracted from an open–source, 1 arc–second (approximately 30 m) resolution, U.S. Geological Survey (USGS).

Land Cover data was downloaded from High–Resolution Land Use and Land Cover (LULC) Map of the Central Region of Vietnam – 1/3 arcsecond (approximately 10 m) resolution and Water Base of United Nations University global repository of data with 400 m resolution for Australia/ Pacific data.

Digital Soil Survey Data was collected from Global Hydrologic Soil Groups – 1/480 decimal degrees (approximately 250 m) resolution– Distributed Active Archive Center for Biogeochemical Dynamics (DAAC).

Climate data

Precipitation data: hourly–series data for five flood events in Nhat Le and Upper Sunter river basin and a six–hours period data for Vu Gia–Thu Bon river basin.

Design storm data: hourly–series data for 2, 5, 10, 25, 50, 100, and 200 years.

Flow data

Daily discharge data (Station No: Meteorology 745) are used for the calibration of the hydrological model in the Upper Sunter river basin, hourly discharge data of Kien Giang station for Nhat Le river basin and a six–hour period of Nong Son stations for Vu Gia–Thu Bon river basin.

2.3. Model development

The watershed and streams in the study area were first delineated from a 30–meter spatial resolution DEM using the HEC–GeoHMS tool. The HEC–GeoHMS permits users to visualize spatial data, perform spatial analysis, document watershed properties, delineate stream and sub–basins, and building inputs data for hydrologic models [49].

The next step in the model development is deriving input parameters for each sub–basin (Loss, transform and routing parameters). For those parameters, the dataset of LULC and soil map was used to calculate the CN grid. With the calculated CN grid, the losses and transformations in sub–basins can be estimated [49]. Precipitation that does not create to surface runoff is identified as losses. The total runoff volume of watershed was controlled by losses mainly, which influence to the magnitude of peak streamflow [50]. Soil infiltration and

initial abstraction are the major losses components. Initial abstraction mentions to the total depression storage and vegetation interception that do not donate to runoff. The infiltration losses were measured by using the Natural Resources Conservation Service (NRCS, formerly Soil Conservation Service) curve number method (SCS–CN). The SCS–CN method calculates precipitation excess as a functioning of cumulative precipitation, soil group, and land use.

A hydrograph is showing the discharge against time. The unit hydrograph is the hydrodynamic flow that flows directly as a result of a unit of precipitation per unit time and is used to determine the theoretical shape of the hydrograph during precipitation period. Using the parameterization of this method, it is possible to estimate the time and intensity of peak flows generated in the catchment. The SCS Unit Hydrograph method was applied to the simulated watersheds [50]. For this method, the input to the HEC–HMS model is the river basin time lag. This parameter is a factor-adjusted estimate of the condensation time, which is the time required for direct runoff to travel from the furthest point in the river basin to the outlet. This time depends on the hydraulic length of the watershed, watershed slope and maximum retention in the watershed. For sub-basins receiving flows from the upstream catchment, channel routing is used to transmit discharge through the primary channel to the catchment outlet. Sub-basins that do not accept flows from the upstream sub-basin will not include routing elements. The routing component of the HEC–HMS controls the attenuation of the flow due to energy resistance and can therefore control the magnitude and duration of the peak flow. It does not influence the total amount of runoff volume developed in a river basin.

The schematic diagram shows steps that required for running the model, calibrating, validating and simulating the design floods.

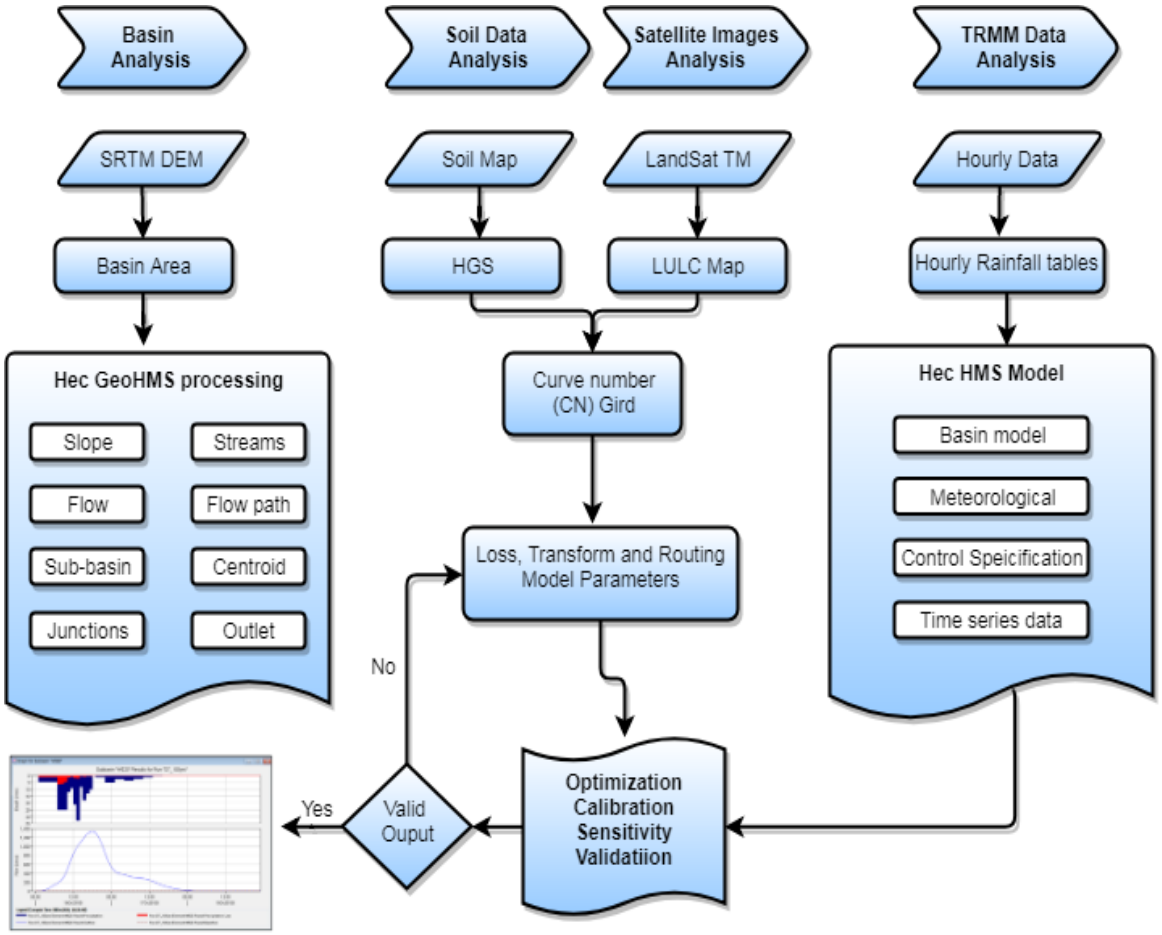

Figure 2. Flow chart of the study.

2.4. Model calibration and validation

The model was manually calibrated for daily and six–hours and hourly time–step for simulation with three different case study areas. The simulated runoff was compared with the measured runoff for the river basin. In order to get good calibration, this study will determine the key parameters and parameter accuracy required for calibration. Therefore, the calibration of the model is mainly carried out by changing model parameters including loss parameters (f_0 – Initial intensity and f_c – Stable permeability intensity); Parameters of the unit line (t_{lag} – transmission time and C_p – flood peak coefficient); Flood parameters (K – coefficient specific to infusion time and X – coefficient for river length). Statistical indicators were used to assess the model performance. Statistical indices were applied to evaluate the performance of the model, containing the coefficient determination (R^2), the root–mean–square error (RMSE), Nash–Sutcliffe model efficiency coefficient (NSE), the relative errors of peak discharge and runoff volume.

$$RMSE = \sqrt{\frac{1}{n}\sum_{i=1}^{n}(O_i - F_i)^2} \quad (1) \qquad Nash = 1 - \frac{\sum_{i=1}^{n}(O_i - F_i)^2}{\sum_{i=1}^{n}(O_i - \overline{O})^2} \quad (2)$$

$$R^2 = 1 - \frac{\sum_{i=1}^{n}(O - \overline{O}) * (P - \overline{P})}{\sqrt{\sum_{i=1}^{n}(O - \overline{O})^2 * (P - \overline{P})^2}} \quad (3) \qquad Re\,Q_{max} = \frac{(F_{max} - O_{max})}{O_{max}} 100 \quad (4)$$

$$Re\,W = \frac{(W_F - W_o)}{W_o} 100 \quad (5)$$

where O_i is observed discharge, $\overline{O}$ is average observed discharge, F_i is calculated discharge; F_{max} and O_{max} are maximum observed and calculated discharge; W_o and W_F are total observed and calculated volume.

After calibration, the models were validated using the same input parameters as determined by the calibration process but with different simulation time. Models for three study areas were calibrated for three years and validated for two years.

2.5. Model Application

In order to develop the implementation of the results, this study will design a storm for discharge calculation at the outlet with seven return periods (2, 5, 10, 25, 50, 100, 200 years). For the Vu Gia–Thu Bon river basin, in order to simulate the design storm, the study was used the design frequencies of 0.5%, 1%, 2%, 5% 10%, 20%, and 50%, and used flow data series largest from 1977 to 2005 to calculate the frequency of the largest flow rate at Nong Son hydrological station according to PIII distribution.

For the Upper Sunter river basin, seven flood scenarios were performed to gain the peak values of designed storm events. Fisher–Tippet Type I method can be used to calculates the extreme value distribution based on time series data. The extraction of the highest daily rainfall of each year was ranked from the maximum values. Then, the extreme rainfall value R_{24} is calculated for the specified return period Tr after the plotting position Fm. Two reduction factors also calculated for the data reduction factor ym and the reduction factor from return period yr, respectively. The rainfall depth proceeds in order to get the Depth Duration Curve as input for Frequency Storm Modelling in the HEC–HMS.

$$F_m = 1 - [(m–0.44)/(N_T+0.12)] \quad (6)$$

$$y_m = – \ln [– \ln (F_m)] \quad (7)$$

$$y_r = – \ln [– \ln (1 – 1/T_r)] \quad (8)$$

$$R_{24} = Ay_r + B \quad (9)$$

where NT is total data and m is data rank, R_{sm} is the maximum rainfall data for each year, and several parameter formula are $c_1 = \sum y_m 2$; $c_2 = \sum y_m$; $d_1 = \sum y_m$; $d_2 = NT$; $F_1 = \sum R_{sm} y_m$; $F_2 = \sum R_{sm}$; $Det = c_1 d_2 – c_2 d_1$; $A = (d_2 F_1 – d_1 F_2)/Det$; and $B = (c_1 F_2 – c_2 F_1)/Det$.

For the Nhat Le river basin, these design storms were gathered from the hydrological report of Quang Binh Irrigation and Drainage Management Company.

3. Result and Discussion

3.1. HEC–HMS

In this study, the Upper Sunter river basin with a total area is 330 km^2, dived into 18 sub–basins; the Vu Gia–Thu Bon river basin was contained 57 sub–basins with a total area is 10,350 km^2; and the Nhat Le river basin was separated to 20 sub–basins, with a total area is 2,647 km^2. For each basin the SCS–CN, initial abstraction, and percentage of the impervious area are differences.

3.2. Calibration and Calibration

Results of the HMS model for the selected rainfall duration have been calibrated using discharge observation data. To perform the calibration process, four parameters, such as Muskingum–K, Muskingum–X, lag time, and impervious, has been adjustment. This research operates 3 periods of precipitation events for each river basin calibration to gain the optimal value for the precipitation model. In order to get the optimal value for each simulation, the model efficiency was tested for each simulation using some objective value such as root means square error (RMSE), R^2, Nash–Sutcliffe (NS), and PBIAS. The following table was presented the optimal parameters for each calibration simulation.

The model performance output for each calibration case can be viewed in Table 1. It can be seen that the average acceptable value is shown from the result of second simulation. Hence, the parameter used in second simulation can used for validation simulation in the Upper Sunter river basin.

Table 1. The criteria for calibrating parameters in the HEC–HMS model.

River basin	Simulation	RMSE	R^2	NSE
Upper Sunter	11/03–19/33/2007	9.64	0.41	0.31
	12/08–18/08/2004	5.94	0.54	0.43
	08/02–16/02/2005	8.03	0.27	0.16
Vu Gia–Thu Bon	20/10–22/10/2001	109.1	0.81	0.83
	24/10–26/10/2002	215.4	0.86	0.83
	20/10–22/10/2003	245.8	0.75	0.76
Nhat Le	07/10–09/10/2005	201.81	0.86	0.83
	30/09–03/10/2006	131.14	0.78	0.72
	03/10–05/10/2007	92.96	0.92	0.90

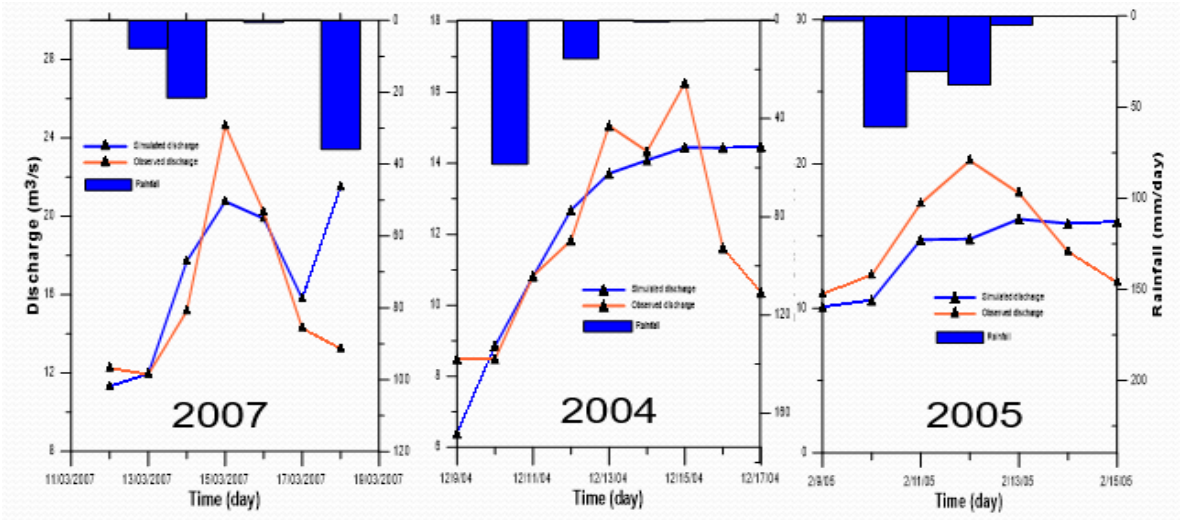

Figure 3. The model results of calibration simulation for the Upper Sunter river basin.

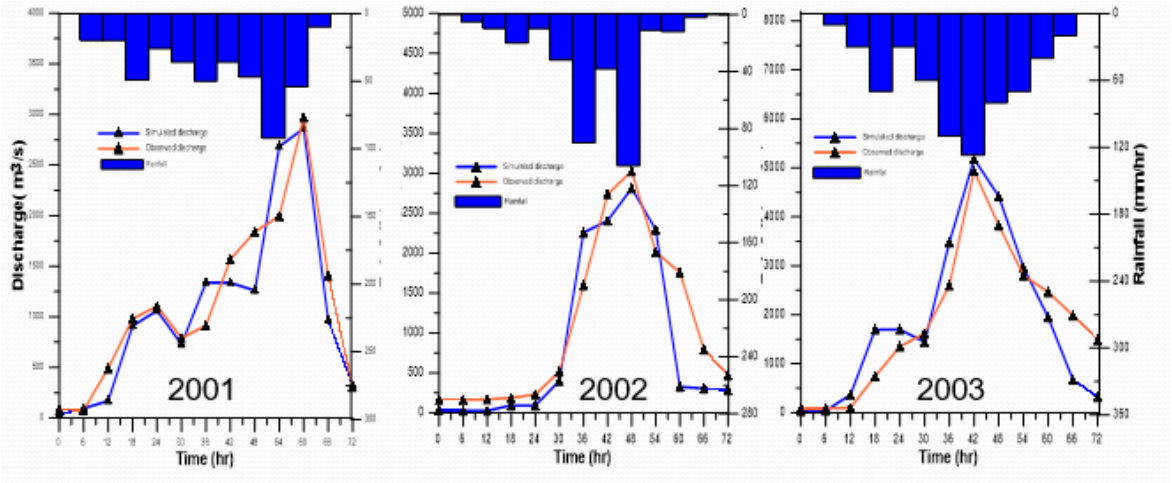

Figure 4. The model results of calibration simulation for the Vu Gia–Thu Bon river basin.

Calculation results of the hydrological simulation for the Vu Gia–Thu Bon river in typical floods of 2001, 2002, 2003 showed that the relative between calculation lines and actual measurement lines stick to each other in terms of oscillation phase and peak flood value. The difference in maximum flow between calculation and the actual measured value is negligible. Peak deviation errors at inspection stations are within the acceptable range. The results of the calculation of the NASH coefficient are relatively good, ranging from 0.75 to 0.83. It can be seen that the calculated discharge was consistent with the observed discharge. NSE coefficients are higher than 0.70 in both calculation and validation scenarios. Also, a high value of R^2 (above 0.78) presented the close correlation between simulated and observed curves. In terms of shape and peak time, the results of this model seem close to the real data presented in Figure 5.

Using the calibration parameters of the model HEC–HMS as described above, the project will be validated for 2 flood seasons in each river basin. The results of validation for the years are presented in table 2 and in Figures 6.

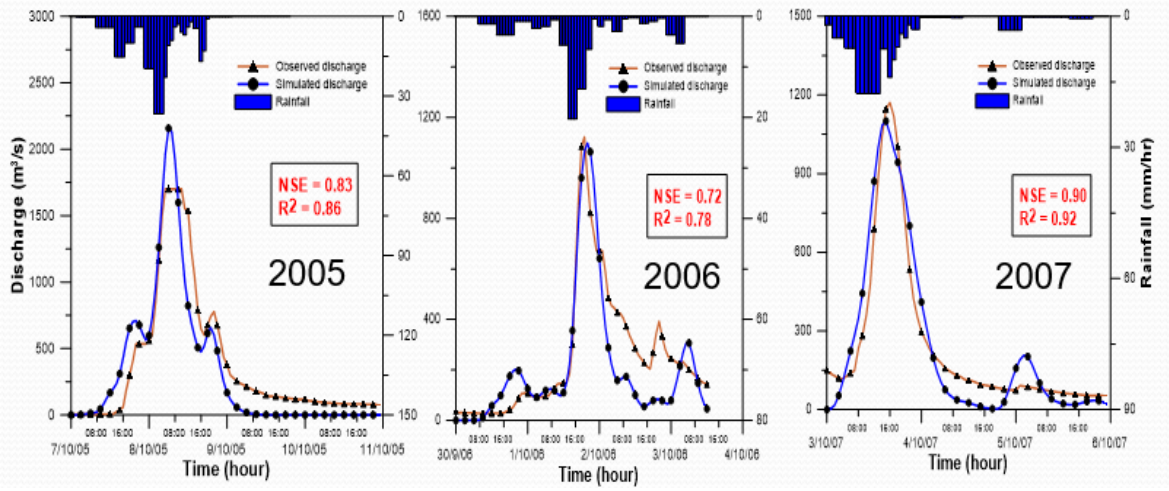

Figure 5. The calibration model result for the Nhat Le river basin.

Table 2. The statistical performance measures for validation.

River basin	Simulation	RMSE	R^2	NSE
Upper Sunter	23/2–04/03/2003	4.23	0.38	0.21
	02/02–13/02/2006	9.20	0.58	0.55
Vu Gia – Thu Bon	25/10– 7/10/2004	145.1	0.82	0.83
	22/10–24/10/2005	230.7	0.86	0.80
Nhat Le	02/10–05/10/2010	130.98	0.89	0.84
	15/10–17/10/2011	263.47	0.89	0.70

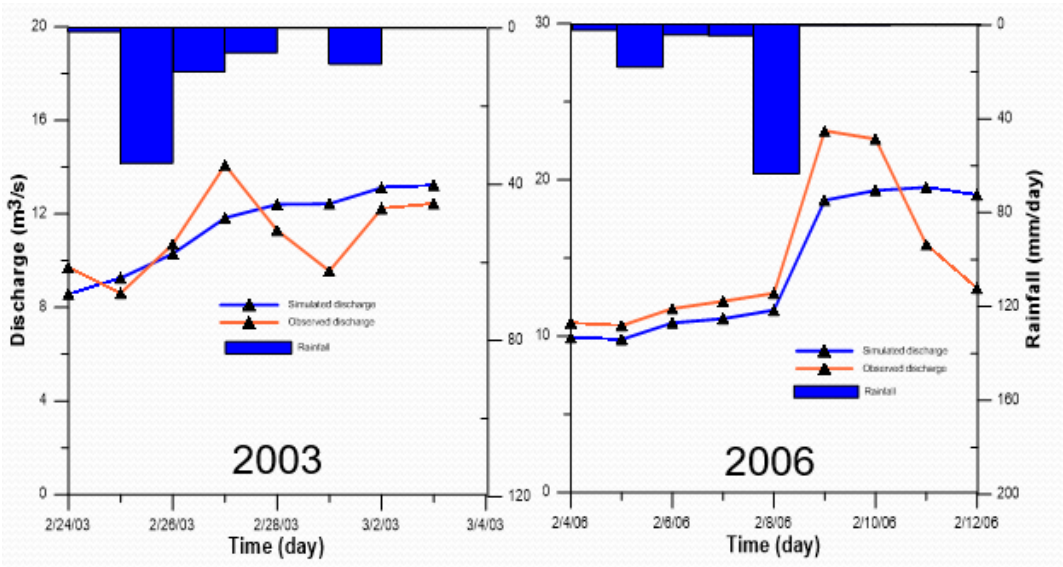

Figure 6. The validation model result for the Upper Sunter river basin.

Each model results of the optimum value were validated with 2 durations of precipitation for the daily hydrograph. Although the value of R^2 for simulation 1 is not too high, the effective output of the model for each validation case can be classified as acceptable. This shows that in the Upper Sunter river basin, the optimized parameters from calibration 2 can be used for flood modeling. The assumption of lower values of model efficiency comes from the limitation of hourly discharge data. In addition, the chosen optimized parameter with Muskingum K = 30; Muskingum x = 0.01; and Percent Impervious = 0; Initial Abstraction=0 and the number of routing = 1 can be performed to simulate the design storm.

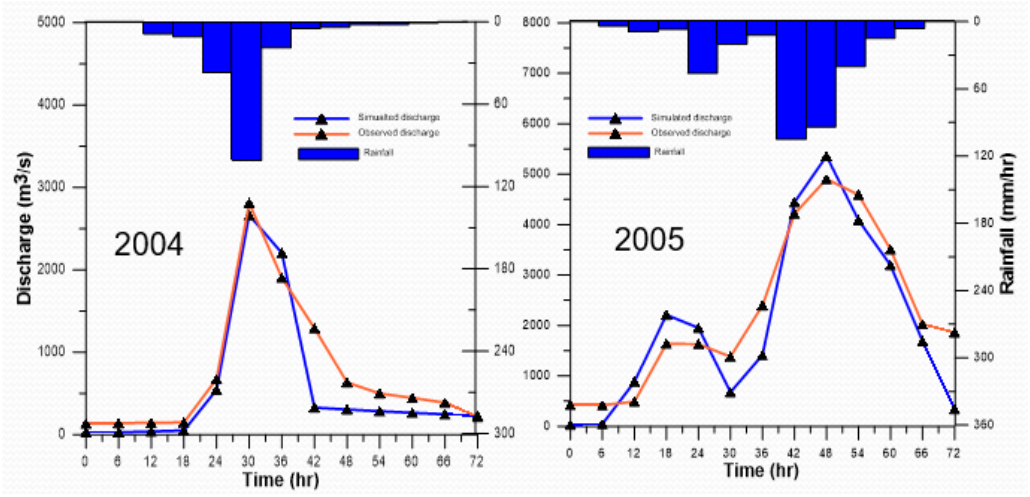

Figure 7. The validation model result for the Vu Gia–Thu Bon river basin.

The validation results with the floods in 2004 and 2005 assessed the accuracy of the hydraulic simulation. The calculation results and the real data measured at the Nong Son stations have shown relatively appropriate results. The calculation results are similar to the observed data. Evaluate results with the NASH coefficient for very good results in the range above 0.8. Thus, the selected optimized parameter with Muskingum K = 1.1, 3, 5, and 10; Muskingum x = 0.01 and 0.1; and Percent Impervious = 25; Initial Abstraction= 470 and the number of routing = 1 can be performed to simulate the design storm.

With the results as shown in figure 7 and the suitability of flood line at the Vu Gia–Thu Bon river basin, it shows that the set of parameters can be applied to the next steps of flood simulation with the design flood frequency and for future studies in the Vu Gia–Thu Bon river system.

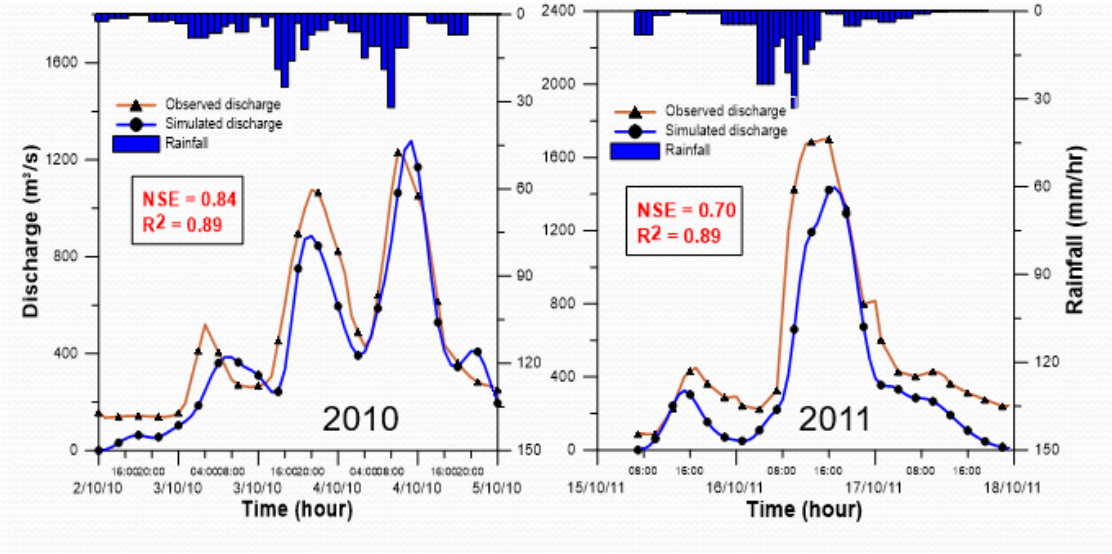

Figure 8. The validation model result for the Nhat Le river basin.

The results of this model seem to close to the real data which is shown in the results for validation. This means that the HMS model simulated well for flood events in the Nhat Le river basin. Therefore, the selected optimized parameter initial abstraction = 75 and 70, percentage of the impervious area = 75, Muskingum K = 1 and 2, and Muskingum X = 0.01. Consequently, this model is possible of estimating the peak discharges corresponding to the design storm for the Nhat Le river basin.

3.3. Design storm

This research simulates seven return periods from 2 years to 200 years. In the Upper Sunter river basin case study, design storm events were estimated by using Fisher Tippet I Distribution method. The calculation results are value of 24-hour of precipitation for the selected return period. Moreover, the analysis of storm events was performed using the Depth-Duration-Frequency (DDF) curves representing precipitation depth to time concentration. In the Vu Gia–Thu Bon case study, to calculate the 3–day rainfall designed for 7 future scenarios 2, 5, 10, 50, 100, 200 years, the project selected rainfall from October 20 to October 22, 2003, to calculate (the rainfall in 2003 is the largest rainfall in the computation period). Last but not least, design storms were obtained from the hydrological report of Quang Binh Irrigation and Drainage Management Company for the Nhat Le river basin.

The discharges hydrographs result with seven design storms (2, 5, 10, 25, 50, 100 and 200 years return period) for three river basins are presented in figure 13. It can be seen that the graph of each simulation shows a similar shape and grows higher as the return period is higher.

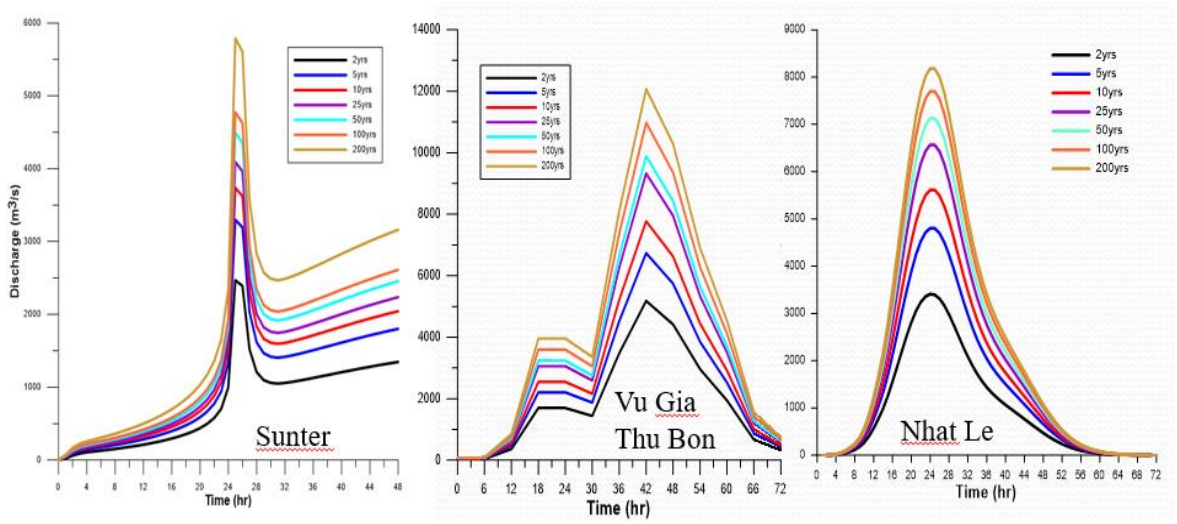

Figure 9. The hydrographs for design storm simulation.

Table 3. The peak discharges of design storm for three case study area.

	River basin		
Return period	**Upper Sunter**	**Vu Gia–Thu Bon**	**Nhat Le**
2 years	2329.4	5383.2	3409.4
5 years	3257.0	6736.6	4805.1
10 years	3871.1	7789.2	5612.6
25 years	4647.1	9327.6	6657.1
50 years	5222.9	9887.3	7127.6
100 years	5794.3	10974.9	7700.9
200 years	6363.6	12072.3	8183.3

Summarize the peak discharge data of each graph is presented in Table 3. The peak discharge simulated at the outlet is increasing with the increase of the return period. These results of hydrograph can be used as the input of the HEC–RAS model for making an inundation map or can be applied for practical tasks in projects related to design dams and waterworks.

4. Conclusions

This research shown that the HEC–HMS hydrological model is conformable to tropical climate conditions. The model is on the basis of topographical, hydrological, soil type and land use characteristics of the study area. The river basin features and initial values were analyzed using HEC–GeoHMS in ArcGIS in order to calibrate model. The rainfall-runoff models were performed using extreme precipitation events and initial results showed a difference between observed and simulated discharge and peak discharge in the research area. Therefore, model calibration was carried out to optimize the parameters. To know the most influential parameter in the simulation, a sensitivity analysis was performed and the results presented that the curves number is the most sensitive parameter come next the lag time.

This research developed successful three hydrological models to assess flooding behavior due to rainfall events in three study areas in Upper Sunter, Vu Gia–Thu Bon and Nhat Le river basins, which the result could be the baseline for the early warning hazard of flooding area. Based on the simulation result, we can see that the errors are the difference in each case study. With the detail input data and shortly time step, we will get more accuracy with observation data. The model calibration and validation result show an acceptable value of model efficiency. The overall performance of the HEC–HMS model is great in terms of relative error functions, Nash Sutcliffe efficiency and coefficient of determining consistent with the selected loss, transform and flow routing methods. Therefore, it can be suggested that the adjusted parameters can be further used for another river sub-basin within the river basin and adjacent river basin. The design floods for seven different return periods for the three study areas were determined. These results can be used in further studies in order to simulate inundation maps and also for water management purposes.

Lastly, the methodologies established in this study can also be applied to other ungauged river basins and regions with similar characteristics. We recommend further researches in these river basins to produce more detailed information for modeling work by considering the effectiveness of meteorological and hydrological measurements (poor in quantity and quality) to establish the optimum number of stations and their adequate distribution in the river basin.

Author contribution statement: Calculation; manuscript writing and editing: H.T.N.M.; methodology; results analysis and discussions: N.T.T.L., H.T.N.M.; data processing and analysis: N.T.T.L.

Competing interest statement: The authors declare no conflict of interest.

References

1. McMillan, H.; Krueger, T.; Freer, J. Benchmarking observational uncertainties for hydrology: Rainfall, river discharge and water quality. *Hydrol. Process.* **2012**, *26*, 4078–4111.
2. Yen, H.X.; Wang, D.; Fontane, R.; Harmel, M. Arabi. A framework for propagation of uncertainty contributed by parameterization, input data, model structure, and calibration/validation data in watershed modeling. *Environ. Model. Softw*. **2014**, *54*, 211–221.
3. Abbaspour, K.C. Modelling hydrology and water quality of the European Continent at a subbasin scale: calibration of a high–resolution large–scale SWAT model. *J. Hydrol*, **2015**, *524*, 733–752.
4. Abbaspour, K.C. Uncertainty in Estimation of Soil Hydraulic Parameters by Inverse Modeling: Example Lysimeter Experiments. *Soil Sci. Soc. Am. J.* **1999**, *63*, 501–509.

5. Rouholahnejad, E. A high resolution spatiotemporal distribution of water resources quantity and quality in the Black Sea Basin. *Water Resour. Res.* **2014**, *50*, 5866–5885.
6. Hall, J.; Arheimer, B. Understanding Flood Regime Changes in Europe: A state of the art assessment. *Hydrol. Earth Syst. Sci.* **2014**, *18*, 2735–2772.
7. Barnett, T.; Pierce, D. Human–Induced Changes in the Hydrology of the Western United States. *Science* **2018**, *319*, 1080–1083.
8. Lin, S.; Jing, C. Evaluating DEM source and resolution uncertainties in the Soil and Water Assessment Tool. *Stoch. Environ. Res. Risk Assess*. **2013**, *27*, 209–221.
9. Beven, K.; Binley, A. The future of distributed models: Model calibration and uncertainty prediction. *Hydrol. Process*. **1992**, *6*, 279–298.
10. Legates, D.; McCabe, G. Evaluating the use of "goodness–of–fit" measures in hydrologic and hydroclimatic model validation. *Water Resour. Res*. **1999**, *35*, 233–241.
11. N. Ajami.; Q. Duan.; S. Sorooshian. An integrated hydrologic Bayesian multimodel combination framework: Confronting input, parameter, and model structural uncertainty in hydrologic prediction. *Water Resour. Res*., **2007**, *43*.
12. O. Wani.; A. Scheidegger. Parameter estimation of hydrologic models using a likelihood function for censored and binary observations. *Water Res.*, **2017**, 121, 290–301.
13. Sharma, A.; Tiwari, K. A comparative appraisal of hydrological behavior of SRTM DEM at catchment level. *J. Hydrol.* **2014**, *519*, 1394–1404.
14. Wang, H.; Wu, Z. A Comprehensive Study of the Effect of Input Data on Hydrology and non–point Source Pollution Modeling. *Water Resour. Manag.* **2015**, *29*, 1505–1521.
15. Bormann, H.; Breuer, L. Assessing the impact of land use change on hydrology by ensemble modelling (LUCHEM) IV: Model sensitivity to data aggregation and spatial (re–) distribution. *Adv. Water Resour.* **2009**, *32*, 171–192.
16. Bastola, S.; Murphy, C. The role of hydrological modelling uncertainties in climate change impact assessments of Irish river catchments. *Adv. Water Resour.* **2011**, *34*, 562–576.
17. Najafi, M.; Moradkhani, H. Assessing the uncertainties of hydrologic model selection in climate change impact studies. *Hydrol. Process.* **2011**, *25*, 2814–2826.
18. Niehoff, D. Land–use impacts on storm–runoff generation: scenarios of land–use change and simulation of hydrological response in a meso–scale catchment in SW–Germany. *J. Hydrol.* **2002**, *267(1–2)*, 80–93.
19. Price, K. Effects of watershed topography, soils, land use, and climate on baseflow hydrology in humid regions: a review. US Environmental Protection Agency, USA, **2011**, *35*, 465–492.
20. DeFries, R. Land–use change and hydrologic processes: a major focus. *Hydrol. Processes* **2004**, *18*, 2183–2186.
21. Yang, X.; Ren, L.; Singh, V.P.; Liu, X.; Yuan, F.; Jiang, S.; Yong, B. Impacts of land use and land cover changes on evapotranspiration and runoff at Shalamulun River watershed, China. *Hydrol. Res.* **2012**, *43(1–2)*, 23–37.
22. Horritt, M.S.; Bates, P.D. Evaluation of 1D and 2D numerical models for predicting river flood inundation. *J. Hydrol.* **2002**, *268(1–4)*, 87–99.
23. Behbahani, R. The effect of base map scale on the accuracy of floodplain zoning using GIS. *J. Appl. Sci.* **2006**, *6(1)*, 20–26.
24. Bates, P.D. Remote sensing and flood inundation modeling. *Wiley Inter. Sci.* **2004**, *18(1–2)*, 2593–2597.

25. Borga, M. Accuracy of radar rainfall estimates for streamflow simulation. *J. Hydrol.* **2002**, *267(1–2)*, 26–39.
26. USACE. Engineers, Hydrologic Modeling System (HEC–HMS) Applications Guide: Version 3.1.0. Institute for Water Resources, Hydrologic Engineering Center, 2008.
27. Oleyiblo, J.O. Application of HEC–HMS for flood forecasting in Misai and Wan'an catchments in China. *Water Sci. Eng.* **2010**, *3*, 14–22.
28. Wahren, F.T.; Julich, S.; Nunes, J.P.; Gonzalez-Pelayo, O.; Hawtree, D.; Feger, K.H.; Keizer, J.J. Combining digital soil mapping and hydrological modeling in a data scarce watershed in north–central Portugal. *Geoderma* **2016**, *264*, 350–362.
29. Steinman, A. Event and Continuous Hydrologic Modeling with HEC–HMS. *IJETSR* **2009**, *135(1)*, 119–124.
30. Feldman, A. Hydrologic Modeling System HEC–HMS, Technical Reference Manual, USA: U.S. Army Corps of Engineers. Hydrologic Engineering Center, 2009.
31. Yener, M.K. Modeling studies with HEC–HMS and runoff scenarios in Yuvacik Basin, Turkiye. International Congress on River Basin Management, 2009.
32. Knebl, M.R.; Yang, Z.L.; Hutchison, K.; Maidment, D.R. Regional scale flood modeling using NEXRAD rainfall, GIS, and HEC–HMS: a case study for the San Antonio River Basin Summer 2002 storm event. *J. Environ. Manage.* **2004**, *75*, 325–336.
33. Enard, B.; Kavetski, D. Understanding predictive uncertainty in hydrologic modeling: The challenge of identifying input and structural errors. *Water Resour. Res.* **2010**, *46(5)*, W05521.
34. William, J. Hydrologic Modeling of a Probable Maximum Precipitation Event Using HEC–HMS and GIS Models – A Case Study of Two Watersheds in Southern Virginia. Thesis in Civil Engineering, Virginia Polytechnic Institute and State University, 2012, pp. 269.
35. Kalita, D. A study of basin response using HEC–HMS and subzone reports of CWC. Proceeding of 13th National Symposium on Hydrology, Roorkee, New Delhi, 2008.
36. Oudin, L.; Andréassian, V. Dynamic averaging of rainfall–runoff model simulations from complementary model parameterizations. *Water Resour. Res.* **2006**, *42(7)*, W07410.
37. Rathod, P. Simulation of Rainfall–Runoff Process Using HEC–HMS – Case Study: Tapi River, India. Proceeding of 20th International Conference on Hydraulics, 2015.
38. Abdullah, J. Estimation of Peak Discharges Using Flood Frequency Analysis and Hydrological Modeling System. In International Symposium on Flood Research and Management, Singapore, 2015.
39. Muthukrishnan, E. Calibration of a simple rainfall–runoff model for long–term hydrological impact evaluation. *URISA J.* **2006**, *18(2)*, 33–40.
40. Tassew, B.; Belete, M.; Miegel, K. Application of HEC–HMS Model for Flow Simulation in the Lake Tana Basin: The Case of Gilgel Abay Catchment, Upper Blue Nile Basin, Ethiopia. *Hydrology* **2019**, *6(1)*, 21.
41. Merwade, V. Terrain Processing and HMS–Model Development using GeoHMs. School of Civil Engineering. Purdue University, USA, 2012.
42. World Bank. In Jakarta Tantangan Perkotaan Seiring Perubahan Iklim. The World Bank, Jakarta, Indonesia, 2017.
43. Emam, A.; Mishra, B.; Kumar, P.; Massago, Y.; Fukushi, K. Impact Assessment of Climate and Land–use Changes on Flooding Behavior in the Upper Ciliwung River, Jakarta, Indonesia. *Water* **2016**, *8(12)*, 559.

44. Nga, T.T. Establishing a flood simulation model for reservoir operation in the Vu Gia–Thu Bon River during the flood season. **2013**, *42*, 18–24.
45. Loi, N.K. Automated procedure of real–time flood forecasting in Vu Gia – Thu Bon river basin, Vietnam by integrating SWAT and HEC–RAS models. *J. Water Clim. Change* **2019**, *10(3)*, 535–545.
46. Son, N.H. Study on the application of flood forecasting model for Vu Gia – Thu Bon River. **2013**, *43*, 118–124.
47. Hau, N.X. Assessment of Climate Change Impact on Floods in the Nhat Le River Basin, Vietnam. *VNU J. Sci.: Nat. Sci. Technol.* **2015**, *31(3S)*, 125–138.
48. Halwatura, D.; Najim, M.M.M. Application of the HEC–HMS model for runoff simulation in a tropical catchment. *Environ. Modell. Softw.* **2013**, *46*, 155–162.
49. Sardoii, E.; Rostami, N. Calibration of loss estimation methods in HEC–HMS for simulation of surface runoff (Case Study: Amirkabir Dam Watershed, Iran). *Adv. Environ. Biol.* **2012**, *6*, 343–348.
50. Tewolde, M.; Smithers, J.C. Flood routing in ungauged catchments using Muskingum methods. *Water SA.* **2016**, *32*, 379–388.

VIETNAM JOURNAL OF HYDROMETEOROLOGY

Research Article

An alternative calibration method for wave-fence interaction in SWASH model

Hoang Tung Dao[1*], Tri Mai[2], Cong Mai[3,4], Tuan Minh Thanh Doan[5]

[1] Hanoi University of Natural Resources and Environment, Vietnam; dhtung@hunre.edu.vn
[2] Hanoi University of Civil Engineering, Vietnam; trimc@nuce.edu.vn
[3] Thuyloi University, Vietnam; cong.m.v@tlu.edu.vn
[4] Delft University of Technology, the Netherlands; C.MaiVan@tudelft.nl;
[5] Ministry of Agriculture and Rural Development, Vietnam; minhthanhbql@gmail.com

*Corresponding author: dhtung@hunre.edu.vn; Tel.: +84–395357993

Received: 8 July 2022; Accepted: 19 August 2022; Published: 25 September 2022

Abstract: The application of brushwood fences along the Mekong deltaic coast has recently played a significant role in wave damping and promoting sedimentation. The insight mechanism of brushwood fence for wave energy reduction is the bulk drag coefficient ($\overline{C_D}$) that is also linked to the well-known Forchheimer coefficients (α, β). The bulk drag coefficient was then applied in the SWASH model for validation in its implementation model, the vegetation model, and showed a good comparison with the physical model in the same settings. The porosity model in the SWASH model applied the Forchheimer coefficient has not been used for validation even though the strong links between the $\overline{C_D}$ and the α, β were indicated. In this study, the validation of wave-fence interaction in the porosity model of the SWASH model is presented and compared to the vegetation model in the previous study. The results show a good agreement of wave heights and wave spectrum between the physical, vegetation and porosity models. Furthermore, the computational and physical model errors, such as BIAS and SI values, are less than 1 mm and 10%, respectively.

Keywords: Wooden fence; SWASH model; Mekong Delta; Darcy-Forchheimer.

1. Introduction

Coastal structures, such as breakwater, sea dikes, porous breakwater and wooden fences, bring a certain level of safety to marine habitats and people living along the coasts. However, the safe level of structures certainly depends on each type of structure applied [1]. For example, hard or grey structures, breakwater, and sea dikes create an acceleration of sediment transport at the upstream flow. In contrast, erosion apparently occurs on the downstream side of the structures due to breaking sediment equilibrium. On the other hand, porous structures or hybrid structures, such as either submerged or emerging structures, may reduce and occasionally stop the erosion at the downstream site. In the better case, a nature-based solution that combines a porous structure and a natural ecosystem can create a good situation for both inhabitants and natural vegetation, such as mangroves, along the coast.

The Mekong deltaic coastline has been under serve erosion conditions for more than a decade. The consequence of eroding the coastal zone brings many negative impacts to the living habitats along the coast. For example, natural marine ecosystems, mangroves, are now

facing a dangerous situation when the reduction of mangroves belt to the shore has been up to 50 to 100 m per year [2]. Furthermore, erosion phenomenon occurs along the coast can threaten the economic stability and the safety of civilization.

Along the Mekong deltaic coast, wooden fences are built in front of mangrove belts to reduce wave and flow energies and to increase the sedimentation inside the downstream basin. Furthermore, wooden fence structures with a maximum of three rows of vertical bamboo poles form a frame to keep horizontal brushwood, such as bamboo and tree branches [3–5]. The results of about 80% incoming wave height reduction were recorded at Nha Mat, Bac Lieu [3–6] and simulated in numerical studies [7–9]. However, due to a lack of understanding of flow over wooden fences, the study [10] carried out flow resistance experiments to indicate the bulk drag coefficient ($\overline{C_D}$) and the Forchheimer coefficients (α, β) of the wooden fences. Thereafter, the study [9] used the bulk drag coefficient for validating the wave-fence interaction data from the physical model with the simulated data in the SWASH model, developed by Delft University of Technology [9].

In the SWASH model, the vegetation implementation model simulates the interaction of waves and cylinders based on the well-known bulk drag coefficient. This coefficient can be indicated by the relationship between flow patterns and the array of cylinders [11–12], which is also influenced by the characteristic of cylinders themselves, for example, the cylinder surface, the cylinder diameters, and positions between cylinders [13–14]. On the other hand, the porous implementation model considers the famous Forchheimer coefficients from the Darcy-Forchheimer equations to indicate the drag forces [15–16] if the array of cylinders can be considered as permeable media. Therefore, the drag forces on porous media were then indicated as the linear and nonlinear forces caused by the effect of laminar and turbulent friction, respectively [17–18].

In the previous study [9], well agreements between physical and numerical models were presented, which applied the bulk drag coefficient found in the study [10]. However, the interesting simulation for the porous implementation model has been abandoned. Therefore, in this study, this simulation of the porous model is presented that validates the measurement data and the numerical modelling of the vegetation model [9].

2. Method

2.1. Physical model

The physical model of wave-fence interactions was conducted in the wave flume at the Hydraulic Engineering Laboratory at Delft University of Technology. The settings of wave piston, wave gauges and wooden fences are shown in Figure 1.

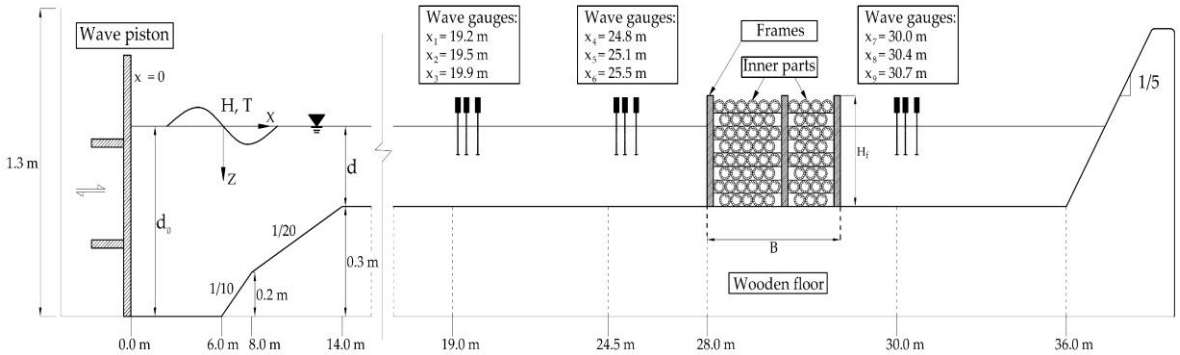

Figure 1. The cross profile is used in physical and numerical models [9].

The wave conditions were put on the west side of the flume, while a schematized dike was located on the east side. The horizontal bed is to schematize the gentle foreshore along the Mekong deltaic coast, creating a breaking zone for waves. However, the flume in the

laboratory was virtually short and made an impossible design for a gentle slope. Therefore, steep slopes were combined to simulate similar breaking phenomena. Furthermore, waves were intended to break at x = 14.0 m before reaching the fence at x = 28.0 m on the horizontal bed (Figure 1).

Wave conditions were used in physical and numerical models, including irregular wave heights (H_s) and peak wave periods (T_P) ranged from 0.035 to 0.075 m and from 1.1 to 2.7 seconds, respectively. Three water depths (d) were used as 0.15, 0.20, and 0.25 m corresponding to three fence thicknesses. The settings for wooden fences were inhomogeneous with bamboo cylinders with diameters of about 0.004 m. The setup and structures are shown in Figure 2. Wooden fences used in this physical model had three different thicknesses, B = 0.28, 0.40, and 0.66 m, while the height was fixed at 0.30 m. In every test, the number of cylinders in m^2 was also fixed at 8705 cylinder/m^2 resulting in a density of 0.10 or porosity of 0.90. Moreover, wave data were recorded by a total of nine wave gauges (WGs) from WG1 to WG9 (Figure 1) with a sampling frequency of 100 H.

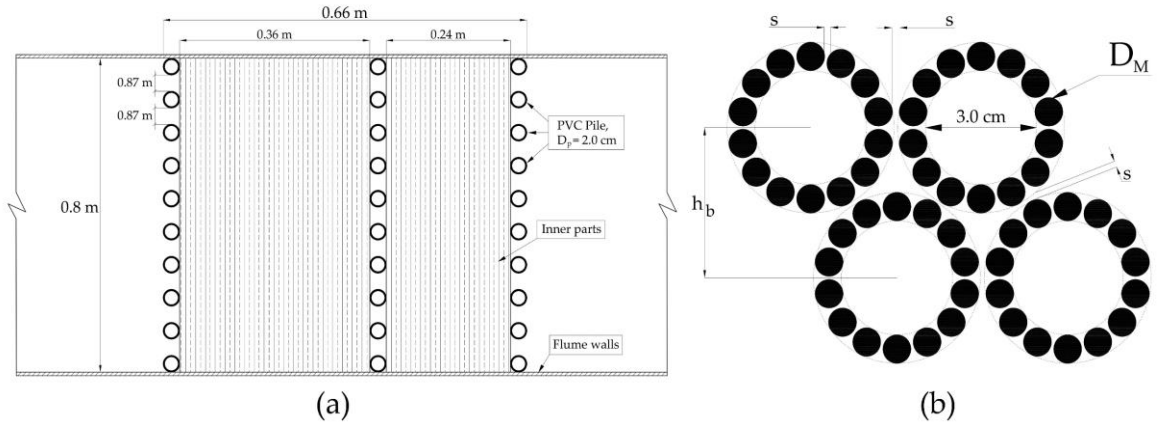

Figure 2. The wooden fence setup. The top-view (a) of the fence and the inner parts (b) structure [9].

2.2. Numerical model

SWASH model is the time-phased averaging model, which can simulate hydrostatic and non-hydrostatic free-surface flow based on the nonlinear shallow water equation [19]. This model can also accurately account for many waves and flow processes on the nearshore [20].

The government equations for wave propagation in a cross-shore profile are:

$$\frac{\partial u}{\partial x}+\frac{\partial w}{\partial z}=0 \quad (1)$$

$$\frac{\partial \eta}{\partial t}+\frac{\partial}{\partial x}\int_{-d}^{\eta} u dz=0 \quad (2)$$

$$\frac{\partial w}{\partial t}+\frac{\partial uw}{\partial x}+\frac{\partial ww}{\partial z}+\frac{1}{\rho}\frac{\partial (P_{nh})}{\partial z}+\frac{\partial \tau_{zz}}{\partial z}+\frac{\partial \tau_{zx}}{\partial x}=0 \quad (3)$$

$$\frac{\partial u}{\partial t}+\frac{\partial uu}{\partial x}+\frac{\partial wu}{\partial z}+\frac{1}{\rho}\frac{\partial (P_h+P_{nh})}{\partial x}+\frac{\partial \tau_{xz}}{\partial z}+\frac{\partial \tau_{xz}}{\partial x}=0 \quad (4)$$

where x is the horizontal coordinate and z is the upward coordinate relative to the still water level. u and w are horizontal and vertical velocities, respectively. η is the free surface elevation relative to the still water level, t is the time. The pressure contribution P is separated into the hydrostatic pressure P_h and nonhydrostatic pressure P_{nh}. The turbulent stresses τ are calculated from a constant turbulent viscosity.

At the bottom boundary, bottom stress is applied, following a quadratic friction law, as:

$$\tau_b=c_f\frac{U|U|}{\eta+d} \quad (5)$$

where U is the depth-averaged velocity; c_f is friction coefficient which is based on Manning's roughness coefficient n [13]:

$$c_f = \frac{n^2 g}{d^{1/3}} \quad (6)$$

The settings of SWASH model are based on the physical model and study [9]. In detail, the 1D-mode was applied with the profile, as shown in Figure 1. A horizontal resolution was set at 0.02 m, and the initial water level was set to zero. The physical condition for SWASH was the vertical turbulence viscosity, which was set as 3×10^{-4} (m^2/s), and the bed friction coefficient, which applied Manning's roughness coefficient as a default factor as 0.019 ($m^{-1/3}s$) [19]. The interpretation for this setup was described in the study [9].

In the SWASH model, two options can be applied to simulate the interaction between waves and wooden fences, the vegetation and porous implementation model. The vegetation model takes into account a number of cylinders in an area and the bulk drag coefficient to calculate the reduction of incoming wave heights as the following equation:

$$\frac{H}{H_0} = \frac{1}{1+\tilde{\beta}x} \quad (7)$$

where H_0 (m) and H (m) are the incoming and transmission wave heights, respectively and the parameter $\tilde{\beta}$ is calculated from [21] yielded as:

$$\tilde{\beta} = \frac{1}{3\sqrt{\pi}}\overline{C_D}DNH_0k\frac{sinh^3(k\alpha H_f) + 3\sinh(k\alpha H_f) + cosh^3(k\alpha H_f) - 3\cosh(k\alpha H_f) + 2}{[\sinh(2kd) + 2kd]\sinh(kd)} \quad (8)$$

where the parameter αH_f is the water depth from the fence's toe to the water surface with H_f is the fence height, k is the wave number and $\overline{C_D}$ is the bulk drag coefficient.

On the other hand, the porous implementation model considers the computational domain to simulate the interaction between waves and porous coastal structures. The mean flow through a porous medium, therefore, is described by the mean volume Reynolds-averaged Navier-Stokes equations. The flow conditions, including laminar and turbulent flow, then is modelled as the respective frictional forces inside the porous medium by the empirical formula of Van Gent [18]:

$$F_D = a\rho u + b\rho|u|u \quad (9)$$

where a (s/m) and b (s^2/m^2) are the friction factors representing viscosity and turbulence dominance, ρ (kg/m^3) is water density, and u (m/s) is the flow velocity. These factors depend on the porosity (n), cylinder diameter (D) and viscosity of water (v), indicated as:

$$a = \alpha\frac{(1-n)^2}{n^3}\frac{\nu}{gD^2} \quad (10)$$

$$b = \beta\frac{1-n}{n^3}\frac{1}{gD} \quad (11)$$

where g (m/s^2) is gravitational acceleration, the set-parameter α and β are the dimensionless parameter representing friction terms.

Moreover, the study [10] stated that the importance of α was always minor and much less than the β in turbulent conditions. Therefore, that study found the relationship between the bulk drag coefficient ($\overline{C_D}$) and the β in turbulent flow conditions as yielded as:

$$\beta = \frac{2n}{\pi}\overline{C_D} \quad (12)$$

This relationship then allows comparing the interaction between wave and fence in different methods, the porous and vegetation models. The details can be found in the study [9].

2.3. Validation

The validation was given a good agreement between the physical and numerical vegetation model, which uses the bulk drag coefficient as shown in Figure 3a [9]. In this study, the validation continues by using the β values calculated directly from $\overline{C_D}$ in Equation 12. In Figures 3a and 3b, the comparison of $\overline{C_D}$ and β in the same relationship with KC number, with $KC = uT_p/D$ where u is flow velocity in front of the fence, T_P is peak wave periods.

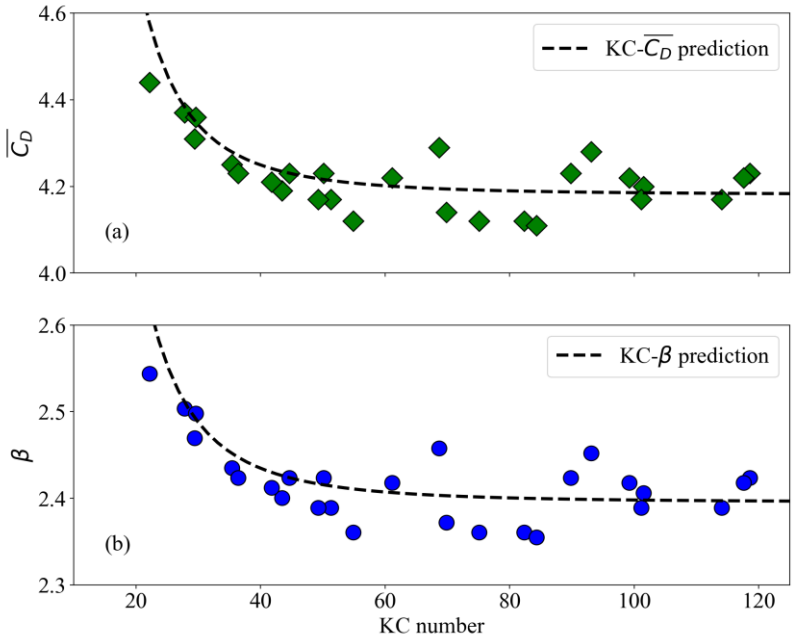

Figure 3. Relationship of the bulk drag coefficient ($\overline{C_D}$) and KC number (a); And the dimensionless coefficient (β) and KC number (b).

Furthermore, the errors between physical and numerical data that is the predictive skill of SWASH are calculated with two parameters, such as bias and scatter index, defined as:

$$bias = \frac{1}{N}\sum_{i=1}^{N}(\varepsilon_{compute}^{i} - \varepsilon_{measure}^{i}) \quad (13)$$

$$SI = \frac{\sqrt{\frac{1}{N}\sum_{i=1}^{N}(\varepsilon_{compute}^{i} - \varepsilon_{measure}^{i})^2}}{\frac{1}{N}\sum_{i=1}^{N}\varepsilon_{measure}^{i}} \quad (14)$$

where $\varepsilon_{compute}$ and $\varepsilon_{measure}$ are the statistical wave values simulated by SWASH and measured in the wave flume, respectively, and N is the total number of data points in the considered data set [22].

3. Results and Discussion

3.1. Wave heights

Figure 4 shows the standing waves of four cases for all models, such as physical (red diamonds), vegetation (solid black line) and porosity (blue dashed line) models. As can be seen, SWASH gives a good simulation which shows the reflection in front and transmission behind the fences for both vegetation and porous models. Moreover, standing waves are compared to each other in Figure 4, showing that the two implementation models agree well with measurement data.

3.2. Surface elevation and Wave spectrum

Figure 5 indicates the water elevation at three locations, x = 19.2 m, 25.3 m (in front of the fence) and x = 30.0 m (behind the fence), of three models, physical model (dashed black line), vegetation model (solid green line), and porous model (solid blue line). The results show a good agreement between the three models even though several phases are delayed between numerical and physical models.

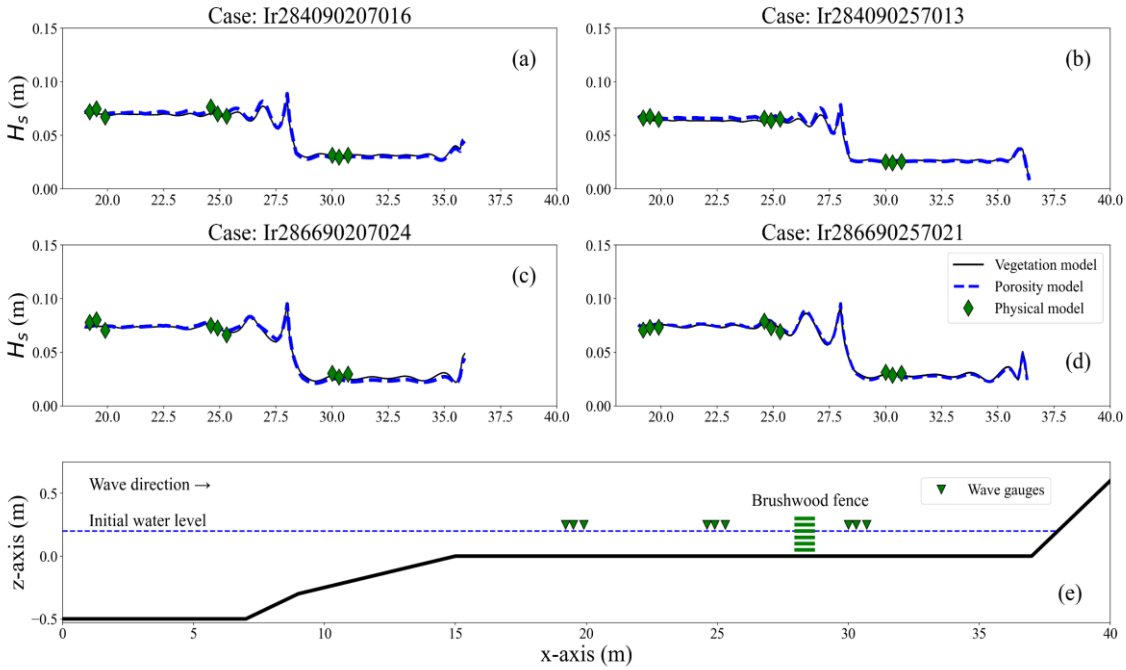

Figure 4. Standing wave heights in four cases: (a) $d = 0.2$ m, $H_s = 0.07$ m, $T_P = 1.6$ s, $B = 0.4$ m; (b) $d = 0.25$ m, $H_s = 0.07$ m, $T_P = 1.3$ s, $B = 0.4$ m; (c) $d = 0.2$ m, $H_s = 0.07$ m, $T_P = 2.4$ s, $B = 0.66$ m; and (d) $d = 0.25$ m, $H_s = 0.07$ m, $T_P = 2.1$ s, $B = 0.66$ m. The profile and measured points are presented in (e).

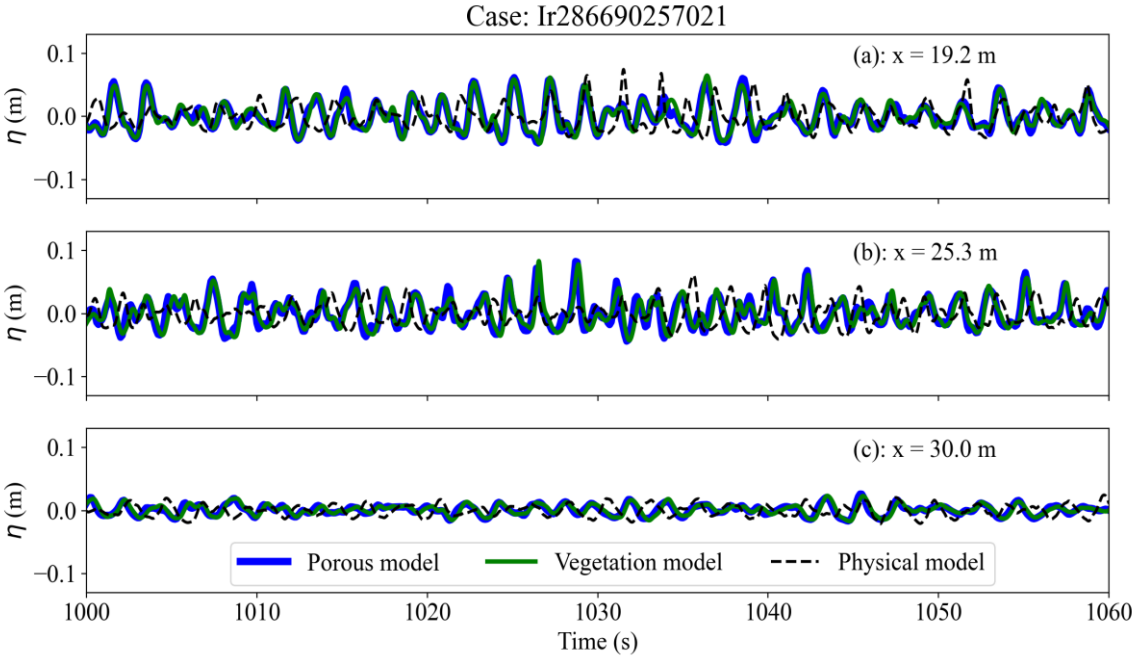

Figure 5. Surface elevation at three locations, in front of the fence x = 19.2 m (a) and x = 25.3 m (b) and behind the fence x = 30.0 m (c).

Figure 5c also indicates the phases lagged due to porous media/vegetation obstruction. It can be seen that water elevation generated from both porous and vegetation models are quite comparable but have less agreement between them and the physical model. This is due to the physical mechanism of wave reduction inside the wooden fence of the physical model might have more inflow between cylinders and larger drag force than described in the SWASH model.

Wave spectra densities of all cases were derived by applying the Fast Fourier Transform (FFT) method to the surface elevation (Figure 5). The wave spectrum of a case at a total of nine wave gauges (Figure 4e) is indicated in Figure 6. As can be seen, all wave spectral densities of all models have a good agreement. There are different densities at frequency of 0.5 for location x = 19.5, 19.9, and 24.9 m. The reflection could cause these differences due to different mechanisms in front of the fence between the three models. Even though the highest spectral densities at x = 24.6, 24.9, and 25.3 m are slightly similar at a frequency of 0.5, the second densities at a frequency of 0.85 show a difference.

Furthermore, in the physical model, the second peak generally represents the second wave interacting with the first wave. In other words, the first wave is slower than the second one, which is shorter, leading to the second peak of spectral densities. The more wave-wave interactions, the more peaks appear. In SWASH, this phenomenon is somehow absurd and challenging to understand.

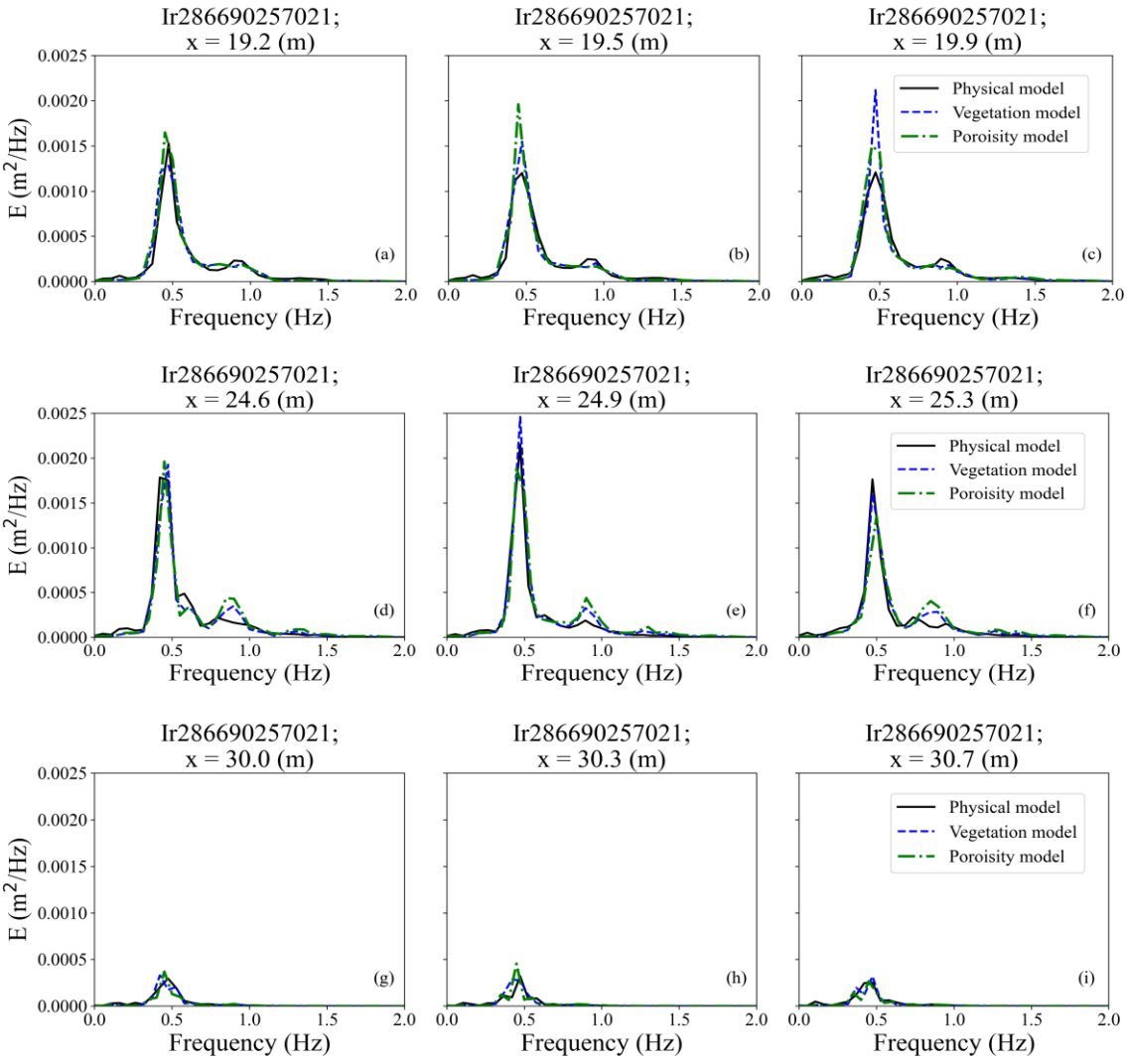

Figure 6. Wave spectrum at nine locations from (a) to (i) of the case: H = 0.07 m, Tp = 2.1s, d = 0.25 m and B = 0.66 m.

3.3. Wave height errors

The skill of SWASH is calculated from Equations 13 and 14 and shown in Figure 7 and Figure 8 for incoming wave heights (in front of the fence) and transmitted wave heights (behind the fence), respectively. The bias and SI parameter gives a good agreement between implementation models (vegetation and porous models) and the physical model. Moreover, for incoming wave heights, the errors are below 5% (Figure 7).

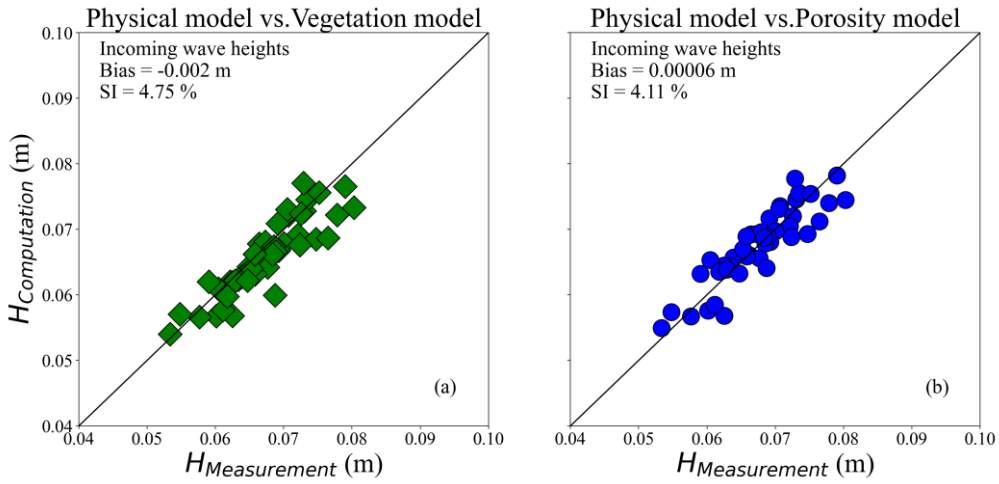

Figure 7. Errors between measurement and numerical data of incoming wave heights for vegetation (a) and porosity (b) implementation model.

However, the transmission wave heights error of the vegetation model is significantly lower than the porous model (Figure 8a). It is shown that the SI value of the vegetation model is about 6%, while this value is nearly double at about 11% for the porous model (Figure 8b). This result means that the skill of SWASH for transmission wave heights for both models is acceptable, but the vegetation model is more accurate than the porous model.

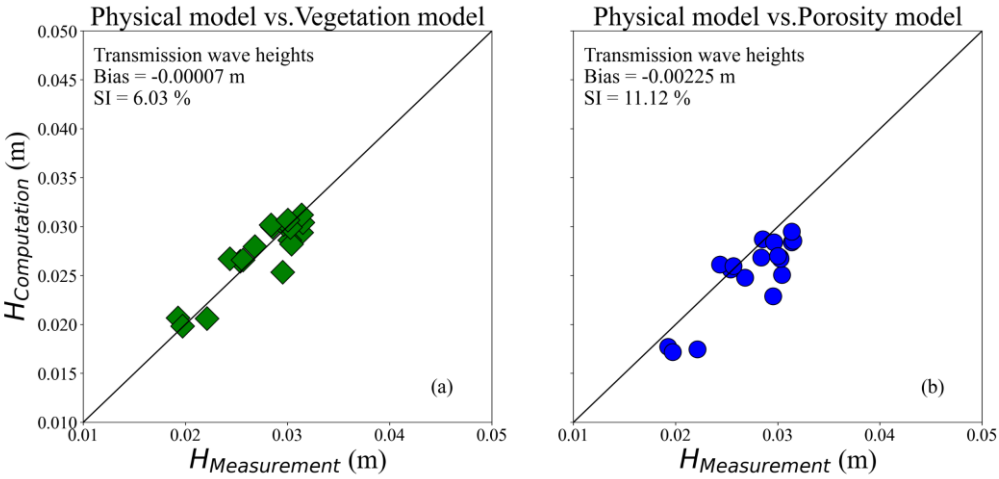

Figure 8. Errors between measurement and numerical data of transmission wave heights for vegetation (a) and porosity (b) implementation models.

4. Conclusion

This study presents an alternative method for validating wave-fence interaction in the SWASH model, the porous implementation model. This model applied the dimensionless friction coefficient (α, β) in the famous Darcy-Forchheimer equations for particularly wooden fences used in the study [9]. Furthermore, the β coefficient has a strong link with the

bulk drag coefficients found in the study [10], which is only effective in the turbulent flow condition.

The validation results of the porous model show a good agreement with the physical and vegetation model for standing wave heights, surface elevations, and wave spectral densities. Moreover, good bias and SI indicate the skill of SWASH even though the errors of the vegetation model are slightly better than the porous model. This study also opens new windows to simulate wave-fence interaction, and more topics, such as sediment transport, and 3D simulation of wave-fence, will be studied in the future.

Author contribution statement: Conceived and designed the experiments; Analyzed and interpreted the data; contributed reagents, materials, analysis tools or data; manuscript editing: H.T.D.; Performed the experiments; contributed reagents, materials, analyzed and interpreted the data, wrote the draft manuscript: H.T.D.; Reviewer and edit: T.M., T.C., T.M.T.D.

Acknowledgement: The first author (Hoang Tung Dao) is grateful for being supported by Delft University of Technology, the Netherlands; Hanoi University of Natural Resources and Environment, Hanoi, Vietnam.

References

1. Schoonees, T.; Mancheño, A.G.; Scheres, B.; Bouma, T.J.; Silva, R.; Schlurmann, T.; Schüttrumpf, H. Hard structures for coastal protection, towards greener designs. *Estuaries Coasts* **2019**, *42(7)*, 1709–1729.
2. Duke, N.; Wilson, N.; Mackenzie, J.; Nguyen, H.H.; Puller, D. Assessment of Mangrove Forests, shoreline condition and feasibility for REDD in Kien Giang Province, Vietnam, Deutsche Gesellschaft für Technische Zusammenarbeit (GTZ), 2010, pp. 1–128.
3. Schmitt, K.; Albers, T. Area coastal protection and the use of bamboo breakwaters in the Mekong Delta. *Coastal Disasters Clim. Change Vietnam, Elsevier* **2014**, 107–132.
4. Albers, T.; San, D.C.; Schmitt, K. Shoreline Management Guidelines: Coastal Protection in the Lower Mekong Delta, GIZ. Eschborn, Germany, 2013.
5. Van Cuong, C.; Brown, S.; To, H.H.; Hockings, M. Using Melaleuca fences as soft coastal engineering for mangrove restoration in Kien Giang, Vietnam. *Ecol. Eng.* **2015**, *81*, 256–265.
6. Van, C.M.; Ngo, A.; Mai, T.; Dao, H.T. Bamboo Fences as a Nature-Based Measure for Coastal Wetland Protection in Vietnam. *Front Mar. Sci.* **2021**, *8*, 1430.
7. Dao, T.; Stive, M.J.F.; Hofland, B.; Mai, T. Wave Damping due to Wooden Fences along Mangrove Coasts. *J. Coastal Res.* **2018**, *34(6)*, 1317–1327. doi: 10.2112/JCOASTRES-D-18-00015.1.
8. Tri, M.C.; Vuong, N.V.; Dat, H.D.; Anh, N.T.T.; Tung, D.H. Numerical simulation of wave transmitting through a bamboo fence. *J. Sci. Technol. Civil Eng.* **2019**, *13(1V)*, 75–83. (In Vietnamese)
9. Dao, H.T.; Hofland, B.; Suzuki, T.; Stive, M.J.F.; Mai, T.; Tuan, L.X. Numerical and small-scale physical modelling of wave transmission by wooden fences. *J. Coastal Hydraul. Struct.* **2021**, *1(4)*, 1–21.
10. Dao, H.T.; Hofland, B.; Stive, M.J.F.; Mai, T. Experimental assessment of the flow resistance of coastal wooden fences. *Water* **2020**, *12(7)*, 1910.
11. Williamson, C.H.K. The natural and forced formation of spot-like "vortex dislocations" in the transition of a wake. *J. Fluid Mech.* **1992**, *243*, 393–441.
12. Schewe, G. On the force fluctuations acting on a circular cylinder in crossflow from subcritical up to transcritical Reynolds numbers. *J. Fluid Mech.* **1983**, *133*, 265–285.

13. Lou, S.; Chen, M.; Ma, G.; Liu, S.; Zhong, G. Laboratory study of the effect of vertically varying vegetation density on waves, currents and wave-current interactions. *Appl. Ocean Res.* **2018**, *79*, 74–87.
14. Zdravkovich, M.M. Flow induced oscillations of two interfering circular cylinders, *J. Sound Vib.* **1985**, *101(4)*, 511–521.
15. Darcy, H.P.G. Les Fontaines publiques de la ville de Dijon. Exposition et application des principes à suivre et des formules à employer dans les questions de distribution d'eau, etc. V. Dalamont, 1856.
16. Forchheimer, P. Wasserbewegung durch boden. *Z. Ver. Deutsch Ing.* **1901**, *45*, 1782–1788.
17. Ergun, S. Fluid flow through packed columns. *Chem. Eng. Prog.* **1952**, *48*, 89–94.
18. van Gent, M.R.A. Wave interaction with permeable coastal structures. *Int. J. Rock Mech. Min. Sci. Geomech.* **1996**, *6(33)*, 277A.
19. Zijlema, M.; Stelling, G.; Smit, P. SWASH: An operational public domain code for simulating wave fields and rapidly varied flows in coastal waters. *Coastal Eng.* **2011**, *58(10)*, 992–1012.
20. Smit, P.; Zijlema, M.; Stelling, G. Depth-induced wave breaking in a non-hydrostatic, nearshore wave model. *Coastal Eng.* **2013**, *76*, 1–16.
21. Suzuki, T.; Hu, Z.; Kumada, K.; Phan, L.K.; Zijlema, M. Non-hydrostatic modeling of drag, inertia and porous effects in wave propagation over dense vegetation fields. *Coastal Eng.* **2019**, *149*, 49–64.
22. Zijlema, M. Modelling wave transformation across a fringing reef using SWASH. *Coastal Eng. Proc.* **2012**, *33*, 1–12.

VIETNAM JOURNAL OF HYDROMETEOROLOGY

Rerearch Article

Open and collaborative tools for disaster management and risk reduction

Vasil Yordanov[1,2*], Xuan QuangTruong[3], Thi ThanhThuy Pham[3], Thanh Dong Khuc[4], Maria Antonia Brovelli[1,5]

[1] Department of Civil and Environmental Engineering (DICA) Politecnico di Milano, Italy; vasil.yordanov@polimi.it
[2] Vasil Levski National Military University, Veliko Tarnovo, Bulgaria
[3] Hanoi University of Natural Resources and Environment, Vietnam; txquang@hunre.edu.vn; pttthuy.tdbd@hunre.edu.vn
[4] Hanoi University of Civil Engineering, Vietnam; dongkt@huce.edu.vn
[5] Istituto per il Rilevamento Elettromagnetico dell'Ambiente, CNR-IREA, via Bassini 15, 20133; maria.brovelli@polimi.it

*Corresponding author: vasil.yordanov@polimi.it; Tel.: +39–3283316133
Received: 12 July 2022; Accepted: 24 August 2022; Published: 25 September 2022

Abstract: In recent years geo-information technologies have significant increase in various domain implementations. Such methodologies and applications are gathering more interest in aspects such as data collection, processing, analyses, and dissemination. Covering the full processing cycle, these technologies are impacting many fields, even those where traditionally there were no or few geospatial specialists. A relevant example can be the domain of Disaster Management and Risk Reduction (DMRR), where geo-information is providing powerful tools for effective management in the prevention, preparedness, response and recovery processes, which are of high interest to authorities and stakeholders. However, in certain cases, an important aspect is still under-considered - the "power of the crowd", which can bring vital knowledge and strength. Recently, also hazard specialists started to elicit the participation of citizens and to promote collaborative approaches in their mitigation strategies, whether it is for data collection (local or remotely), or to reduce the time a certain task is done, or simply to further disseminate knowledge and practices. As it is becoming a multi-field and multi-application domain, with our contribution we want to present the state of the art of the open and collaborative tools that are applied in DMRR, regardless of the hazard type, of the used platform (mobile, desktop) and the approach (remote, onsite). In addition, tools currently applied in other domains, but that can be fruitfully used also in DMMR will be included in our speech.

Keywords: Disaster Management; Risk Reduction; Hazards; Collaborative; Open; VGI.

1. Introduction

Natural and man-made hazards are often turning into hard to mitigate or control disasters which, in recent years, are with increased intensities and frequencies. As such stakeholders, local authorities and first responders usually are working together to adopt and implement the most suitable mitigation measures according to different scenarios and hazards. In reality, developing proper mitigation strategies and disaster management, as a whole, are far from being a straightforward problem. Usually, it is taken as a multi-fold problem since most of the hazard events are occurring suddenly with fast evolvement in time and changing local

conditions derailing the planned actions and making the first responders also vulnerable and not fully efficient. In other cases, problems during the preparation and response phases are mainly due to a lack of local knowledge, i.e., having complete and exhaustive knowledge of the local environment and hazard related factors.

As such lack of understanding can be considered as a drawback, in the last decade scholars are actively advocating and adopting contributions from citizens that are able to provide information and knowledge from the perspective of locals [1–2]. In fact, [1] adopted the term Volunteered Geographic Information (VGI) by which is meant the involvement of citizens (professionals and non) to contribute on volunteering basis with information (having also a spatial attribute). In the literature can be noted several suggestions where citizens can actively contribute also in the disaster domain, simply starting from data collection but also to higher level tasks as helping to identify what are the actual problems and how they can be analysed and resolved [3–4]. In specific hazard domains, can be highlighted several adoptions of the VGI, namely, for earthquakes [5–6], floods [7]. Where it is interesting to that the mentioned worked are utilizing the developments in mobile phones and Web 2.0 in the form of social networks. Fewer works can be found where citizens are contributing directly to early warning systems [8–9], building resilience [10], yet many examples of projects for crisis mapping can be found [11–12]. On the other hand, the tools that can actually be utilized by single volunteers or in a collaborative manner in the disaster domain are scarce. In the rest of this paper, we would like to discuss and present the tools that are either focused on a specific hazard or in general, but also such that are not developed for the disaster domain, yet still can be useful. Firstly, will be presented few desktop solutions, followed by mobile tools.

2. Desktop collaborative tools

2.1. OpenStreetMap

OpenStreetMap (OSM) is probably one of the most extensive and effective crowdsourced projects [13] in the geospatial domain. OSM is bringing a street-level spatial data globally and it is mainly relying on volunteers for providing up-to-date and accurate information (~≈8.3 mil registered users by the beginning of 2022 [14]). Single features are mapped through nodes, while linear and areal features are in contained as a list of nodes, named ways. More than just adding map elements users can also add attribute information to them using key = value predefined schema, for example, highway = motorway defines major divided road equivalent to freeway or autobahn.

Even though, OSM was not established as a disaster management project it finds great applicability mainly due to the fact that can be used as a two-way hub for providing valuable spatial information. One way could be defined only as data exploitation, meaning that everyone can access, browse and obtain the already available data, therefore, not just to look at it but also to import it in their environment for processing and analysing spatial data. Where the second way, is actually giving the possibility to the user for contributing to the global map with the matic-specific data, usually organized in collaborative campaigns. Below will be presented tools that can be used in the disaster domain in both data exploitation also in data contribution manner.

2.2. InaSAFE

InaSAFE is a software that allows the users to combine datasets from different sources like scientists, local governments and communities to produce hazard scenarios that can be used for planning, preparedness and response activities. It is developed as a Free and Open Source Software (FOSS) plugin for QGIS [15]. In such way the licensing allows the user not only to use it for free but also to contribute to its improvement and to adapt it according to the needs.

At its core, InaSAFE relies on the information available at OSM, in case it is not provided addition from the user. However, it is required to provide minimum specific information

according to the type of hazard under consideration. For example, if the case is to estimate the numbers of building exposed to a certain flooding event it is needed to input a flood depth layer after the inundation and the building can be directly downloaded from OSM (if mapped). A similar example can be seen on Figure 1 where is reported a possible affected population for the Bengawan Solo flood.

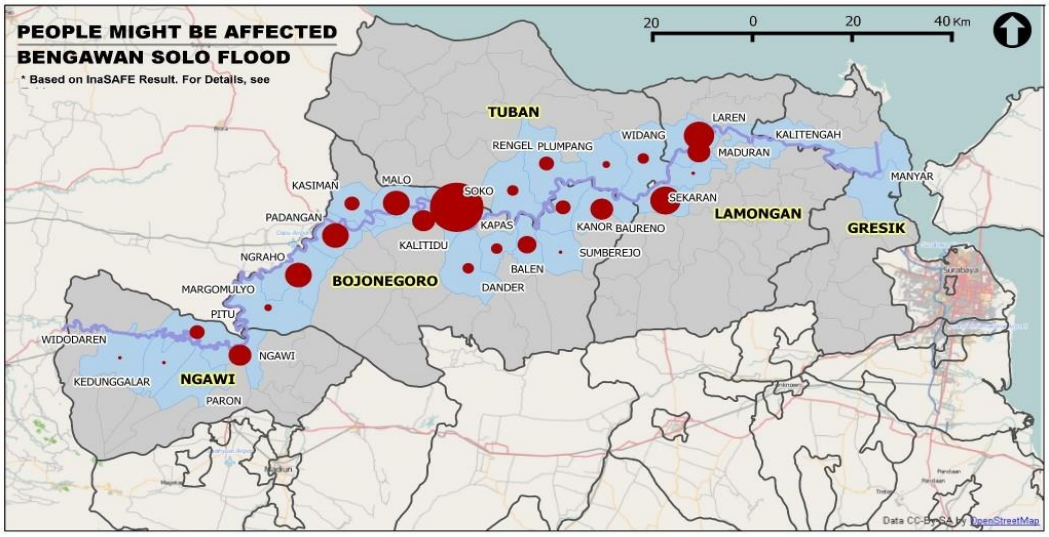

Figure 1. InaSAFE for Bengawan solo flood contingency plan, Institution: BPBD Jawa Timur (via inasafe.org).

2.3. Humanitarian OSM Team

The HOT is not a tool in the scope of this work, however their work is closely related to developing FOSS tools for supporting disaster management, therefore will be briefly introduced. The work of the team is entirely based on the collaborative principle, as their work is focused on open mapping for humanitarian actions and community development. The HOT actions are based on the work of international volunteers which are contributing either remotely or in the field with spatial data and information pre- and post-events. Their main tool of use is the OSM, however, they are dedicated also into developing FOSS tools. Two of the tools will be discussed below.

2.4. Tasking Manager

The role of the Tasking Manager is to breakdown larger mapping projects into small and feasible tasks that can be completed in a collaborative manner in a short time. The goal of the task (e.g., map buildings) is predefined and each user can contribute depending on the own level of expertise. Subdividing into smaller projects allows easier managing and monitoring of the overall aim.

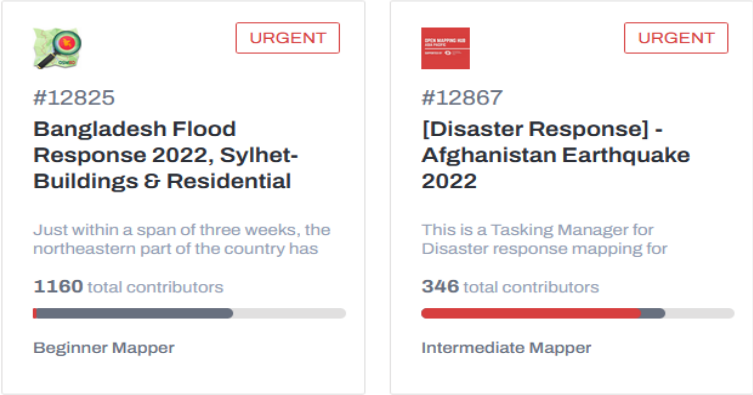

Figure 2. Example of mapping task with different expertise levels.

2.5. OpenAerialMap

OpenAerialMap is another tool developed by HOT which serves as a platform to host aerial imagery (from satellites or unmanned aerial vehicles) where every user can obtain or contribute freely. The general goal is to be a hub for high-resolution imagery that can be useful during disaster preparedness and response. Currently (at the time of writing), the platform collects more than 11,000 images from almost 1,000 contributors, and the spatial resolution of the images can vary from a few centimetres to a bit more than 10 cm.

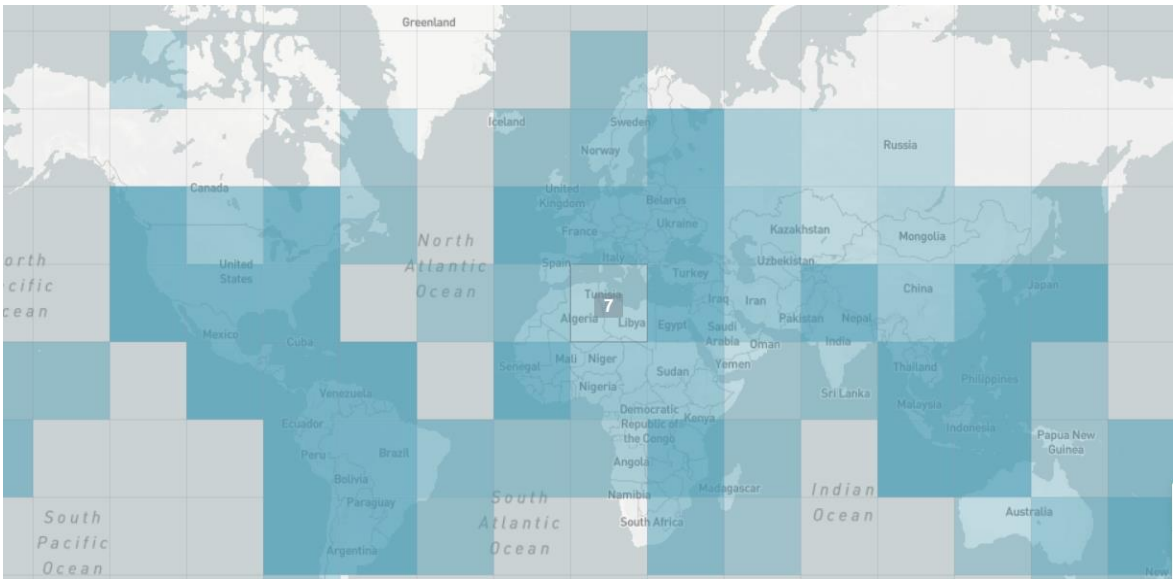

Figure 1. Global map of aerial collections. Colour tiles represent the number of images in it (dark blue means more collections).

3. Mobile tools

Nowadays smartphones and tablets are used by millions of people and with their expansions scholars and practitioners adopted another aspect for VGI contribution - by the means of portable devices, citizen can now be used as “sensors”, i.e., actively or passively to provide valuable geospatial information [16]. The “active” contribution is when the citizen knowingly is providing information using a dedicated application, on the other hand, “passive” is referred when the citizen is sharing an information (e.g., social media publication) but it has an added value to a specific field. Below will be discussed two mobile applications, where the first one is for generic data collection, still can be used for risk reduction actions, while the second is a hazard specific.

3.1. QField

QField is a data collection app also built under the FOSS license. Users are allowed to manage the data by adding and editing spatial and non-spatial data. One of the main advantages of the application is that it hides in itself all the potential of QGIS by using the same QGIS libraries, but it is developed for Android and allows portability. In fact, QField can sync with QGIS and transfer pre-configured projects. The application utilizes the built-in GPS module for positioning the user and can be easily integrated with WebGIS developing system. The data collection form can be created according to the needs of the survey and can be implemented for a variety of case studies (e.g., river monitoring, geological mapping, infrastructure assessment, etc.).

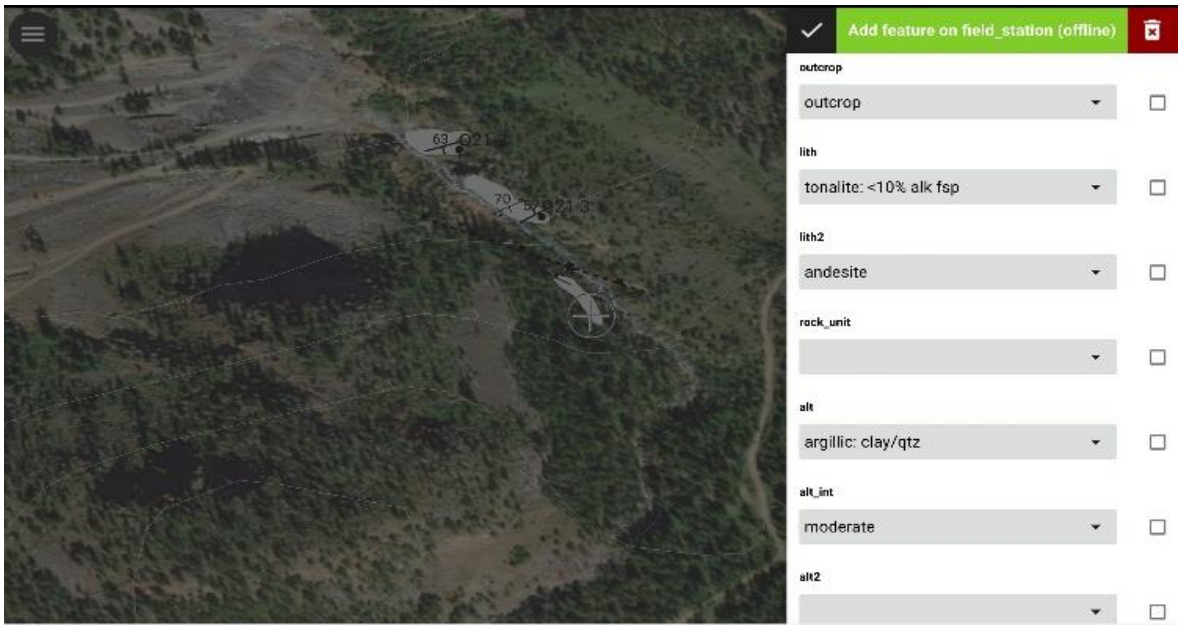

Figure 2. Example of form for geological mapping (via qfield.org).

3.2. Landslide Survey

LandslideSurvey mobile application was developed for thematic data collection, i.e., collection of the location and related information for landslides. The main goal of it is to provide the tool for easy and multi-source landslide inventory compiling. In fact, by design choice the mobile application does not show the mapped records from other users, this was made following the assumption that redundant data can help in validating entries, but also can contribute with additional information. The application is designed according to the proficiency level of the user into the topic (professional and non). Accordingly, the user interface guides through the compiling process of each entry, following a standard geological questionnaire. At a minimum the user should provide the type of the landslide and a photo of it, the application stores the location of the phone through a built-in positioning module. Once the record is saved, the application syncs with the server and in cases the smartphone is not connected to internet service, it syncs once online.

As a complementary to the app has been developed a LandslideSurvey plugin for QGIS, which allows the user to download locally the information from the server (including location and related information). A simple LandslideSurvey WebApp was also developed which allows the user to browse online the landslide records and explore simple statistics related to them.

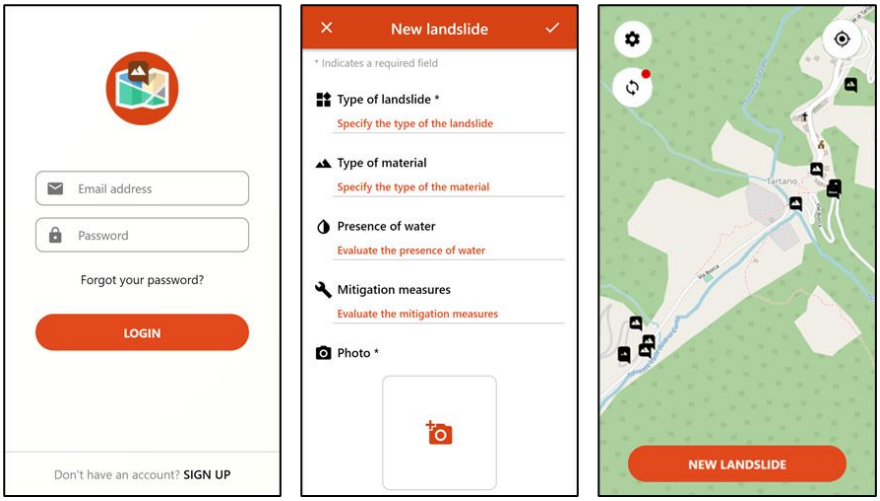

Figure 3. Screenshots from the LandslideSurvey Mobile App.

4. Conclusions

In this work, we have discussed some of the tools that can be used in Disaster Management and Risk Reduction actions in an open and collaborative manner. As it can be noted most of the tools are actually relying on OpenStreetMap which is perhaps the best example of open and collaborative effort in the geospatial domain. Based on its success is possible to derive additional tools and products that are specifically applicable for better development of hazard preparedness and response plans. Throughout the research phase for this contribution were noted other tools in the scientific literature. Mostly those tools could not be actually found or tested, which highlighted a problem related to the lack of maintenance of a product after the project end. However, during a full cycle for DMRR actions the volunteering contribution of citizens is always adding value with insights and information which, with certainty, will lead to more and new tools, applications that will be able to improve the activities related to planning, preparedness and response to hazards.

Author contribution statement:

Conceived and designed: V.Y., M.A.B., T.T.T.P.; Analyzed and interpret the data: V.Y., T.D.K.; Manuscript editing add: V.Y., M.A.B., X.Q.T.; Wrote the draft: V.Y., M.A.B.; Reviewer and edit: V.Y., M.A.B.

Acknowledgments: The work is partially funded by the Italian Ministry of Foreign Affairs and International Cooperation within the project "Geoinformatics and Earth Observation for Landslide Monitoring" - CUP D19C21000480001 (Italian side) and partially funded by the Ministry of Science and Technology of Vietnam (MOST) (Vietnamese side) by the Bilateral Scientific Research project between Vietnam and Italy, code: NĐT/IT/21/14. The authors would like to thank Edoardo Pesina for the help during the mobile application development.

Competing interest statement: The authors declare no conflict of interest.

References

1. Goodchild, M.F. Citizens as sensors: the world of volunteered geography. *GeoJournal* **2007**, *69*, 211–221. https://doi.org/10.1007/s10708-007-9111-y.
2. Glantz, M.H.; Ramírez, I.J. Improvisation in the time of disaster. *Environ.: Sci. Policy Sustainable Dev.* **2018**, *60*, 4–17. https://doi.org/10.1080/00139157.2018.1495496.
3. Haklay, M. Citizen science and volunteered geographic information: Overview and typology of participation. In: Sui D., Elwood S., Goodchild M. (eds) Crowdsourcing Geographic Knowledge: Volunteered Geographic Information (VGI) in Theory and Practice. Springer Netherlands, Dordrecht, **2013**, pp. 105–122.
4. Kocaman, S.; Gokceoglu, C. Possible contributions of citizen science for landslide hazard assessment. *Int. Arch. Photogramm Remote Sens. Spatial Inf. Sci.* **2018**, *XLII-3/W4*, 295–300. https://doi.org/10.5194/isprs-archives-XLII-3-W4-295-2018.
5. Earle, P. Earthquake Twitter. *Nat. Geosci.* **2010**, *3*, 221–222. https://doi.org/10.1038/ngeo832.
6. Shan, W.; Feng, J.; Chang, J.; Yang, F.; Li, Z. Collecting earthquake disaster area information using smart phone. Proceeding of the 2012 International Conference on System Science and Engineering (ICSSE), **2012**, pp. 310–314. https://doi.org/10.1109/ICSSE.2012.6257197.
7. Kouadio, S.; Douvinet, J. A smartphone application to help alert in case of flash floods. Proceeding of the 2015 2nd International Conference on Information and Communication Technologies for Disaster Management (ICT - DM), **2015**, pp. 252–257.
8. Marchezini, V.; Trajber, R.; Olivato D.; Muñoz, V.A.; de Oliveira Pereira, F.; Luz, A.E.O. Participatory early warning systems: Youth, citizen science and Intergenerational dialogues on disaster risk reduction in Brazil. *Int. J. Disaster Risk*

Sci. **2017**, *8*, 390–401. https://doi.org/10.1007/s13753-017-0150-9.
9. Marchezini, V.; Horita, F.E.A.; Matsuo, P.M.; Trajber, R.; Trẹo-Rangel, M.A.; Olivato, D. A review of studies on participatory early warning systems (P-EWS): Pathways to support citizen science initiatives. *Front Earth Sci*. **2018**, *6*, 184. https://doi.org/10.3389/feart.2018.00184.
10. Cieslik, K.; Shakya, P.; Uprety, M.; Dewulf, A.; Russell, C.; Clark, J.; Dhital, M.R.; Dhakal, A. Building resilience to chronic landslide hazard through citizen science. *Front Earth Sci* **2019**, *7*, 278. https://doi.org/10.3389/feart.2019.00278.
11. Norheim-Hagtun, I.; Meier, P. Crowdsourcing for crisis mapping in Haiti. *Innovations: Technol. Governance Globalization* **2010**, *5(4)*, 81–89, https://doi.org/10.1162/INOV_a_00046.
12. Humanitarian open street map team. Online available: https://www.hotosm.org/. (Accessed 15-July-2022).
13. Haklay, M.; Weber, P. Open street map: User-generated street maps. *IEEE Pervasive Comput.* **2008**, *7*, 12–18. https://doi.org/10.1109/MPRV.2008.80.
14. Stats - Open street map Wiki. Online available: https://wiki.openstreetmap.org/wiki/Stats. (Accessed 15-July-2022).
15. QGIS development team. QGIS Geographic Information System. Open source geospatial foundation Project, 2020. http://qgis.osgeo.org. Qgisorg.
16. Yordanov, V.; Biagi, L.; Truong X.Q.; Tran, V.A.; Brovelli, M.A. An overview of geoinformatics state-of-the-art techniques for landslide monitoring and mapping. *Int. Arch. Photogramm. Remote Sens. Spatial Inf. Sci.* **2021**, *XLVI-4/W2-2021*, 205–212.

VIETNAM JOURNAL OF HYDROMETEOROLOGY

Research Article

Estimation of the water regime under different climate scenarios and the importance of the thoroughness of the soil as input layer in a small watershed in Central-Hungary

Hop Quang Tran[1*,2], Zsolt Zoltán Fehér[3]

[1] Department of Geoinformatics, Physical and Environmental Geography, University of Szeged, Hungary; feher.zsolt@agr.unideb.hu
[2] Faculty of Water Resources, Hanoi University of Natural Resources and Environment, Vietnam; hoptran@geo.u-szeged.hu
[3] Faculty of Agricultural and Food Sciences and Environmental Management, University of Debrecen, Hungary; feher.zsolt@agr.unideb.hu

*Corresponding author: hoptran@geo.u-szeged.hu
Received: 12 July 2022; Accepted: 24 August 2022; Published: 25 September 2022

Abstract: The indicators of climate change in Central Europe, Hungary is showing a trend of decrease in rainfall, increase in temperature and especially extreme weather that is becoming more usual and unpredictable. The current study presents the application of the MIKE SHE model to examine the role of unsaturated soil settings and the effects of climate change on various hydrological parameters and water balance components. The input data has been provided by Lower-Tisza District Water Directorate. The one-at-a-time method utilized in this study allows for the investigation of the impact of various input parameter combinations on the estimated values of different hydrological parameters and water balance components. The findings demonstrated that the level of detailedness of the soil as an input parameter significantly influences the results of the modelled groundwater circulation and therefore the dynamics of the water regime. According to the simulation results of the temperature increase, the water table can be regarded as the primary water supply that replenishes the streams. The simulation results show that the groundwater table and evapotranspiration are the two main driving forces in the Dong-ér catchment's water regime. These findings will be used as a reference for water resource management and irrigation infrastructure planning in the context of complex climate change contexts.

Keywords: Climate change; Dong-ér catchment; Water balance; MIKE-SHE.

1. Introduction

According to the most recent report of the United Nation's Intergovernmental Panel on Climate Change (IPCC – Sixth Assessment Report), climate change is having a significant impact on the hydrological cycle and leading to an increase in extreme weather events worldwide. The period from 2011 to 2020 has shown a warming of 1.09^{o}C compared to before the first industrial revolution and the 5 years from 2016 to 2020 is the hottest period from 1850 to the present [1]. In general, the 1.5°C temperature limit *"will be exceeded in the 21st century"* under medium or higher emissions scenarios. The report also introduced the term equilibrium climate sensitivity (ECS) to allow more reliable predictions of future warming. Global warming will exacerbate droughts, increase evapotranspiration, and thus increase the frequency of extreme rains and floods.

The temperature increase in Hungary is in line with the general trend in the world, but the data from the Meteorological Service of Hungary (OMSZ) indicates, that the temperature in Hungary has increased by +1.2^{o}C over the last 4 decades, compared to the period before the first industrial revolution [2]. This is the level approach to the minimum allowed under the Paris Climate Agreement. 2019 is the hottest year on record since 1901 in Hungary [3]. Analysis of measurements from the Water Scarcity Management Observationary Network operated by the National Directorate of Water Management of Hungary (OVF) shows, that the impacts of climate change are making droughts more frequent, more intense, and longer. Rising mean temperatures are associated with rising urban temperatures [4–6], which increases energy demands in summer. The spread of various invasive pests [7–8], the significant increase in forest water use [9], and the general increase in water demand are also foreseeable.

According to the National Directorate of Water Management of Hungary (OVF), extreme weather events are becoming more common in Hungary as a result of climate change, and an increase in the frequency of high-intensity precipitation events should be expected soon, potentially increasing the magnitude of local water damages [10]. As a result, changing climatic effects have a direct impact on agriculture, causing greater damages primarily due to droughts and directly affecting agricultural sustainability as well as food security [11–12]. Water management is becoming increasingly important in mitigating the effects of extreme weather conditions. The importance of more effective and sustainable water resource management, planning, and consumption has never been greater [13-14].

According to [15], only local water balance models are reliable for making efficient and economically sustainable water use decisions in the dry season and water retention in the rainy season. Understanding the state of the water regime is becoming increasingly important. In the presence of both inland excess water and drought conditions, an integrated approach is required to evaluate the complex interrelationships of hydrological processes and changes in water balance from various perspectives, thereby providing effective solutions to the complex modelling challenges. The Tisza River Basin Management Plan provides an excellent introduction to the subject [14].

The geographical information system (GIS) can now be used thanks to recent advances in information technology. In addition, various mathematical and physical-based hydrological modelling software has made related research possible [16]. Among the various models, the MIKE SHE model stands out as a tool for implementing integrated water resource management. The model is capable of simulating the interaction of surface water and groundwater [17]. [18] published a model based on MIKE SHE where they simulated the excess water accumulation processes, and water regime, and generated excess water maps for the Dong-ér watershed. The findings indicate that the integrated MIKE SHE model is relatively calibrated and can be used to compute and analyse several other elements of climate change in the connection between hydrological parameters and water balance.

Among the benefits of the MIKE SHE model is that it offers a complete, integrated water balance calculation capability for calculating the entire regional and catchment-level water balance for any temporal and spatial scale. Areal fluxes, storage fluctuations, and water balance changes are the typical elements of the results regarding the water balance [19]. These results can further be used to integrate, map, and visualize hydrological processes between different hydrological parameters [17]. The overall water balance fluctuation estimate for the entire model catchment area is computed. Furthermore, each hydrologic component's water balance changes. The value of these characteristics is crucial because it serves as the basis for evaluating the water balance in the Dong-ér catchment. Temperature and rain are the two principal factors that impact a catchment's water balance,

either directly or indirectly. These are the two primary forces at work in the hydrologic cycle. The issue is how climate change affects the model estimates of the hydrological parameters and the results of the water balance components. research. Permutation of the input dataset has an effect on model findings, and it is required to examine the sensitivity of the model on the input dataset and enables to discover which inputs have the largest influence on the model results [20]. Setting up sensitivity analysis is required to increase accuracy and optimize the calibration process [21]. Sensitivity analysis is an effective method for identifying influential model parameters and thereby making the model structure more robust [22]. Furthermore, the sensitivity analysis is capable for parameter estimations and explains the model's responses to changes in the input dataset. The one-at-a-time method, in which sensitivity measures are derived by adjusting each parameter separately while leaving all other parameters intact, is the easiest approach to conceive among the several approaches of sensitivity analysis that have been utilized in the literature. The method's shortcoming is that it can only do local sensitivity analysis at a single location in the parameter distribution rather than the complete distribution [20]. However, using the MIKE SHE model's flexible simulation framework on both the geographical and temporal scales, this disadvantage may be overcome, providing us with a more integrated and complete perspective.

The aim of the current study is to simulate different climatic conditions and to evaluate the influence of input parameters on hydrological parameters and water balance components using sensitivity analysis. However, in order, to be able to carry out these integration analyses, the hydrological models usually require various representative and reliable hydrological and meteorological datasets [23]. In the current framework, this is particularly complicated, given the limited data availability in the Dong-ér catchment at the chosen modelling scale. However, the variable parameters and the water calculation module were developed and used by the authors to simulate and assess with an integrated approach, which climate change manifestation has a more significant impact on the results of the hydrological parameters and water balance components. This can be achieved by applying the one-at-a-time method. To achieve the goals, it is required to 1) verify the suitability to determine the advantages and disadvantages of the MIKE SHE environment in the case of the area under study; 2) to simulate the hydrological system and the complete water regime under different combinations of input variables; 3) to compare the simulation results and determine the most affected factors thus mostly sensitive to the permutations of the input dataset. These results may make it possible to predict and assess the impacts of the ongoing climate change on water balance components and different hydrological parameters.

2. Materials and methods

2.1. Study area

The 2127 km^2 Dong-ér inland excess water protection management system is located in the central-southern part of the Danube–Tisza Interfluve Sand Ridge, about 50 km from the Serbian border (Figure 1). The western part of the watershed belongs to the eastern part of the Bugaci Sand Ridge, where the slightly undulating plain and the series of ridges stretching in the northwest-southeast direction, the wind furrows, is an area covered with wet bogs and peat. The average relative relief is 3.5 m/km^2. In the sediment near the surface of the area, shifting sand shows dominance; its thickness can vary from a few meters to 50-60 m. Most of its waters flow into the Dong-ér Brook. Incidentally, the initial stages of the Dong-ér stream belong to this landscape [24]. The western, higher area consists mainly of highly permeable sandy sediments. The eastern part is mainly covered by river sediments with minimal gradient and lower hydraulic conductivity.

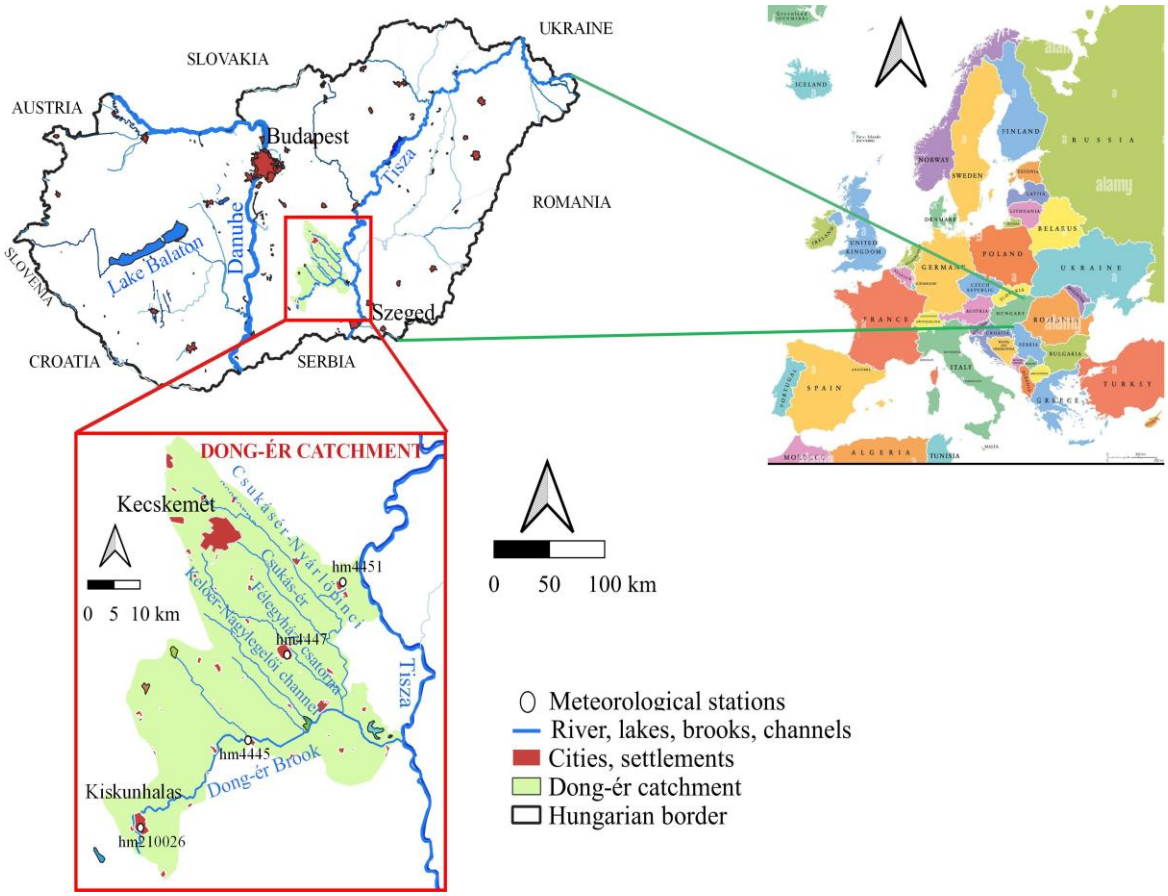

Figure 1. The Dong-ér stream watershed.

In the initial section of the Dong-ér stream, the surface water transport is minimal, the occasionally drying-up river bed is revealed only through wetland vegetation. Consequently, the area's water resources cannot be exploited; therefore, groundwater mostly plays the only source for irrigation purposes [25]. 50 years ago, the water table of the Bugaci sand ridge was available at a depth of 2-4 m, but later, significant discharge was observed [24]. The southern part of the Dong-ér catchment, more specifically the area on the right side of the Dong-ér stream, belongs to the Dorozsma-Majsai-Sand Ridge. Most of the Dong-ér catchment belongs to the Kiskunság Loess Ridge, which is an alluvial cone plain covered with loess and sand. The value of the relative relief here is 5 m/km^2. In the northwest-southeast direction between Kiskunfélegyháza and Kecskemét, a 1.5 m thick loess covers the sand dunes [24]. In the catchment area, the almost parallel canal system collects and transports the excess water to the Dong-ér stream, and then flows on into the Tisza. Only when an extreme Tisza flood wave forms does the gravitational flow end. The Dong-ér stream's flow rate during the normal period is around 2-3 m^3/s; however, in years, when inland excess water is formulated in spring, the runoff can exceed 20-30 m^3/s, and in extreme drought summer periods, the stream is often dries up completely [26]. The speed of the prevailing north-west wind is about 2-3 m/s, thus the surface forms are predominantly shaped by aeolian effects and the area's topography has fundamentally shaped the water networks. The Dong-ér stream's dominant flow direction is SW-NE, while the tributaries are flowing perpendicularly, following the characteristic natural deflationary depressions. In years, when the rainfall exceeds the average, the water table usually rises above the surface in deflationary depressions, forming temporarily flooded regions [27].

The climate projections released by the United Nation's Intergovernmental Panel on Climate Change (IPCC) forecasts, that the average temperature increase of our planet may exceed 1.5^{o}C in 2052 [28]. Two regional climate models and two climate scenarios from

the Meteorological Service of Hungary (OMSZ) indicate, that the average temperature in Hungary could increase by 3-4ºC by the end of the 21st century, hence the 2˚C threshold will be exceeded in the near future. The Dong-ér watershed is particularly exposed to temperature rise, and is one of the driest areas in Hungary, hence, the risk of drought will increase in the future [27]. The mean annual precipitation total in the catchment over the past two decades is 611 mm, meanwhile in extreme cases, it can exceed 800 mm (1999, 2010, 2014) or can represent desert conditions with the extremely minimal 203 mm (2000, 2011, 2021, 2022). Between 2000 and 2018, the lowest monthly mean temperature was -5.2ºC (February 2012 and January 2017), the highest was +24.5ºC (August 2018). Snow cover has disappeared over the past decade, although the long-term average snow cover is 20 cm thick.

Non-irrigated cropland dominates the area with about 40%, followed by pasture with 13%, and deciduous forest with 10% of the total study area. The rest are various small land uses, such as transitional forest-shrub, discontinuous urban structures, and complex cultivation patterns. The agrotopographic map indicates an extremely heterogeneous soil distribution pattern, predominantly chernozem, humid sand, blown sand, sandy, and saline soils. Each soil type found in the area typically has a high infiltration potential. Since the 1970s, there has been a decreasing trend in precipitation, which has led to a significant lowering of the water table, which today averages more than 2 meters [29]. Recently, in periods of sustained rainfall, water scarcity can be restored in the lower parts of the Sand Ridge. In the recent 20 years, the water table has occasionally risen to harmful levels and caused surface flooding [30].

2.2. Basic concepts of the water regime model in the catchment area

The unsaturated soil settings and temperature sensitivity analysis focused on the impact of changes in the modelled hydrological parameters and water balance component outcomes. Based on data from the Hungarian National Geological Institute (MÁFI), the unsaturated data were uniformly and spatially adjusted. Taking into account the results of the long-term climate forecast models IPCC [28] and OMSZ [31] for the temperature increase for 2050, the temperature data series of the reference model for 2018 (BS scenario) was increased by +0.3ºC, +0.5ºC, +0.7ºC and +1.5ºC. All other parameters were left unchanged and the differences between the three hydrological models were compared (Figure 2).

2.3. Data requirements of the current model

In the MIKE SHE model, the input data depends entirely on the purpose of the hydrological process simulation and the problem that the model is intended to solve. Obviously, there are essential input data, such as the catchment area, the topography and the water network of the investigated area. This includes data that changes little or remains unaffected over the long term, such as the watershed topography, water networks (rivers and lakes), soils and geological features. In addition, there are data that change within a relatively short period of time, like precipitation, temperature, evapotranspiration, and vegetation (leaf area index and root depth). Mitigating these factors is critical to modelling a variety of processes, including water management. Table 1 presents the basic input data requirements of the MIKE SHE modelling environment.

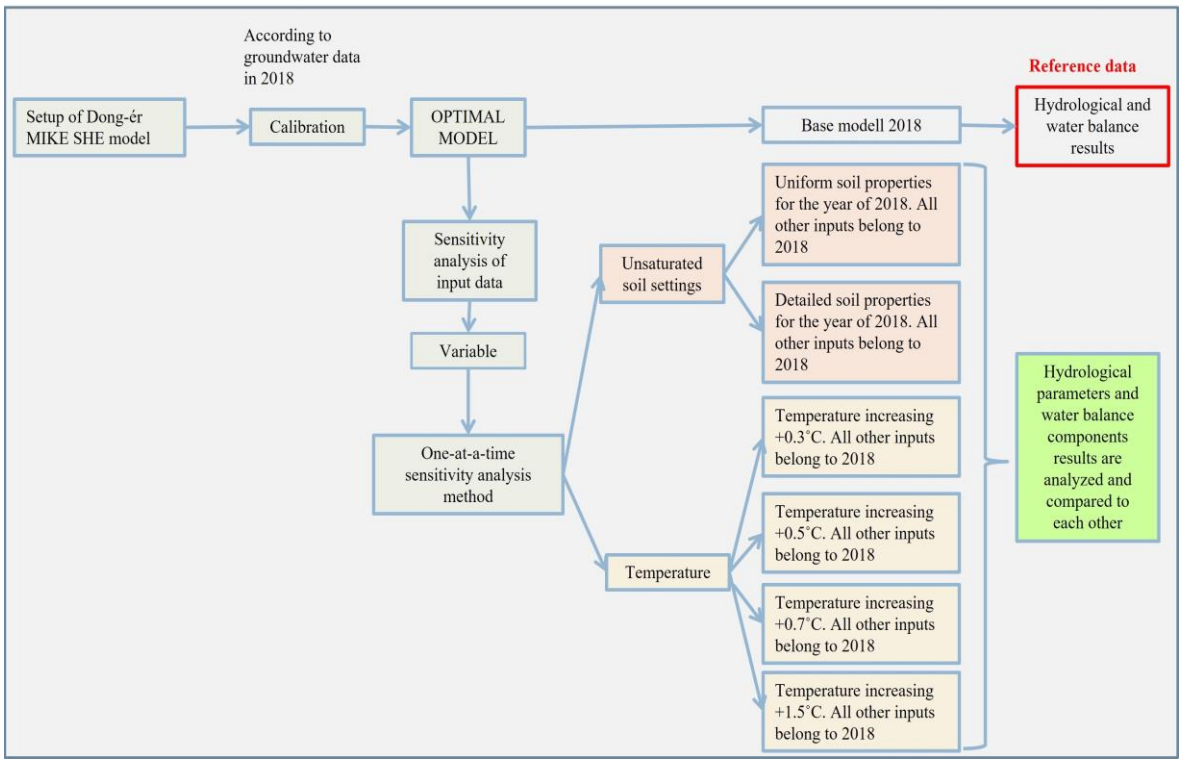

Figure 2. Schematic structure of the research workflow.

Table 1. Input features and included data sources of the MIKE SHE model.

Data	Format	Notes
Catchment area	Shape	
Water networks	Shape	
Geometry data of water networks	Shape and Excel table	It can be divided into two main classes. The first group includes streams from the previous era, that provide routings and survey cross-sections and process them into 3D point features. ATIVIZIG manages the stream attributes in a different way, where the path lines are provided as polylines, and the cross-section data is defined by longitudinal profile and various cross-section data.
Digital Elevation Modell (DEM)	Tiff	10×10m spatial resolution, spatial reference: Hungarian Datum 1972/ EOV. In order to run the MIKE SHE model, the DEM data must be converted to a spatial distribution grid point file (dfs2). The point file was created with ArcGIS Desktop and could be converted to a dfs2 file using MIKE Zero Toolbox [19]. The resulting spatial distribution grid can be imported into the model.
Precipitation	Excel table	Daily mean temperature dataset provided by the Hungarian Meteorological Office (OMSZ).
Temperatures	Excel table	Daily precipitation totals at individual gauges provided by the Hungarian Meteorological Office (OMSZ).
The potential evapotranspiration (ET_P)		Potential evapotranspiration (ET_P) can be estimated in a simplified way based on the correlation with the temperature (T). The following function describes a good relationship between the two phenomena [32]: $ET_p = ET_{ref} = e^{0.07T}$
Surface water level	Excel table	Surface water level dataset for the Dong-ér catchment provided by ATIVIZIG.

Data	Format	Notes
Subsurface water level	Excel table	The water table shows longer temporal autocorrelation as it is less influenced by the dynamics of external environmental phenomena than the unsaturated zone or the water level of the streams. The water table time series provided by ATIVIZIG consists of 33 groundwater gauges and their geospatial locations between 2010 and 2018.
Landcover	Shape	In our model, we distinguished 23 classes of land use [33], based on the CORINE dataset [34-35].
Rivers and lakes	mhydro	Hydrodynamic module built with MIKE Hydro River model
Root depth	Text	Mean root depth values estimated using CORINE classes [18].
Leaf Area Index (LAI)	Tiff	Estimation of average LAI values by CORINE category using MODIS remotely sensed images [36].
Geological layers	Shape and Excel table	The hydraulic parameters of the upper 10 m layer of the soil with the RETC software built by [37], the ratio of soil layers for each soil type according to the data of MÁFI, the data of bulk density by [38] were determined. Deeper geologic parameters were spatially estimated from 13 drill hole logs provided by ATIVZIG.
Computational layers	Shape and Excel table	The MIKE SHE model discretizes the numerical vertical calculation grid by explicitly defining the bottom level of each computational layer. The spatial distribution of the lower level is even; The value of the bottom aquifer limit is set to -75 m. To correct the relief layers, the minimum layer thickness is set at a value of 2 m. The outer boundary conditions are defined based on a fixed head type based on a spatially distributed and time-varying dfs2 file, which is extracted from the specified water table. A fixed water table is determined based on the daily groundwater level data from 2010 to 2018. The specified groundwater level is divided into 200 m × 200 m grid cells. MIKE SHE then interpolates both temporally and spatially from the dfs2 file to the local head boundary at each local time step [19].

2.4. Output features of the MIKE SHE model

The output results obtained from the simulation depend on the selected modelling workflow. According to the User guide (2017), the MIKE SHE model saves the results in three groups of files. The ASCII files store the catalogue of the simulation output files (.sheres). Every constant information of the simulation is stored in binary files (.frf). The dynamic results of the simulation are stored as, 1-d time-series (dfs0), 2-d spatial datasets (dfs2), and 3-d datasets (dfs3).

Basically, MIKE SHE considers all water inflows into the hydrological system to be positive, while all outflows or water losses are negative. As storage increases, the amount of water stored in the watershed increases. A positive change in the water balance is when the sum of the change in storage and the total outflows is less than the total inflows (Storage + Outflow Inflow).

The following tables summarize the hydrological parameters and water balance components considered in the current study Table 2 and Table 3.

Table 2. Output hydrological parameters used for the current study [19].

Hydrological parameters	Data type	Unit	Notes
Actual evapotranspiration	Evapotranspiration rate	mm/day	Evapotranspiration occurring under actual soil moisture conditions in the period under study for the given climate [39]
Actual transpiration	Evapotranspiration rate	mm/day	Evaporation of water occurs mainly through the pores of the leaves.
Actual soil evaporation	Evapotranspiration rate	mm/day	Actual soil evaporation depends on factors such as soil properties, land use, and vegetation.
Depth of overland water	Water depth	m	Represents the actual amount of water on the surface.
Overland flow in the x-direction	Discharge	m^3/sec	Runoff on a slope has a positive x-direction
Overland flow in y-direction	Discharge	m^3/sec	Downward water movement is positive
Infiltration to unsaturated zone (UZ)	Infiltration	mm/day	Water movement toward the system is positive
Unsaturated zone deficit	Deficit	mm	The deficit of the unsaturated zone represents the amount of air in the soil pores. A decreasing deficit indicates wetter soil, while an increasing deficit indicates drier soil.
Average water content in the root zone	Water content	-	
Groundwater flux in the x-direction	Discharge	m^3/sec	Positive for water flow from south to north
Groundwater flux in the y-direction	Discharge	m^3/sec	Positive for water flow from west to east
Groundwater flux in the z-direction	Discharge	m^3/sec	Positive when the water flow is directed downwards

Table 3. Output water balance components used for the current study [19].

Water balance component		Units
Precipitation		mm
Evapotranspiration	Evapotranspiration (ET) Infiltration include ET Exfiltration include ET	mm
Flows	Overland boundary inflow (OL Bou.Inflow) Overland flow to river (OL->River/MOUSE) Subsurface boundary outflow (SubSurf.Bou.Outflow) Baseflow to river Baseflow from river	mm
Storages	Canopy storage change (CanopyStor.Change) Snow storage change (SnowStor.Change) Overland storage change (OL Stor.Change) Subsurface storage change (SubSurfStor.Change) includes both unsaturated (UZ Stor.change)- and saturated zone storage changes (SZ Stor.change)	mm
Water balance changes		mm

2.5. Calibration and validation of the hydrodynamic model

The preliminary hydrodynamic model for the catchment described earlier in this study, lacks several data (e.g. channel water levels and discharge) to perform proper calibration and validation. The model built by [18] was calibrated based on the 2018 spring water table conditions. The cross-validation of these simulation results with the measured water table depths resulted in a non-negligible RMS error of 45 cm. This high value can be considered

reasonable given the lack of input parameters and the limited information content of the input datasets (e.g. topographic maps, vegetation conditions, soil properties). The results of some measuring points show a slightly larger difference and a different trend than reality. This is because many parameters are necessary for calibration to make the model more complete. The additional data sets include saturated hydraulic conductivity to calibrate unsaturated flow, specific yield and specific storage to calibrate groundwater flow. Due to data limitations, these parameters were not examined.

As it was previously described, the unsaturated zone has been completely upgraded from the original model. Figure 3 and Figure 4 compares the simulation results with the actual groundwater data measured at each monitoring gauge.

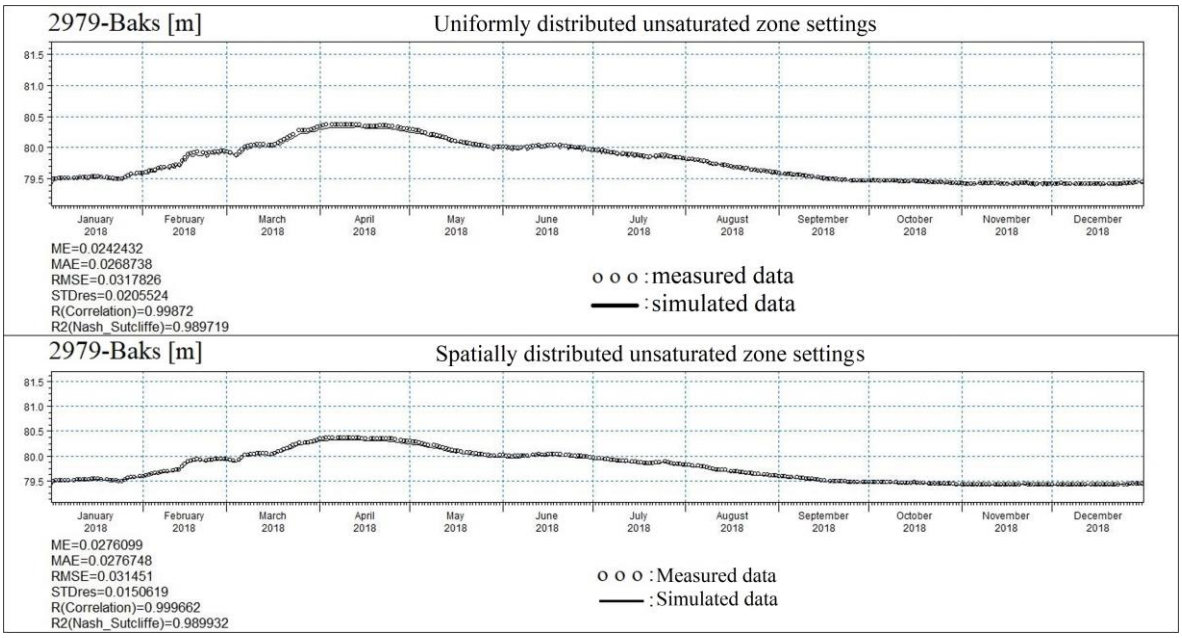

Figure 3. Example of calibration results for the Dong-ér basin for 2018 for groundwater well No. 2979 in Baks village.

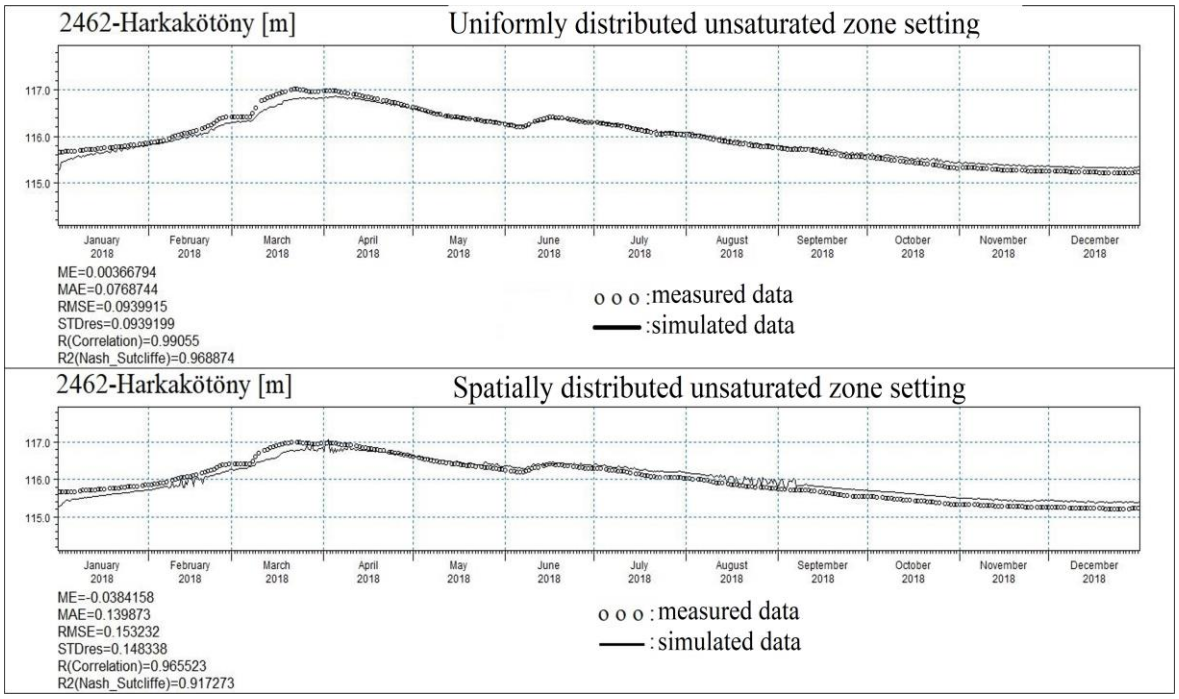

Figure 4. Example of calibration results for the Dong-ér basin for 2018 for groundwater well No. 2462 in Harkakötöny village.

The results show that the spatially more detailed structure of the input data for the unsaturated zone gives similar results for groundwater. In both results, the simulated data "fit" the measured data and the observed trends also represent reality. However, the simulation results for the processes in the unsaturated zone and those occurring in the spatially distributed model are certainly different from the results of the uniformly distributed model. The disadvantage of defining the unsaturated zone with a more detailed spatial distribution is that the simulation shows a large difference in time. The uniform distribution model version takes about 20 hours to run, while the model I developed took more than 72 hours of calculation time. There is also a significant difference in the amount of disk space required, with the results of the simulation of the model built with the uniformly distributed unsaturated zone taking up about 330 GB, while the one with the more detailed spatial distribution took up 497 GB of disk space.

3. Results

3.1. 2018 base model

The year 2018 was chosen as the baseline year for the simulation of the integrated hydrological process and the hydrological regime of the Dong-ér basin, for the following reasons:

1) The preliminary model by [18] is based on water table depth measurements from 2018; 2) the 2018 baseline model with spatially distributed unsaturated zone was calibrated and validated by consideration of surface water level, water yield and groundwater data; 3) 2018 Corine surface cover data was applied; 4) Data for 2018 vegetation characteristics (leaf area index, root depth) were determined by [18]; 5) Overall, the year 2018 had an average amount of precipitation (573 mm) compared to the extreme years 2000 and 2014. Thus, the baseline simulation for the year 2018 is suitable for carrying out sensitivity analyses and the simulated results can be used as references for comparison with the simulation results of other scenarios. Figures 5 and 6 compare the models using either the uniform or the spatially distributed unsaturated zone in terms of hydrological parameters (for the whole of 2018 and the whole catchment) and hydrographic components.

Figure 5 shows that there are significant differences between the results of the simulation with uniform and more detailed spatially distributed soil properties in the following parameters: actual evapotranspiration, actual evapotranspiration, and actual soil evaporation. Thus, for soil types built with horizontal distribution, the values of evapotranspiration processes are smaller than for soils with uniform distribution. Because of the detailed horizontal and vertical distribution of the surface soil types, a decrease in infiltration and consequently an increase in the deficit of the unsaturated zone can be observed in the case of spatially distributed soil properties in the simulation. The average water content in the root zone is slightly higher for the uniformly distributed soil properties due to higher infiltration than for the spatially distributed case. For the unsaturated zone water content parameter, the values are equal in both cases, but no specific conclusion can be drawn, since several parameters have an influence on the water content in the unsaturated zone, such as infiltration, groundwater elevation, and evaporation. The surface runoff and groundwater flow in the x- and y-directions parameters are so small that the numbers are equal to zero due to rounding. In addition, difference in the z-direction groundwater flow can also be observed, yet the simulation result of the model built with spatially distributed soil properties shows that the groundwater rises 70 mm higher than in the case of the uniformly distributed model.

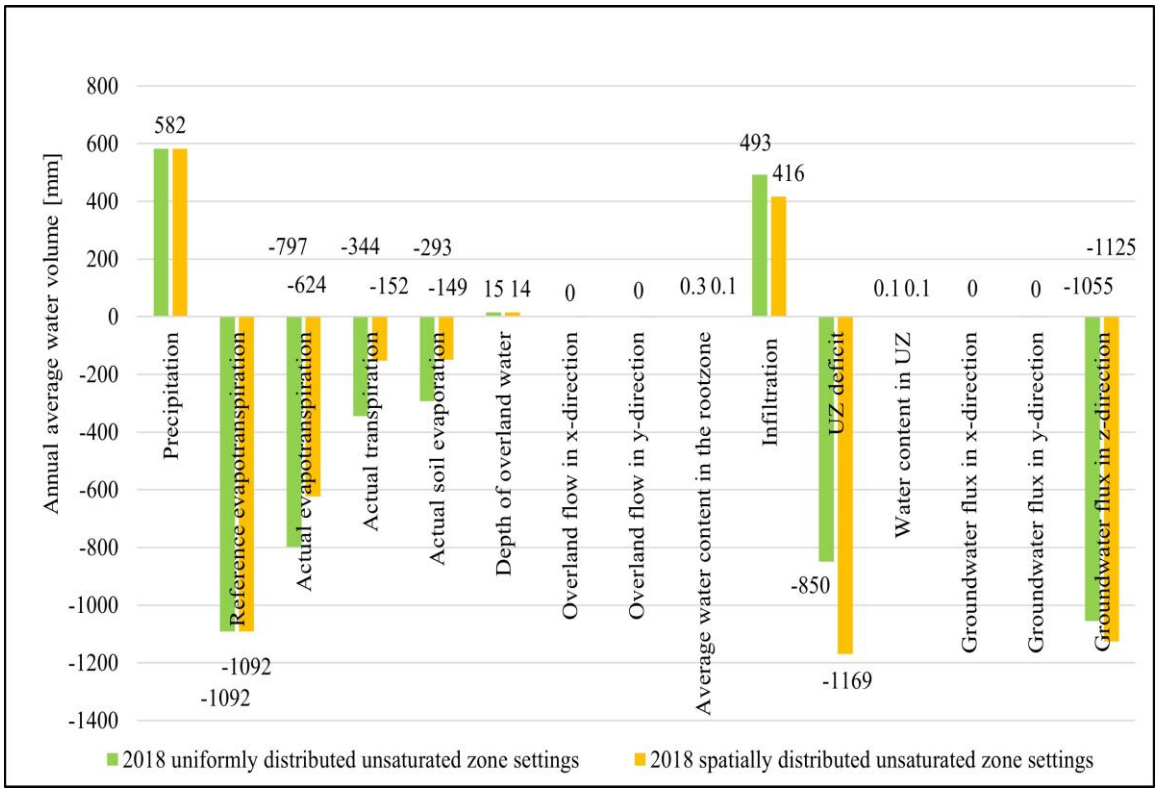

Figure 5. Hydrological results of the simulation of the Dong-er catchment with uniform and detailed soil properties for the year of 2018.

The water balance comparison (Figure 6.), suggests a significant difference in the groundwater (unsaturated and saturated zone). For the uniformly defined soil properties, the simulation estimated a 129 mm lower groundwater table compared to the model run with detailed soil properties. Multiplying this difference by the catchment area (2,127 km^2), there is a difference of more than 270 million m^3 of water between the two model estimates. This is a substantial amount of water that greatly affects the accuracy of the water balance calculation. The result suggests that the soil composition of the study area plays an important role in the estimation of groundwater resources and thus the water balance. For the simulation with detailed soil properties, the values of surface runoff, subsurface runoff and near-surface runoff are larger than those of the steady-state version. The vertical distribution of the soil results in more groundwater inflow from the outer catchment (1269 mm) than the uniformly defined soil profile (1132 mm). Overall, the difference in water balance between the two settings is 277 mm, corresponding to about 580 million m^3 of water. This can be considered a large difference, so We consider it necessary to adjust the unsaturated zone soil as detailed as possible.

Based on the above results, the Dong-ér small catchment was modelled with the unsaturated zone based on the more detailed spatially distributed soil properties. The hydrological parameters were investigated using the annual average runoff of the entire catchment and the water volume accumulated over the entire catchment and the study year for the hydrometeorological components.

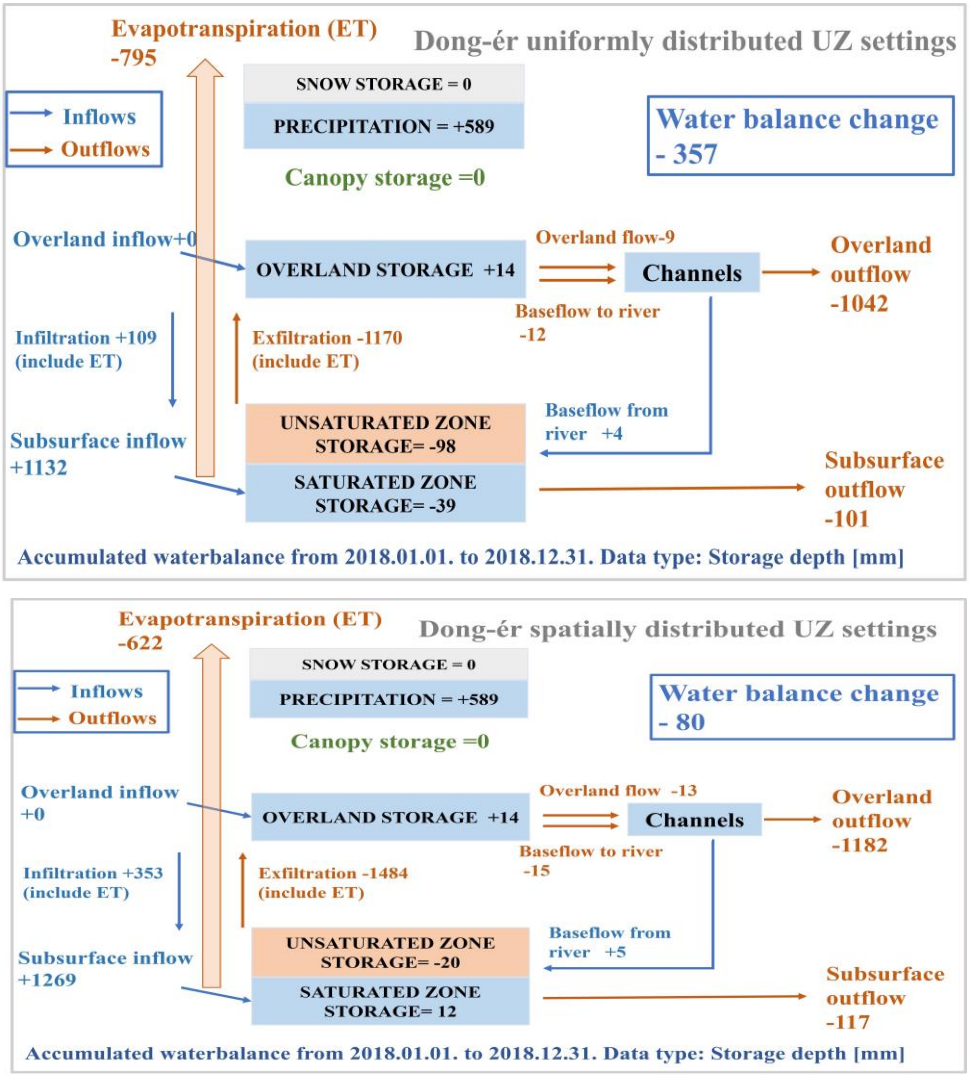

Figure 6. Hydrography results for Dong-er catchment with uniform and detailed soil properties simulation for the year of 2018.

3.2. Scenario-based simulation of the effects of temperature rise on the hydrological system

Several important climatic elements will change in the future, due to the increase in temperature, and these changes will have a major impact on the hydrological regime of the area. Therefore, sensitivity analyses were performed to determine the influence of temperature changes on hydrological parameters and water balance components. In addition to temperature data for 2018, the consequences of the daily temperature increases of +0.3°C, +0.5°C, +0.7°C and +1.5°C were analyzed, according to the IPCC [28] and OMSZ [31] climate forecast models. This was followed by a comparative evaluation of the results of the five scenarios (Figure 7). All other parameters, except temperature, were left unchanged in the model scenarios for 2018.

The model results show that the evapotranspiration (ET) parameters (reference ET, actual ET, actual transpiration, actual soil evaporation) increase gradually with the temperature. The surface runoff along the x- and y-coordinate axes is so small in each scenario that the values are rounded to zero. In the root zone, the water content decreases with temperature increase, here again rounding the values to equal 0.1 mm. This shows that the effect of a temperature rise of +0.3°C is reduced by 0.2 mm. The results of the four temperature rise scenarios hardly differ from each other. With respect to infiltration, it is obvious and natural that infiltration decreases with temperature rise, and even more so with a temperature rise of +0.3°C, infiltration decreases substantially and decreases gradually for

temperature rises of +0.5°C, +0.7°C and +1.5°C. This phenomenon is also observed in the unsaturated zone deficit. No change is observed in the x- and y-directions for groundwater movements. In the z-direction (upward), groundwater movements differ by only 1-8 mm (Figure 7). The results of the simulation suggest that the most sensitive to temperature increases among the hydrological parameters are surface processes (evaporation, transpiration, surface water depth, infiltration, and the deficit of the unsaturated zone). Due to the nature of the Carpathian Basin and the direction of deep groundwater movement, it is not sensitive to temperature increases.

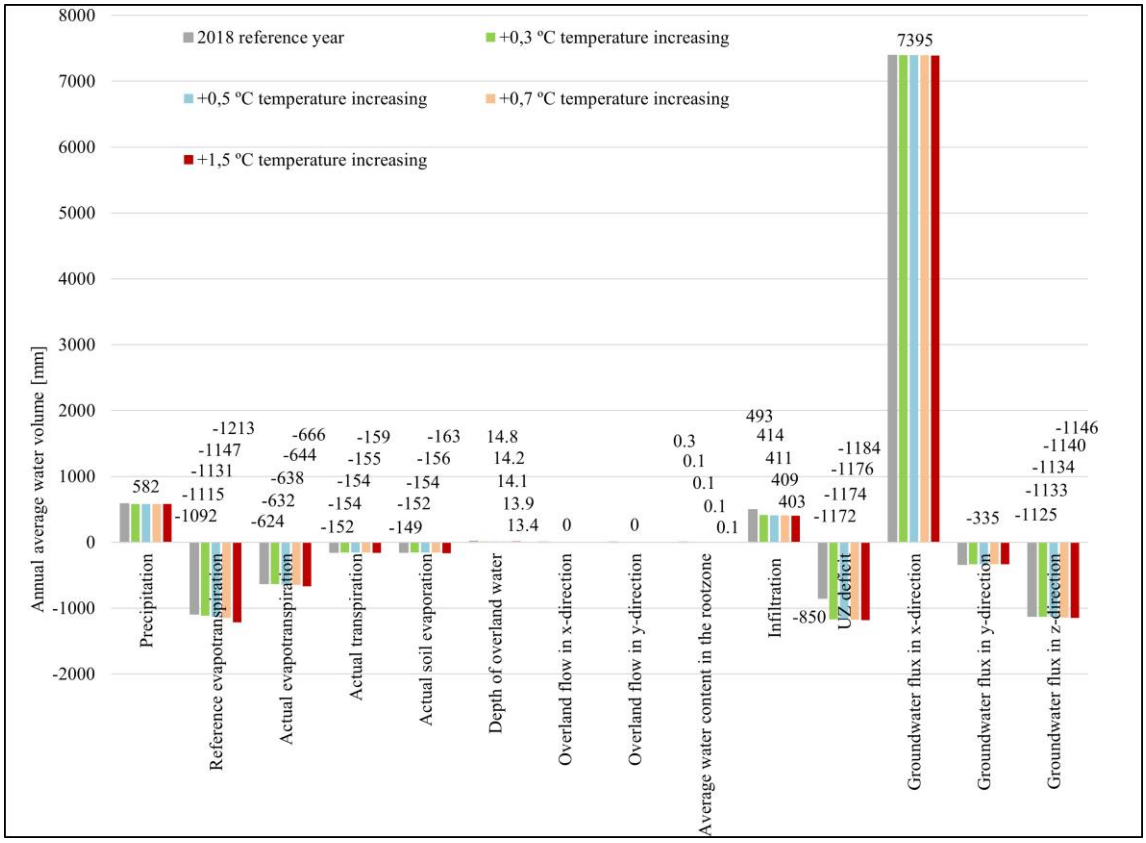

Figure 7. Effect of temperature increases of +0.3°C, +0.5°C, +0.7°C and +1.5°C on the simulated hydrological parameters.

The exploration of relationships between water balance components and temperature changes was investigated using water balance calculation. The results of the simulations indicate that evapotranspiration increases significantly (5 mm to 22 mm) with increasing temperature, thus substantially reducing the amount of infiltration into the open surface receiving basins in the form of springs. Intensive evaporation of water surfaces and evaporation from plants, and a reduction in near-surface flows feeding the channel, while the near-surface outflow component from the channel remains unchanged (5 mm), reduces the water content of the channel. The results in Table 4. show that the values of groundwater inflow, surface runoff and evapotranspiration are larger in relation to the amount of precipitation falling and the other indicators. Consequently, these components are of great importance in the water balance, as the study of precipitation events has shown. The groundwater inflow components show the highest significance. It can therefore be concluded that the water balance of the study catchment is highly dependent on groundwater inflow from the external catchment. The groundwater (unsaturated and saturated zone) shows a decreasing trend with increasing temperature. This result is also confirmed by the fact that the water scarcity problem in the Danube-Tisza basin shows an increasing trend [29].

Table 4. Changes in water balance components due to temperature increase of +0.3°C, +0.5°C, +0.7°C and +1.5°C compared to the reference year.

Parameters [mm]	**2018**	**(+) 0.3˚C**	**(+) 0.5˚C**	**(+) 0.7˚C**	**(+) 1.5˚C**	**%**	**%**	**%**	**%**
Precipitation	589	589	589	589	589	0%	0%	0%	0%
Evapotranspiration (ET)	-622	-631	-637	-642	-664	1%	2%	3%	7%
Overland boundary inflow	0	0	0	0	0	0%	0%	0%	0%
Overland boundary outflow	-1195	-1192	-1185	-1182	-1172	0%	-1%	-1%	-2%
Canopy storage change	0	0	0	0	0	0%	0%	0%	0%
Snow storage change	0	0	0	0	0	0%	0%	0%	0%
Overland flow to river	-13	-12	-12	-12	-11	-8%	-8%	-8%	-15%
Overland storage change	14	14	14	13	13	0%	0%	-7%	-7%
Unsaturated storage change	-20	-22	-25	-24	-29	-10%	-25%	-20%	-45%
Saturated storage change	12	9	8	3	-5	-25%	-33%	-75%	-142%
Baseflow to river	-15	-15	-15	-14	-14	0%	0%	-7%	-7%
Baseflow from river	5	5	5	5	5	0%	0%	0%	0%
Subsurface boundary inflow	1269	1273	1273	1273	1269	0%	0%	0%	0%
Subsurface boundary outflow	-117	-116	-115	-115	-113	-1%	-2%	-2%	-3%
Infiltration includes evapotranspiration	353	348	343	336	316	-1%	-3%	-5%	-10%
Exfiltration includes evapotranspiration	-1484	-1485	-1482	-1481	-1469	0%	0%	0%	-1%
Water balance change	-93	-98	-100	-106	-132	-5%	-8%	-14%	-42%

The surface inflow component from the outer catchment is zero under both temperature conditions, and consequently, the surface watersheds are correctly determined. The canopy water and snowpack for each temperature increment have values less than 0.03 mm, thus they are equivalent to zero when rounded. Groundwater discharge components vary slightly (1%-3%). This suggests that, on the one hand, groundwater feeds deep riverbeds and cavities and, on the other hand, groundwater is subject to additional downward seepage. It is important for the water balance of the area that the groundwater influence from external catchments is stable. The results show groundwater inflows fluctuating between 1,269 mm and 1,273 mm, which can be considered stable. However, this amount is not able to compensate for the water losses (Table 4).

Simulated water balances for the whole of 2018 show a value of around -93 mm, which means, that practically 200 million m^3 of water leaving the water system. The temperature increases of +0.3°C, +0.5°C, +0.7°C and +1.5°C can result in 5% (5 mm), 8% (7 mm), 14% (13 mm) and 42% (39 mm) less water in the Dong-ér catchment, i.e. nearly 11 million m^3, 15 million m^3, 28 million m^3 and 83 million m^3 less water than the 2018 baseline, respectively. In other words, increased temperatures result in increased water loss through evapotranspiration, leading to a significant reduction in the water availability of the catchment. Consequently, groundwater resources (unsaturated zone and saturated zone water resources), hydrological regime, infiltration, and surface runoff to the channel components are more sensitive to changes in evapotranspiration (varying from 1% to 7%), making these components more sensitive to temperature increases due to climate change.

4. Conclusions

The unsaturated zone deficit, infiltration into the unsaturated zone, evapotranspiration and overland flow parameters appear to have a significant impact on the diurnal hydrological circulation and appear to be very sensitive to changing climatic conditions.

Based on the relationship between the manifestations of climate change and the components of the hydrological regime, the subsurface boundary inflow and evapotranspiration are likely to be the two main driving forces that form and regulate the

hydrological regime of the Dong-ér catchment. According to the models, the water balance in the Dong-ér catchment is largely determined by the subsurface marginal inflow, as it continuously supplies about ~90% of the surface water. The subsurface marginal inflow shows no close relationship to temperature changes or extreme precipitation events. Therefore, this parameter is unlikely to be affected by the manifestations of climate change. Evapotranspiration, on the other hand, is strongly dependent on temperature. Due to the warming trend, the water retention of the Dong-ér Stream showed a decreasing trend, especially in areas where the water table is lower than the bottom of the stream. The components that play important roles in the water regime of the Dong-ér catchment are, in descending order: marginal surface inflow, marginal surface runoff, evapotranspiration, and precipitation. The components most sensitive to climate change include changes in subsurface storage, infiltration including evapotranspiration, overland flow to the stream, changes in overland storage, and evapotranspiration components.

In the model structure, the soil composition plays an important role in estimating both the groundwater balance and the water balance. When simulating with detailed soil properties, the results for surface runoff, subsurface runoff, near-surface runoff and near-surface flows exceed the values of the steady-state version. Therefore, it is strongly recommended to define the soil properties in the unsaturated zone in as much detail as possible.

Based on the modelled water balance changes, the temperature increases of +0.3°C, +0.5°C, +0.7°C and +1.5°C cause a larger volume of water loss than our measurements indicated during the drought year of 2018 in the Dong-ér catchment area. Ultimately, this leads to the water regime of the catchment area getting into a state of water scarcity. In the context of climate change, the rising temperature has a major impact on evapotranspiration, thereby greatly affecting the water balance of the Dong-r catchment. The limitation of the one-at-time method is that it does not take into account temperature-dependent parameters such as potential evapotranspiration, LAI [36], vegetation change. This causes certain errors in the output, but these errors are insignificant compared to the fluctuations in the system's water resources.

The results of the study have also demonstrated the effectiveness of the MIKE SHE model and its water balance calculation module as useful tools for the analysis and assessment of the impacts of climate change. In addition, the need for a large amount of high-quality data, the difficulty of monitoring environmental parameters, as well as changing environmental conditions and the uncertainty of their predictability for the future are the main challenges and therefore need to be improved by which values of the calculated parameters cannot be absolutely accurate but can provide a good approximation and highlight the ongoing trends more effectively.

Author contribution statement: Set up the input data of model; Analyzed and interpreted the data; Materials, analysis tools or data; Simulated the model; Analyzed and interpreted the results; Wrote the draft manuscript: H.Q.T.; Collected the data; analyzed and interpreted the data; Analyzed and interpreted the results; Materials, manuscript editing: Z.Z.F.

Acknowledgement: We are greatly thankful to Professor Emeritus János Rakonczai for his constant support, help and willingness to share his experiences and encourage the writing of the present work. We would like to acknowledge Dr. Péter Kozák and his colleagues at the Lower-Tisza District Water Directorate for their professional advice and support. The study was conducted in association with the DHI Group which provided us with the student license for the MIKE SHE software. The work was funded by the National Research, Development and Innovation Office of Hungary, "Water-related researches at the University of Debrecen" under grant agreement No. TKP2021-NKTA-32.

Competing interest statement: The authors declare no conflict of interest.

References

1. IPCC. Climate Change 2021: The Physical Science Basis. Contribution of Working Group I to the Sixth Assessment Report of the Intergovernmental Panel on Climate Change Cambridge University Press, 2021. Online available at: https://www.ipcc.ch/report/ar6/wg1/downloads/report/IPCC_AR6_WGI_Full_Report.pdf.
2. Rakonczai, J.; Ladányi, Zs.; Blanka, V.; Fehér, Z.S.; Kovács, F. A Globális környezeti válzozások fontosabb magyarországi hatásai. -In: RAKONCZAI, J. (ed.): Elfogyasztott jövőnk? Globális környezeti és geopolitikai kihívásaink, Budapesti Corvinus Egyetem, Budapest, 2021, pp. 275.
3. OMSZ. 2019 is the warmest year since 1901 in Hungary (in Hungarian), 2020. Online available at: https://www.met.hu/omsz/OMSZ_hirek/index.php?id=2729.
4. Unger, J., Gál, T.; Rakonczai, Mucsi, Szatmári, J.; Tobak, Z.; van Leeuwen, B.; Fiala, K. Modeling of the urban heat island pattern based on the relationship between surface and air temperatures. *Q. J. Hung. Meteorogical Serv.* **2010**, *4(114)*, 287–302.
5. Gál, T.; Skrabit, N.; Molnár, G.; Unger, J. Projections of the urban and intra-urban scale thermal effects of climate change int he 21st century for cities in Carpathian Basin. *Hung. Geog. Bull.* **2021**, *70(1)*, 19–33. https://ojs.mtak.hu/index.php/hungeobull/article/view/4920/4466.
6. Fricke, C.; Pongrácz, R.; Unger, J. Comparision of daily and monthly infra-urban thermal reactions based on LCZ classification using surface and air temperature data. *Geog. Pannonica* **2022**, *26(1)*, 1–11.
7. Szép, T. A klímaváltozás erdészeti ökonómiai vonatkozásai. Economic aspects of forestry in climate change. PhD doctoral dissertation, 2010. http://ilex.efe.hu/PhD/emk/szeptibor/disszertacio.pdf .
8. Janik, G.; Hirka, A.; Koltay, A.; Juhász, J.; Csóka, Gy. 50 év biotikus kárai a magyar bükkösökben (50 years biotic damages in the Hungarian beech forests). Erdészeti Tudományos Közlemények [*Forestry Scientific Publications*]. **2016**, *(6)1*, 45–60.
9. Tölgyesi, Cs.; Török, P.; Hábenczyus, A.A.; Bátori, Z.; Valkó, O.; Deák, B.; Tóthmérész, B.; Erdős, L.; Kelemen, A. Underground deserts below fertility islands? Woody species desiccate lower soil layers in sandy drylands. *Ecography* **2020**, *43(6)*, 848–859. https://onlinelibrary.wiley.com/doi/10.1111/ecog.04906.
10. OVF. Effects of climate change, hydrometeorological extremes (in Hungarian), 2016. Online available at: http://www.ovf.hu/hu/korabbi-hirek-2/a-klimavaltozas-hatasai-hidrometeorologiai-szelsosegek.
11. Singh, A. Conjunctive use of water resources for sustainable irrigated agriculture. *J. Hydrol.* **2014**, *519*, 1688–1697.
12. Ladányi, Zs. Climate change impact in a sample area of Danube-Tisza Interfluve. In: Kiss, T. (Ed.): Natural geographical processes and forms. Natural Geography Studies of the 9th National Conference of Geographical Doctoral Students, 2010, 93–98. (in Hungarian). Online available at: http://acta.bibl.u-szeged.hu/68110/1/2009_termeszetfoldrajzi_folyamatok_es_formak.pdf.
13. EU Water Framework Directive. 2004, 1–4. Doi:10.2779/50903.
14. OVF. Tisza River Basin Management Plan by General Directorate of Water Management, 2015. (in Hungarian).
15. Sipos, Gy.; Právecz T. Identification of water retention areas on the Dong-ér catchment using GIS. In: Blanka, V., Ladányi, Zs. (Ed.) Drought and Water Management in South Hungary and Vojvodina. University of Szeged, 2014, 157–167.

16. Tran, Q.H.; Fehér, Z.Zs. Water balance calculation capability of hydrological models. *Acta Agraria Kaposváriensis* **2022**, *26(1)*, 37–53. Doi:10.31914/aak.2877.
17. Graham, D.N.; Butts, M. Flexible, integrated watershed modelling with MIKE SHE. In: Singh, V.P.; Frevert, D.K. (Ed). In Watershed Models. CRC Press. **2005**, 245–272. Doi:10.1201/9781420037432.ch10.
18. Nagy, Zs.; Pálfi, G.; Priváczkiné Hajdú, Zs.; Benyhe, B. Operation of canal systems and multi-purpose water management – Dong-ér catchment (in Hungarian) In: Ladányi, Zs., Blanka, V. (Ed.) Monitoring, risks and management of drought and inland excess water in South Hungary and Vojvodina. University of Szeged. 2019, 83–96.
19. DHI. MIKE SHE Volume 1: User guide. 2017. Online available at: https://manuals.mikepoweredbydhi.help/2017/Water_Resources/MIKE_SHE_Printed_V1.pdf.
20. Hamby, D.M. A review of techniques for parameter sensitivity analysis of environmental models. *Environ. Monit. Assess.* **1994**, *32*, 135–154. Doi: https://doi.org/10.1007/BF00547132.
21. Ibarra, S.; Romero, R.; Poulin, A.; Glaus, M.; Cervantes, E.; Bravo, J.; Pérez, R.; Castillo, E. Sensitivity analysis in hydrological modelling for the Gulf of México. *Procedia Eng.* **2016**, *154*, 1152–1162. Doi: 10.1016/j.proeng.2016.07.531.
22. Bahremnad, A.; de Smedt, F. Distributed Hydrological Modeling and Sensitivity Analysis in Torysa Watershed, Slovakia. *Water Resour. Manage.* **2007**, *22*, 393–408. Doi: 10.1007/s11269-007-9168-x.
23. van Leeuwen, B.; Právetz, T.; Liptay Z.Á.; Tobak, Z. Physically based hydrological modelling of inland excess water. *Carpathian J. Earth Environ. Sci.* **2016**, *11(2)*, 497–510. http://publicatio.bibl.u-szeged.hu/17155/.
24. Dövényi, Z. (Ed). Magyarország kistájainak katasztere. [Cadastre of the small area of Hungary] MTA Földrajztudományi Kutatóintézet. Budapest. 2010. ISBN 978-963-9545-29-8.
25. Kozák, P. Changes in surface runoff on the south-eastern slope of the Danube-Tisza Interfluve Sand Ridge in the context of climate change. In: Farsang, A., Ladányi, Zs., Mucsi, L. (Ed.) Climate change challenges – From global to local. *GeoLitera* **2020**, 109–115. (In Hungarian).
26. Mérnöki, K.K.; Iroda, K.F.T. Harmonized activities related to extreme water management events – especially flood, inland inundation and drought (in Hungarian). 2013. HUSRB/1203/121/145/01, Ref. No.: T-51/2013.
27. Právetz, T.; Sipos, G.; Benyhe, B.; Blanka, V. (). Modelling runoff on a small lowland catchment, Hungarian Great Plains. *J. Environ. Geogr.* **2015**, *8(1–2)*, 49–58. Doi: 10.1515/jengeo-2015-0006.
28. IPCC. Global Warming of 1.5˚C. Thematic Reports. 2018. https://www.ipcc.ch/sr15/.
29. Fehér, Z.Z.S. Large scale geostatistical modelling of the shallow groundwater time series on the Southern Great Hungarian Plain. Two approaches for spatiotemporal stochastic simulation of a non-complete monitoring dataset. PhD Thesis. University of Szeged. 2019. Doi: https://doi.org/10.14232/phd.10122.
30. Szatmári, J.; van Leeuwen, B. (Ed.). Inland Excess Water – Belvíz – Suvišne Unutrašnje Vode, Szeged, University of Szeged. Novi Sad, University of Novi Sad. 2013. Doi: 10.13140/2.1.5143.3920.
31. OMSZ. To the margin of the IPCC Thematic Report assessing a 1.5 degree global temperature rise. 2018. (In Hungarian). https://www.met.hu/ismerettar/erdekessegek_tanulmanyok/index.php?id=2334&hir=Az_IPCC_1,5_fokos_globalis_homerseklet-

emelkedest_ertekelo_Tematikus_Jelentesenek_margojara.
32. Fiala, K.; Barta, K.; Benyhe, B.; Fehérváry, I.; Lábdy, J.; Sipos, Gy.; Győrffy, L. Operational drought and water scarcity monitoring system (In Hungarian). *Hungarian J. Hydrol.* **2018**, *98*, 14–24. http://publicatio.bibl.u-szeged.hu/17598/1/Fiala_et_al2018HidrologiaiKozlony.pdf.
33. EEA. Corine Land Cover 2018. European Environmental Agency. 2018. https://www.eea.europa.eu/data-and-maps/data/external/corine-land-cover-2018.
34. Aune-Lundberg, L.; Geir-Harald, S. The content and accuracy of the CORINE Land Cover dataset for Norway. *Int. J. Appl. Earth Obs. Geoinf.* **2020**, *96(102266)*, 1–10. Doi: 10.1016/j.jag.2020.102266.
35. Feranec, J.; Soukup, T.; Hazeu, G.; Jaffrain, G. (Ed.). European landscape dynamics. Corine land cover data, CRC-Press. *Boca Raton.* **2016**, 9–14. https://doi.org/10.1201/9781315372860.
36. Myneni, R.; Knyazikhin, Y.; Park, T. MCD15A2H MODIS/Terra+Aqua Leaf Area Index/FPAR 8-day L4 Global 500m SIN Grid V006. NASA EOSDIS Land Processes DAAC. 2015. https://doi.org/10.5067/MODIS/MCD15A2H.006.
37. van Genuchten, M.Th.; Leij, J.F.; Yates, R.S. The RETC Code for Quantifying the Hydraulic Functions of Unsaturated Soils. U.S. Salinity Laboratory U.S. Department of Agriculture, Agricultural Research Service Riverside, California. 1991, EPA/600/2-91/065.
38. Pásztor, L.; Laborczi, A.; Takács, K.; Illés, G.; Szabó, J.; Szatmári, G. Progress in the elaboration of GSM conform DSM products and their functional utilization in Hungary. *Geoderma Reg.* **2020**, *21*, e00269. https://doi.org/10.1016/j.geodrs.2020.e00269.
39. Fetter, C.W. Applied Hydrogeology. 3rd Edition, Macmillan College Publishing Company, New York, 1994.

VIETNAM JOURNAL OF HYDROMETEOROLOGY

Research Article

Occurrence and ecological risk assessment of antibiotics in water of Saigon River

Nguyen Phu Bao[1,2*], Pham Hong Nhat[2], Dinh Quoc Tuc[1], Nguyen Thi Minh Hien[3]

[1] Ho Chi Minh City University of Technology; nguyenphubaohien@yahoo.com
[2] Viet Nam Institute fot Tropical Technology and Environmental Protection; phamhongnhat@hotmail.com
[3] Leeds Beckett University; minhhien.25052001@gmail.com

*Corresponding author: nguyenphubaohien@yahoo.com; Tel.: +84–908226432

Received: 5 August 2022; Accepted: 12 September 2022; Published: 25 September 2022

Abstract: The residual antibiotics in the environment have lately caused widespread concerns. However, little information is available on antibiotic pollution and its ecological risk to water resources of Saigon river. Therefore, an investigation of the occurrence and ecological risk of antibiotics in the Saigon river was necessary. Determination of antibiotics was analysed by liquid chromatography tandem mass (LC/MS/MS) and ecological risk assessment of antibiotics was used risk quotient (RQ) methods. Results revealed that the antibiotics concentrations total in water ranged from not determined (ND) to 697.3 ng/L in rainy season and to 869.3 ng/L in the dry season respectively. The ecological risk assessment via the risk quotient (RQ) of Quinolone class (Ciprofloxacin, Enrofloxacin, Norfloxacin and Ofloxacin) in areas affected by livestock, urban living and aquaculture activities were recorded to be higher than 1, indicating that Quinolone class has remained at high risk in the Saigon River. The RQ of Ciprofloxacin in the source area, in particular, has reflected a medium–risk level compared to other antibiotics in the Saigon River's low–risk category. The research findings have revealed the significance and necessity of protecting the Saigon River water from contamination by antibiotics for domestic water supplies and aquaculture.

Keyword: Antibiotics; Ecological Risk Assessment; Aquatic Environment; Saigon River.

1. Introduction

Antibiotics are one of the newest pollutants and are currently being researched for their prevalence and environmental impacts in recent years [1]. In the global study, it has indicated that the presence of antibiotics in surface water has a significant impact on water ecosystems such as antibiotic resistance [2], the inhibition of the pollutant–degrading activity of bacteria [3]. According to a globally representative study by the Water Research Foundation (WRF) [4], there are more than 30 different types of antibiotics present in surface water. Several has a high frequency of occurrence, such as Clindamycin (100%, 3 samples), Monensin (65%, 260 samples), Lincomycin (36%, 600 samples), Erythromycin (21%, 348 samples). Many antibiotics showed up more than 10% of the time (in hundreds of samples), including sulfamethoxazole (18%), trimethoprim (17%, 1087 samples), and sulfamethazine (16%, 715 samples). Antibiotic residues were additionally detected in surface water and wastewater with concentrations approximately 10–1000 ng/L [5]. The quinolones, chloramphenicols, sulfonamides and macrolides appear to be the primary antibiotics recognized in drinking water with the highest concentrations and frequencies of

detection, in which ciprofloxacin has identified values up to 679.7 ng/L [6]. In Guangzhou (China), the concentration of antibiotic residues in tap water is approximately 7.9–679.7 ng/L, which is greater than the level of antibiotics in tap water in 42 other Chinese cities. Synthesis of related studies [7] has revealed that Chinese tap water may contain more antibiotics than other countries' tap water does in terms of antibiotic residues. To assess the level of impact of antibiotics in water or sediment, an ecological risk assessment method is widely used and is expressed as a risk quotient (RQ) [8]. Based on this methodology, a number of studies on risk assessment for Qingshitan Reservoir [9] and the Subtropical River–Reservoir System [10] have been conducted.

The Saigon River takes the responsibility of supplying water to irrigate 58,350 hectares of agricultural land in the basin and providing water for all production and daily activities of Ho Chi Minh area [11]. Many livestock and aquaculture farms use antibiotics and wastewater from hospitals and pharmaceutical firms at the Saigon River's headwaters; domestic wastewater also contains many types of antibiotics that are discharged into water sources. Antibiotics account for 70% in livestock and aquaculture with 13 antibiotics [12] which are utilised in Ho Chi Minh City's hospitals [13]. A number of studies in the Saigon River basin have revealed high concentrations of antibiotic residues FQs, TCs and endocrine disruptors PEs with the occurrence frequency of fluoroquinolones (FQs) in water about 33%, in sludge about 62%; tetracyclines (TCs) in water about 33%, in mud about 57%; phthalate esters (PEs) in water about 25% and in sludge about 100% [14].

Nowadays, research on antibiotic residues and their ecological risks has not been performed. Therefore, the objectives of this study were: (1) to investigate the occurrence of antibiotics and (2) to assess the ecological risks of antibiotics to the water quality of the Saigon River. The research results may examine the status of antibiotic contamination in the river water and its ecological risk level and provide a scientific basis for antibiotic management in the Saigon river basin.

2. Materials and methods

2.1. Sample sites and collection

Based on the environmental and hydrological characteristics of the Saigon river and its main entry tributaries, 12 sampling sites (M1–M12) were deployed in this study (Figure 1). According to Vietnamese Standards [15], from 0 to 50 cm depth, 2 L surface water samples were collected by barometer (Wilco company, US), then immediately loaded into a brown glass bottle and labeled. The water samples were stored in a 4^{o}C refrigerator and pre–treated within 48 h. Sampling Duration: dry season (September 2015) and rainy season (April 2016).

2.2. Sample preparation and detection

Sample extraction: Antibiotics in water were extracted according to the method reported in the literature [16–18], such as Water samples were purified by SPE, which is Oasis HLB (hydrophilic–lipophilic–balance) extraction column (60 mg, 3 mL, Waters). SPE vacuum manifold 12 pos (from Waters Corporation, U.S.A) were used (Figure 2).

Sample analysis: All water samples were analyzed via high–performance liquid chromatography with mass spectrometer double quadrupole detection (HPLC/MS/MS, 6410 B, Agilent) and were referenced in the literature [17–18].

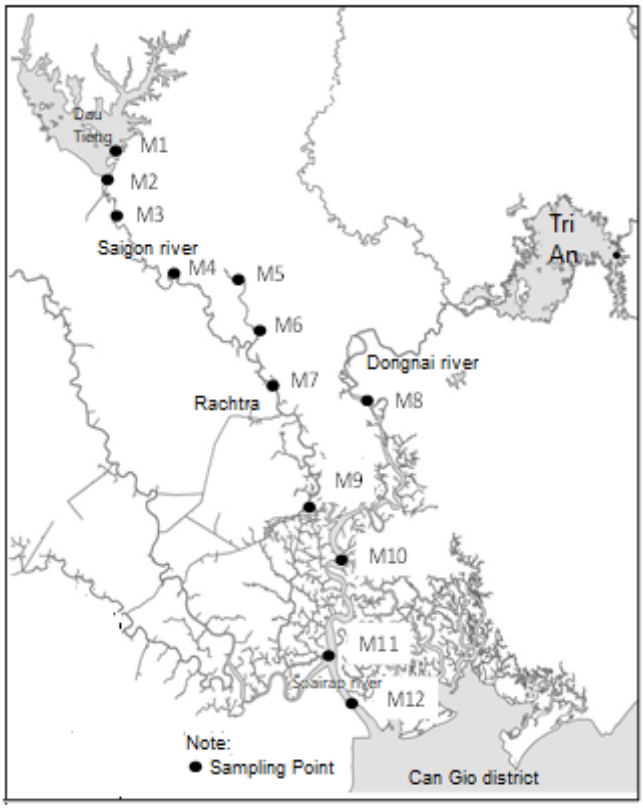

Symbol	Sampling sites	Coordinates
M1	Dautieng reservoir	11°20'16.8"N 106°21'05.0"E
M2	Moi bridge	11°18'29.3"N 106°20'23.9"E
M3	Ben Cui bridge	11°16'45.4"N 106°21'17.8"E
M4	Ben Suc bridge	11°09'22.3"N 106°27'05.6"E
M5	Do bridge	11°09'04.1"N 106°35'16.4"E
M6	Ong Co bridge	11°02'55.2"N 106°36'41.2"E
M7	Phu Cuong bridge	10°58'51.7"N 106°38'33.4"E
M8	Hoa An bridge	10°56'50.1"N 106°48'21.5"E
M9	Bach Dang boating	10°46'33.2"N 106°42'26.2"E
M10	Binh Khanh ferry station	10°40'46.9"N 106°46'09.5"E
M11	Vam Sat	10°31'48.6"N 106°45'18.9"E
M12	Ly Nhon, Can Gio dicstrict	10°26'32.7"N 106°46'52.8"E

Figure 1. The 12 sampling sites (M1–M12) of Saigon river.

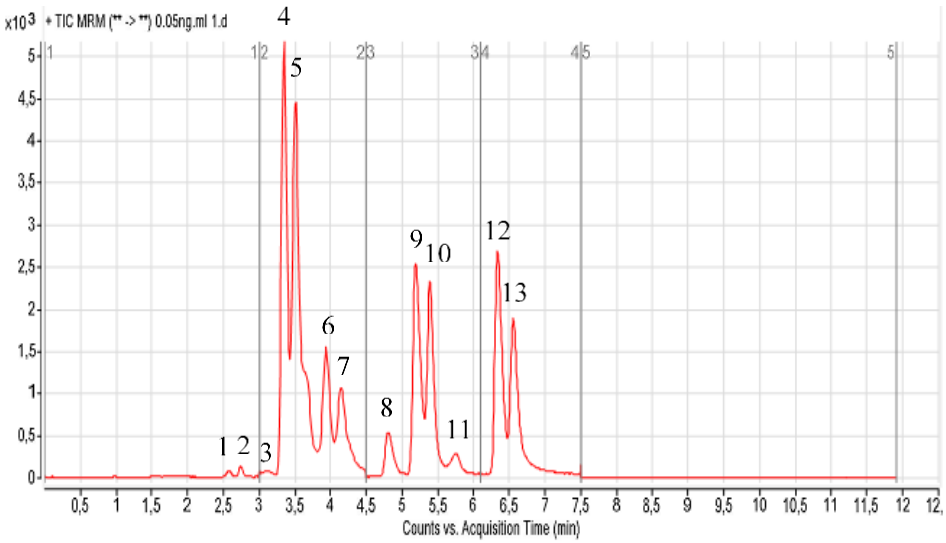

1: atrazin; 2: vancomycin; 3: diuron; 4: trimethoprime, sulfamethazin; 5: ciprofloxacin, 6: ofloxacin; 7: tetracyclin; 8: sulfamethoxazol; 9: enrofloxacin; 10: erythromycin; 11: tylosin; 12: norfloxacine; 13: chlorotetracyclin.

Figure 2. 50 ng/L Standard Chromatogram of antibiotics.

2.3. Ecological risk assessment in water

The antibiotics in the environment are new organic pollutants, their concentration in the aquatic environment is very low, generally in order of magnitude from ng/L to µg/L. In this study, the risk quotient (RQs) method was selected to evaluate the potential risks of antibiotics to aquatic ecosystems. RQs values were calculated according to environmental concentrations (MEC) and predicted no–effect concentrations (PNEC), the formula used was as follows [8, 19]:

$$RQ_{water} = \frac{MEC}{PNEC_{water}} \quad (1)$$

where MEC is the actual measured concentration in the environment (ng/L); $PNEC_{water}$ is the predicted no–effect concentration in the water and it is the maximum drug concentration that will not have an adverse effect on the microorganisms or the ecosystem in the environment under the existing cognition (ng/L); $PNEC_{water}$ values were referenced in the literature [20–21].

Table 1. Predicted no–effect concentrations for antibiotics.

Antibiotic	Observed lowest MIC[1] (ng/L)	Size–adjusted lowest MIC[2] (ng/L)	PNEC (resistance selection)[3] (ng/L)	References
Chlortetracyclin	–	–	1000	as Tetarcyclin
Ciprofloxacin	2000	1000	64	[14–15]
Enrofloxacin	8000	500	64	[14–15]
Erythromycin	16000	8000	1000	[14–15]
Norfloxacin	16000	4000	500	[14, 15]
Ofloxacin	32000	16000	1000	[14–15]
Sulfamethazine	NA	NA	NA	[14–15]
Sulfamethoxazole	1000000	125000	16000	[14–15]
Tetracyclin	16000	16000	1000	[14–15]
Trimethoprim	16000	8000	500	[14–15]
Tylosin	2000	32000	4000	[14–15]
Vancomycin	125000	125000	8000	[14–15]

Notes: [1]The lowest MIC value observed for any species in the EUCAST database; [2]The size–adjusted lowest MIC (Minimal Inhibitory Concentrations) prediction, corresponding to the estimated upper boundary for the MSC (rounded down to the closest concentration on the EUCAST (European Committee on Antimicrobial Susceptibility Testing) testing scale; [3]The PNEC corresponds to the size–adjusted lowest MIC divided by an assessment factor of 10 (rounded down to the closest concentration on the EUCAST testing scale).

Ecological risk classification such as [22]: When RQ ranges from 0.01 to 0.1, the ecological risk assessment of antibiotics in water is low. The environment is in medium risk when RQ ranges from 0.1 to 1, while RQ is more than or equal to 1, the risk is at a high level.

3. Results and Discussion

3.1. Concentration of antibiotics in water

Determination results has revealed 12 antibiotics in water of Saigon River. The antibiotics concentration ranged between not determined (ND) and 697.3 ng/L (rainy season) and 869.3 ng/L (dry season). The highest concentration both was Sulfamethoxazole antibiotic.

The antibiotics concentration total of water (Fig. 3) is ranged from 12.9 to 3,048 ng/L (rainy season) and 3,227 ng/L (dry season). The rank of four antibiotics of highest antibiotics concentration in water of Saigon river was recorded as follows Sulfamethoxazole > Norfloxacin > Ciprofloxacin > Ofloxacin.

Table 2. Highest concentration of four antibiotics in water of Saigon river.

Antibiotics	**Dry season** (ng/L)	**Rainy season** (ng/L)
Sulfamethoxazole	364.2	313.5
Norfloxacin	230.0	207.8
Ciprofloxacin	226.2	188.2
Ofloxacin	220.0	192.6

The highest antibiotic concentration total was observed at sampling site M6 (3,048 – 3,227 ng/L) and the lowest at M1 (about 12.9 ng/L).

The total average concentration of 12 antibiotics varied greatly, ranging from not detected (ND) to 1293.5 ng/L (rainy season) and 1484.2 ng/L (dry season). In addition to natural factors, even in the aquatic environment, antibiotics are also adsorbed by substances suspended in water or by sediment [23].

In terms of antibiotics present in Saigon river water calculated at 12 sampling points, the total antibiotic concentration ranged from not detected (not detected, M1 site) to 3048 ng/L (rainy season), 3048 ng/L (rainy season) and 3227 ng/L (dry season) at Ong Co bridge sampling point (M6 site). The concentration of antibiotics was recored to be insignificantly low at Vam Sat sampling point (point M11) with total antibiotic concentration in the range of 2575 ng/L (rainy season) – 2587 ng/L (dry season) (Figure 3).

The results depicted on the graph (Figure 2) further demonstrate that each area has a distinct total concentration of antibiotics due to various applications and effect sources. Total antibiotic concentration was reported to be highest in livestock production areas, aquaculture areas and lowest in watershed areas, after Dau Tieng reservoir.

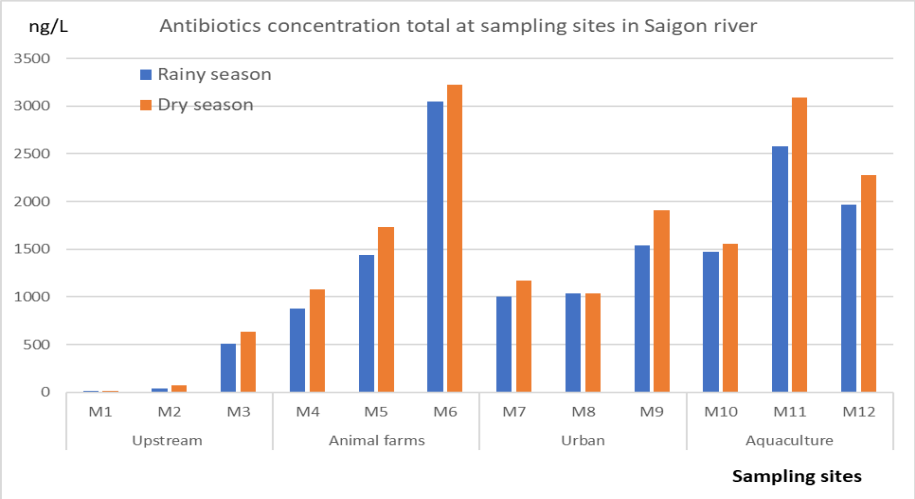

Figure 3. Antibiotic concentration total of water samples in ng/L at each sampling point of Saigon river.

The detection frequency of antibiotics in surface water of Saigon river basin gradually reduced, in the order sulfamethoxazole > norfloxacin > ofloxacin > ciprofloxacin > trimethoprim > enrofloxacin > tylosin > vancomycin > erythromycin > tetracyclin > sulfamethazine > chlotetracycline. Within the majority of the water samples analysis, sulfamethoxazole, trimethoprime, ciprofloxacin, norfloxacin, and ofloxacin frequency and high concentrations were recognised (frequency above 80%) (Table 3).

The frequency and concentration of detected antibiotics is variable depending on the sampling season. Calculating the standard deviation and variance of the antibiotic concentration analysis data also reveals that they are relatively similar and that there is little significant difference between the dry and rainy seasons.

Table 3. Occurrence frequency and antibiotics concentration in water of Saigon river.

Antibiotics	**Rainy season**			**Dry season**		
	Occurrence frequency (%)	Max concentration (ng/L)	Average concentration (ng/L)	Occurrence frequency (%)	Max Concentration (ng/L)	Average Concentration (ng/L)
Ciprofloxacin	83.3	469.3	188.2	83.3	598.3	226.2
Norfloxacin	83.3	540.9	207.8	83.3	604.3	230.0
Ofloxacin	83.3	358	192.6	83.3	386.2	220.0
Enrofloxacin	75.0	192.4	56.8	50.0	86.4	61.4

Antibiotics	Rainy season			Dry season		
	Occurrence frequency (%)	Max concentration (ng/L)	Average concentration (ng/L)	Occurrence frequency (%)	Max Concentration (ng/L)	Average Concentration (ng/L)
Tetracyclin	75.0	104.0	34.4	75.0	142.8	50.2
Chlotetracyclin	75.0	78.83	20.3	75.0	136.4	24.4
Sulfamethoxazole	91.7	697.3	313.5	91.7	869.3	364.2
Sulfamethazine	58.3	85.61	21.3	50.0	67.2	14.5
Trimethoprim	91.7	270.4	104.4	91.7	316.4	130.5
Vancomycin	50.0	311.6	50.2	50.0	214.6	42.6
Erythromycin	75.0	111.6	47.1	75.0	148.4	61.5
Tylosin	75.0	156.0	56.7	75.0	179.2	58.8

3.2. Residual characteristics of antibiotics in water

Antibiotics in to the aquatic environment mainly come from pharmaceutical, medical, animals farm, aquaculture and domestic wastewater [14, 18, 24]. Antibiotics are considered to be ideal antibacterial drugs for humans and animals, they have been widely used in livestock and poultry breeding, aquaculture [12].

Research has quite extensively studied the presence of antibiotics in the aquatic environment on other areas (Table 4).

Table 4. Compared of concentrations of antibiotics in different the aquatic environment with results of study.

No.	Antibiotics	Max conc. of Ho Tay Lake [11]	Max conc. of Truc Bach lake [11]	Max conc. of Yen So Lake [19]	Mean conc. of Dongjiang River [20]	Mean conc. in water of another river [21]	Mean conc. of Saigon river (in rainy season)
1	Chlotetracyclin	NA	NA	NA	NA	690	20.3
2	Ciprofloxacin	55.27	98.56	568.4	169.2	39	188.2
3	Enrofloxacin	16.88	73.01	2.5	NA	40	57.2
4	Erythromycin	NA	NA	NA	0.7	280	47.1
5	Norfloxacin	79	48.88	20.76	62.3	120	207.8
6	Ofloxacin	43.11	211.67	242.91	7.1	270	192.6
7	Sulfamethazine	34.82	LOD	6.91	NA	472	21.3
8	Sulfamethoxazole	89.7	104.29	1619.35	NA	1900	313.5
9	Tetracyclin	NA	NA	NA	44.9	300	34.4
10	Trimethoprim	26.41	69	52.57	NA	710	104.4
11	Tylosin	NA	NA	NA	0.6	280	56.7
12	Vancomycin	NA	NA	NA	NA	NA	20.3

Compared with the concentration of antibiotics in rivers and lakes worldwide, the concentration of the antibiotic in water of the Saigon river was similar or at a moderately low level (Table 2). Of the twelve antibiotics, the highest concentration of antibiotics in water was Sulfamethoxazole and there were significant differences among the values for the other antibiotic at the sampling sites.

This result was similar to some other researches [4, 18, 25]. The highest water Sulfamethoxazole was observed at M6 site (about 697.3–786.2 ng/L) which is located near the high animal farms density. Sulfamethoxazole is a widely used antibiotic in medicine, in the field of livestock and aquaculture, so their presence in the environment with high concentrations is the result of a combination of all waste sources in the basin.

3.3. Ecological risk assessment in water

The ecological risk assessment of antibiotics in water is shown in Table 5 and Figure 3.

Some key characteristics of ecological risk levels through the risk quotient are as follows:

- RQ of Quinolone class (Ciprofloxacin, Enrofloxacin, Norfloxacin and Ofloxacin) in areas affected by livestock, urban living and aquaculture activities were recorded to be higher than 1, indicating that Quinolone class is remained at high risk in the Saigon River.

- In the headwaters of the Saigon River (area 1), the RQs of the Quinolones are reported to be less than 0.1 (except for Ciprofloxacin (RQ: 0.234–0.295), indicating that these CKS substances belonging to the low–risk group in the Saigon River. Particularly for the RQ of Ciprofloxacin in zone 1, the level of risk is moderate.

- The RQ risk quotient for the remaining antibiotics is low (0.0–0.382), indicating a low level of ecological threat.

- Although antimicrobial substances concentrations were discovered at low levels, ecological risk assessment still indicated a higher risk, suggesting that these antibiotics are still toxic to aquatic organisms at low concentrations and thus demand attention.

Table 5. Calculation results of Risk Quotient (RQs) in water of the Saigon river.

Antibiotics	Average		Upstream		Animal farm		Urban		Aquaculture	
	Rainy sea–son	Dry sea–son	Rainy sea–son	Dry sea–son	Rainy sea–son	Dry sea–son	Rainy sea–son	Dry sea–son	Rainy sea–son	Dry sea–son
Chlotetracyclin	0.020	0.024	0.001	0.001	0.019	0.028	0.009	0.009	0.052	0.054
Ciprofloxacin	2.940	3.534	0.234	0.295	3.804	4.269	1.926	1.926	5.797	7.277
Enrofloxacin	0.894	0.959	0.034	0.186	1.663	1.479	0.162	0.162	1.719	1.130
Erythromycin	0.047	0.061	0.005	0.012	0.069	0.095	0.058	0.058	0.056	0.073
Norfloxacin	0.416	0.460	0.062	0.058	0.575	0.680	0.386	0.386	0.640	0.705
Ofloxacin	0.193	0.220	0.034	0.042	0.268	0.288	0.232	0.232	0.237	0.262
Sulfamethazine	NA	NA	NA	NA	NA	NA	NA	NA	NA	NA
Sulfamethoxazole	0.020	0.023	0.004	0.005	0.023	0.027	0.018	0.018	0.033	0.040
Tetracyclin	0.034	0.050	0.001	0.001	0.053	0.083	0.036	0.036	0.046	0.075
Trimethoprim	0.209	0.261	0.038	0.063	0.298	0.371	0.187	0.187	0.313	0.382
Tylosin	0.014	0.015	0.003	0.002	0.028	0.031	0.016	0.016	0.010	0.011
Vancomycin	0.006	0.005	0.000	0.000	0.013	0.009	0.008	0.008	0.004	0.003

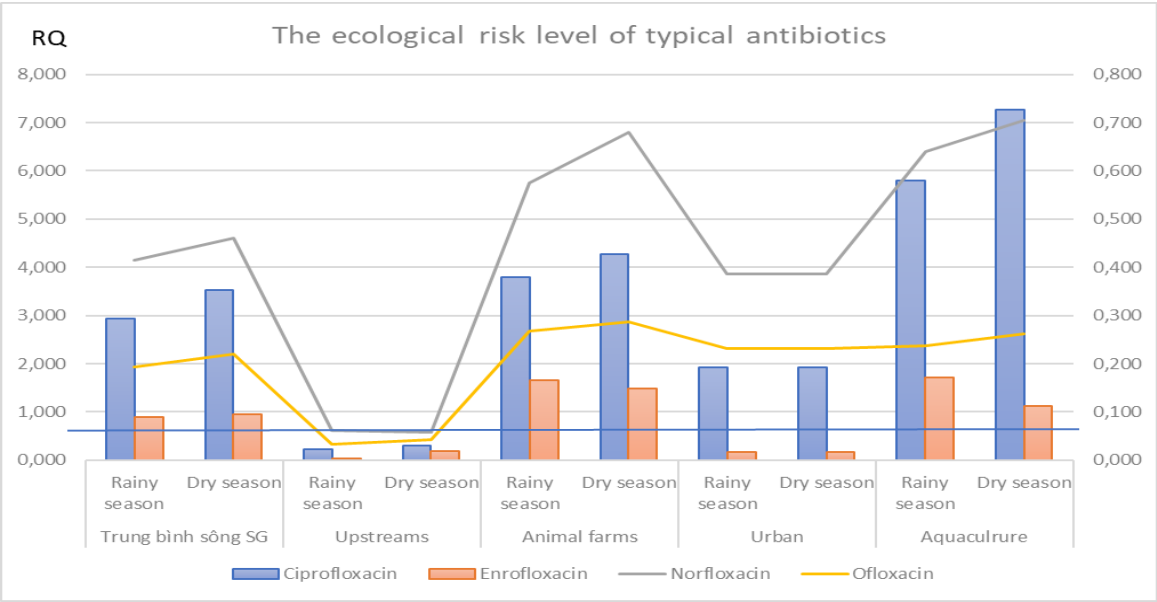

Figure 3. The ecological risk level of typical antibiotics in water of Saigon river.

The most significant degree of ecological risk in the Saigon River is the antibiotics Ciprofloxacin, Enrofloxacin, Norfloxacin, and Ofloxacin with a high RQ risk quotient. Other antibiotics are belonging to the low ecological risk category. The study's main weakness is that it is unable to demonstrate a continuous association between risks on the

Saigon River due to the dispersed nature and diverse sampling locations. The RQ method's results for risk assessment are unrelated, lack homogeneity between the examined positions, and do not accurately reflect the amount of risks.

4. Conclusion

The detection frequency of antibiotics in water was higher 75.0%. Sulfamethoxazole antibiotic was observed to be the highest concentration in water of Saigon river. In terms of spatial distribution, concentrations of antibiotics are distributed variably from upstream to downstream depending on the region. Two areas with total antibiotic concentrations greater than 3,000 ng/L are due to the influence of livestock and aquaculture.

The degree of ecological risk is reported to be low with the majority of RQs less than 1, and only two antibiotics, Ciprofloxacin and Enrofloxacin, have high–risk quotients in livestock, urban living, and aquaculture areas. There are signs of antibiotic pollution in the Saigon river and long–term monitoring of antibiotics' residues is required. In near by future, antibiotic pollution control policy and technology need to be used to protect the water quality of Saigon river.

Author contribution statement: Author contribution statement: Set up the input data of model; Analyzed and interpreted the data; Materials, analysis tools and data; Calculation, analyzed and interpreted the results; Wrote the draft manuscript: N.P.B., D.Q.T.; Analyzed and interpreted the data; Analyzed and interpreted the results; Materials, manuscript editing: P.H.N., N.T.M.H.

Acknowledgement: We are greatly thankful to Vietnam National University, Ho Chi Minh City for sponsoring the project implementation (Project code B2015-20-05), especially the group of researchers sincerely thank Assoc. Prof. Dr. Do Hong Lan Chi has created conditions for the group to perform the topic in the best way.

Competing interest statement: The authors declare no conflict of interest.

References

1. Kümmerer, K. Antibiotics in the aquatic environment – A review – Part I. *Chemosphere* **2009**, *75*, 417–434.
2. Fiedler, T.; Grummt, T.; Heidemeier, J.; Hein, A.; Helmecke, M.; Hilliges, F.; Kirst, I.; Klasen, J.; Konradi, S.; Krause, B.; Küster, A.; Otto, C.; Pirntke, U.; Roskosch, A.; Schönfeld, J.; Selinka, H.C.; Szewzyk, R.; Westphal–Settele, K.; Straf, W. Antibiotics and Antibiotic Resistances in the Environment. Background Challenges Options Action, **2018**, pp. 5.
3. Akhyany, M. Effects of individual antibiotics and their mixtures on single bacterial species, artificial and natural microbial communities. Department of Biological and Environmental Sciences University of Gothenburg, 2013, pp. 25.
4. Bruce, G.M.; Pleus, R.C. A Comprehensive Overview of EDCs and PPCPs in Water. Water Research Foundation, 6666 West Quincy Avenue, Denver, CO 80235–3098, 2015, pp. 22–23.
5. Le Page, G.; Gunnarsson, L.; Snape, J.; Tyler, C.R. Integrating human and environmental health in antibiotic risk assessment: a critical analysis of protection goals, species sensitivity and antimicrobial resistance. *Environ. Int.* **2017**, *109*, 155–169.
6. Wang, Q.J.; Mo, C.H.; Li, Y.W.; Gao, P.; Tai, Y.P.; Zhang, Y.; Ruan, Z.L.; Xu, J.W. Determination of four flfluoroquinolone antibiotics in tap water in Guangzhou and Macao. *Environ. Pollut*. **2010**, *158*, 2350–2358.
7. Bena, Y.; Fua, C.; Hua, M.; Liua, L.; Wong, M.H.; Zheng, C. Human health risk assessment of antibiotic resistance associated with antibiotic residues in the

environment: A review. *Environ. Res.* **2019**, *169*, 483–493.
8. Vryzasa, Z.; Alexoudisa, C.; Vassilioua, G.; Galanisa, K.; Mourkidoub, E.P. Determination and aquatic risk assessment of pesticide residues in riparian drainage canals in northeastern Greece. *Ecotoxicol. Environ. Saf.* **2011**, *74(2)*, 174–181.
9. Huang, L.; Mo, Y. ; Wu, Z.; Rad, S.; Song, X.; Zeng, H.; Bashir, S.; Kang, B.; Chen, Z. Occurrence, distribution, and health risk assessment of quinolone antibiotics in water, sediment, and fsh species of Qingshitan reservoir, South China. *Sci. Rep.* **2020**. https://doi.org/10.1038/s41598-020-72324-9.
10. Chen, Y.; Chen, H.; Zhang, L.; Jiang, Y.; Yew–Hoong Gin, K. Occurrence, Distribution, and Risk Assessment of Antibiotics in a Subtropical River–Reservoir System. *Water* **2018**, 10, 104. doi:10.3390/w10020104.
11. Environmental Technology Center (Entec). Dong Nai River Basin Environmental Planning Project 2010–2015. Ho Chi Minh City, 2010.
12. An, N.Q. Report of antibiotic use in animal in Vietnam. Presentation in the 1st GARP's workshop, 2009.
13. Nguyen, V.K.; Khue, L.N.; Thai, C.H. et al. First report on antibiotic use and resistance in Vietnam hospitals in 2008–2009. A report from the Ministry of Health of the Socialist Republic of Vietnam in collaboration with the Global Antibiotic Resistance Partnership and Oxford University Clinical Research Unit. 2010.
14. Tuan, N.D. Research to evaluate residues of some antibiotics and endocrine disruptors in downstream of Saigon and Dong Nai rivers and propose solutions to monitor and control pollution. Project level of Ministry of Natural Resources and Environment, 2012–2013.
15. Ministry of Science and Technology. Water quality – Sampling – Part 6: Guidance on sampling of rivers and streams. TCVN 6663–6:2008 (ISO 5667–6:2005).
16. Xu, W.H. et al. Determination of selected antibiotics in the Victoria Harbour and the Pearl River, South China using highperformance liquid chromatography–electrospray ionization tandem mass spectrometry. *Environ. Pollut.* **2007**, *145*, 672–679.
17. Gros, M.; Rodríguez–Mozaz, S.; Barceló, D. Rapid analysis of multiclass antibiotic residues and some of their metabolites in hospital, urban wastewater and river water by ultra–high–performance liquid chromatography coupled to quadrupole–linear ion trap tandem mass spectrometry. *J. Chromatography A*, **2013**, *1292*, 173–188.
18. Yen, P.T.T.; Trung, N.Q.; Hai, H.T. Research on determination of the antibiotics Sulfathiazole, Sulfamethazine, Sulfamethoxazole, Sulfamerazine in surface water by liquid chromatography tandem mass LC/MS/MS. *J. Anal. Sci.* **2015**, *20(2)*, 20–29.
19. Chen, Z.F.; Ying, G.G. Occurrence, fate and ecological risk of five typical azole fungicides as therapeutic and personal care products in the environment: a review. *Environ. Int.* **2015**, *84*, 142–153.
20. Bengtsson–Palme, J.; Joakim Larsson, D.G. Concentrations of antibiotics predicted to select for resistant bacteria: Proposed limits for environmental regulation. *Environ. Int.* **2016**, 86, 140–149.
21. de Souza, S.M.L.; de Vasconcelos, E.C.; Dziedzic, M.; de Oliveira, C.M.R. Environmental risk assessment of antibiotics: An intensive care unit analysis. *Chemosphere* **2009**, 77, 962–967.
22. Zhang, P.W. et al. Spatial, temporal distribution characteristics and potential risk of PPCPs in surface sediments from Taihu Lake. *Environ. Sci.* **2016**, *37(9)*, 3348–3355.

23. Tamtam, F.; Mercier, F.; Le Bot, B.; Eurin, J.; Dinh, Q.T.; Clément, M.; Chevreuil, M. Occurrence and fate of antibiotics in the Seine River in various hydrological conditions. *Sci. Total Environ.* **2008**, *393(1)*, 84–95.
24. Thuy, H.T.T.; Nga, L.P.; Loan, T.T.C. Antibiotic contaminants in coastal wetlands from Vietnamese shrimp farming. *Environ. Sci. Pollut. Res. Int.* **2011**, *18(6)*, 835-841. Doi: 10.1007/s11356-011-0475-7.
25. Yen, P.T.T. Research on residual antibiotics assessment in water and aquatic product in lakes of Hanoi. Doctoral thesis in environmental engineering, Hanoi University of Science and Technology, 2017.

VIETNAM JOURNAL OF HYDROMETEOROLOGY

Research Article

Application of numerical models in estimating particulate matter emissions ($PM_{2.5}$ and PM_{10}) from road traffic: A case study in Ha Noi, Viet Nam

Cung Hong Viet[1], Pham Van Sy[2], Tran Van Tra[3], Le Van Linh[3], Truong Ba Kien[1], Ngo Thi Thuy[1*]

[1] Viet Nam Institute of Meteorology, Hydrology and Climate Change; hongviet97@gmail.com; tide4586@gmail.com
[2] Climate Change Department; phamsymt@gmail.com
[3] Water Resources Institute; tranvantra@gmail.com; linhlevan6527@gmail.com

*****Corresponding author: tide4586@gmail.com; Tel: +84–363003245

Received: 2 August 2022; Accepted: 24 September 2022; Published: 25 September 2022

Abstract: The article is developed to analyze the characteristics of particulate matter pollution in Hanoi using observation data at automatic monitoring stations. The estimation method of particulate matter emissions from road traffic is also implemented by the coupled model so-called WRF–SMOKE. The model is applied to estimate $PM_{2.5}$ and PM_{10} emissions from road traffic in Hanoi city for 2021. The results are 325,045.8 tons/year (average 27,087.2 tons/month) and 523,565.9 tons/year (43,630.5 tons/month) respectively. Overall, the comparisons of the estimation result with EDGAR global emissions data and particular matter observation show similarity in terms of spatial and temporal distribution as well as the ratio between PM_{10} and $PM_{2.5}$. This comparison performs the applicability of the numerical coupled model in estimating particular matter emissions.

Keywords: WRF-SMOKE; Emissions; Air pollution; Particulate matter; Road traffic; Hanoi.

1. Introduction

At present, air pollution in general is considered a worrying problem globally due to its impacts on many different fields and social objects. There are significant impacts on human health. It is proved by many studies that the presence of harmful substances in the air contributes to increased mortality or chronic diseases in children. Some common health problems include cardiovascular disease, respiratory disease, and nervous system disease [1–7]. In addition, air pollution can affect the digestive system, urinary tract, and pregnancy [8–10]. Furthermore, extreme weather events caused by air pollution cause harmful effects on the ecosystem (acid rain). Simultaneously, secondary costs such as medical examination and treatment costs, treatment costs, and pollution control... are economic burdens caused by air pollution.

Air pollution is emitted from many different sources. In particular, one of the main sources is transportation activities. Many major cities in the world are currently facing air pollution. Typically, emissions from transport activities in some big cities in Europe account for a relatively high proportion such as in Paris (France) at 29%, Madrid (Spain) at 39%, and London (UK) is 50% [11]. Moreover, this kind of emission in Bangkok city (Thailand) is 60% [12].

Currently, most of the studies on emissions in Viet Nam are applying inventory data sets developed at global and regional scales. Those results in low reliability and accuracy (due to regional variations). Furthermore, forecasting the AQI requires input data which is emission inventory data. At the same time, the implementation of emission inventory has been regulated by the Government in many legal documents. Therefore, the implementation of the estimation study will contribute to the development of emission inventory methods for vehicles and practical results to the construction of a unified emission inventory data set under conditions in Viet Nam.

In this study, pollution emissions specifically particular matter (PM) PM_{10} and $PM_{2.5}$ are inventoried from the traffic sources for Hanoi city. The coupled model namely WRF–SMOKE is used to estimate the particular matter emission that contributes to air pollution in Hanoi urban area. The results of PM_{10} and $PM_{2.5}$ emissions are then compared to that of EDGAR global data and the observation data of PMs concentration as well.

2. Methods and data

2.1. Study area

Hanoi is a city located in the Red River Delta region, with an area of 3,324.92 km^2. Hanoi has a tropical monsoon climate with four distinct seasons a year. In particular, the summer is usually hot, with many thunderstorms and storms. Winters are cold, with a low level of precipitation. The transition time between these two seasons falls between April and October. Hanoi has an average of 1,500–1,700 hours of sunshine annually with an average annual temperature of approximately 23^{o}C. In particular, due to the influence of global warming and urban effects, on summer days, the highest outdoor temperature of the day can reach > 50^{o}C.

The air quality index (AQI) observed at monitoring stations of Hanoi city shows a fluctuation within the unsafe level for human health. In Hanoi, dust pollution in winter and early spring is higher than in other seasons of the year. This is also a common phenomenon for many years and has a regular pattern, particular matter pollution increases in the period from December, January to February and may last into March. This rule has also been shown. quite clearly in the past time when the PM concentration of Hanoi is having significant fluctuations, especially the increase in dust concentration of $PM_{2.5}$ and PM_{10}.

The urbanization process in Hanoi is increasing rapidly (2nd largest population in the country with about 8,053,663 people) [13] leading to an increase in population and a general need for transportation and personal mobility. The number of vehicles operating in Hanoi has increased significantly (including registered vehicles inside and outside the city). This leads to frequent traffic jams occurring at many hours of the day. In parallel, the process of vehicle management is not synchronized between localities. Vehicles such as motorbikes are not registered, and their performance cannot be assessed, making the amount of air pollution worse. [10] performed that road transport activities contribute up to 25% to $PM_{2.5}$ emissions in Hanoi.

2.2. Research data

The necessary data include (i) monitoring data of $PM_{2.5}$ and PM_{10} parameters in Ha Noi; (ii) Survey data on traffic volume (motorcycles, cars under 9 seats, cars 12–24 seats; light trucks 2 axles and heavy trucks over 9 seats) corresponding to different road types (main urban roads; secondary urban roads; main rural roads and secondary rural roads); (iii) Remote sensing data and geographic information; (iv) Global meteorological data and (v) Global emissions data.

2.2.1. $PM_{2.5}$ and PM_{10} monitoring data in Ha Noi

As of 2016, the automatic air quality monitoring network in Hanoi includes 12 stations with 10 stations operated by the Department of Natural Resources and Environment (since 2017), 01 under the Vietnam Environment Administration (since 2010) and 01 private air quality monitoring station belongs to the US Embassy in Vietnam. By July 2019, the French Embassy in Vietnam installed a $PM_{2.5}$ monitoring station at the embassy campus. By May 2020, THT (Korea) Co., Ltd. sponsored and installed 24 automatic sensors to monitor air quality in the Hanoi area. Up to now, there are 37 air quality stations in Hanoi city [14]. In this study, the observed data on air quality at stations is summarized in Table 1.

Table 1. Monitoring data of $PM_{2.5}$ and PM_{10} collected in Ha Noi.

No.	ID	Monitoring station	Monitoring parameters	
			$PM_{2,5}$	**PM_{10}**
1	CCBVMT	Hanoi Environmental Protection Department	2018, 2021, hourly	2017–2018, hourly
2	MK	Minh Khai (Bac Tu Liem)	2018	2017–2018, hourly
3	HD	Hang Dau	2018, daily	2017–2018, hourly
4	HK	Hoan Kiem	2018, daily; 2021, hourly	2017–2018, hourly
5	KL	Kim Lien	2018, daily; 2021, hourly	2017–2018, hourly
6	MD	My Dinh	2018, daily; 2021, hourly	2017–2018, hourly
7	PVD	Pham Van Dong	2018, daily; 2021, hourly	2017–2018, hourly
8	TC	Thanh Cong	2018, daily; 2021, hourly	2017–2018, hourly
9	TMai	Tan Mai	2018, daily	2017–2018, hourly
10	TMo	Tay Mo	2018, daily; 2021, hourly	2017–2018, hourly
11	NVC	Nguyen Van Cu	2010–2019, 2021, hourly	

2.2.2. Vehicle volume data

The data of vehicle volume includes:

Vehicle volume distribution was retrieved from a field survey on the main roads of Hanoi (see Annex Table 1). The traffic survey data is observed 3 times a day from September to November 2021 (07:00–08:00, 11:00–12:00, 16:00–17:00).

Mean daily vehicle volume extracted from COMPASSTECH [16] and Nippon Koei Co., Ltd – Japan [17] (Annex Table 1). The survey location is presented in Figure 1.

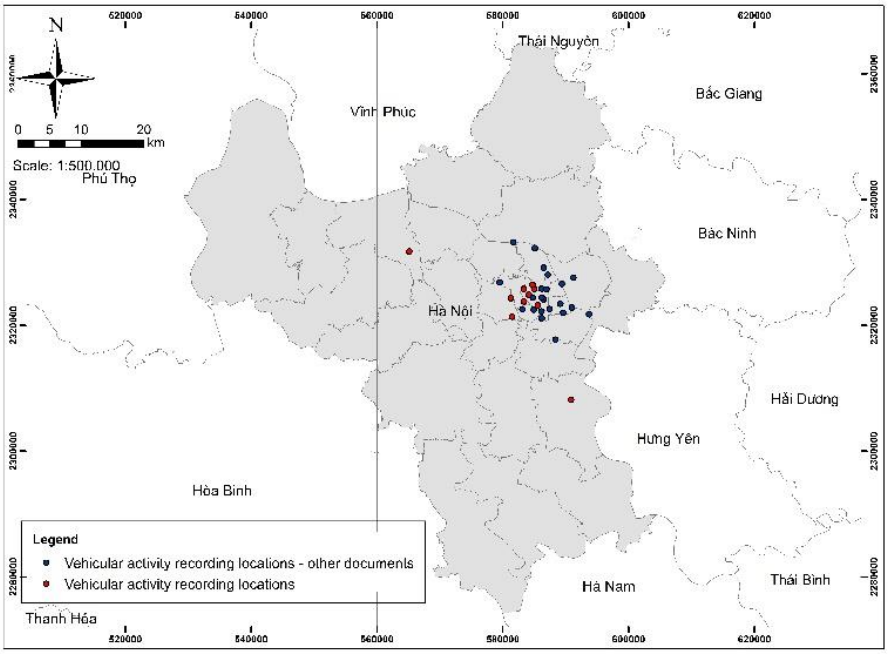

Figure 1. Map of locations with vehicle traffic measurement data.

2.2.3. GIS and remote sensing data

The original data used by the research team to edit the road network is data extracted from the website: http://download.geofabrik.de/index.html. This website includes Viet Nam topographic datasets for various features such as shapefiles. In this case study, the research team used the shapefile of the road object of the dataset, then edit, and classify the types of roads in Ha Noi following the polyline lines under the requirements of the SMOKE model. This editing work was done using ArcGIS software.

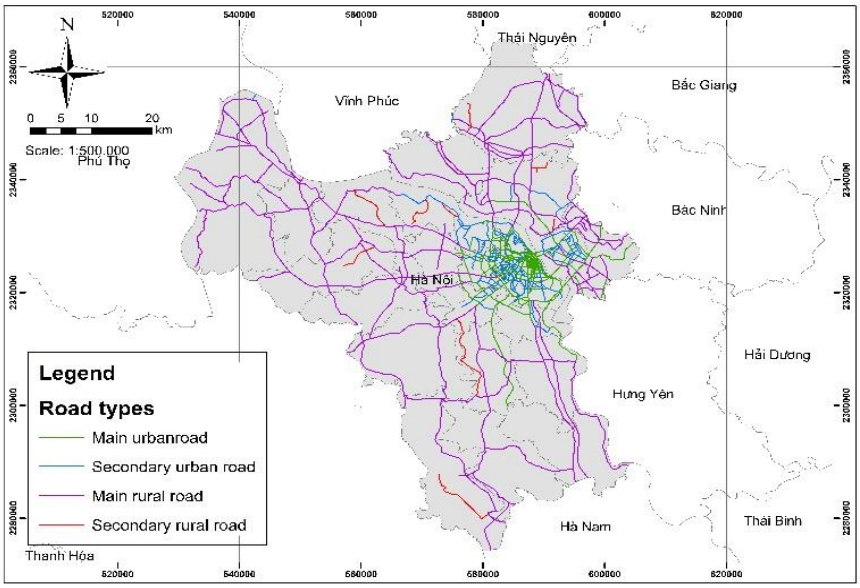

Figure 2. Road network in Ha Noi used in the study.

2.2.4. Global meteorology data

Input data using Global Convection Analysis data source NCEP FNL. Daily data with obs 6 hours apart has a grid resolution of $1^o – 1^o$. This reanalysis is initialized with the forecast data in the Global Forecast System (GFS), however, the reanalysis product will initialize relatively slower than forecast products. The data set parameters include surface pressure, sea surface temperature relative humidity, wind, vertical movements, vortex, soil, ice cover, and ozone. Data source NCEP's reanalysis data with data series from 1999 to the present is freely available at https://rda.ucar.edu/datasets/ds083.2/. This is the input data source for launching the WRF model in the study.

2.2.5. Global emissions data

The global emissions inventory used by the study for the comparison is EDGAR (Emissions Database for Global Atmospheric Research) version 5.0 with data series available continuously from 1970 to 2015. EDGAR 5.0 was selected because it has full information on pollutant types. The EDGAR dataset provides data not only for greenhouse gases but also for common GHG compounds, especially including particular matter ($PM_{2.5}$ and PM_{10}). Furthermore, EDGAR 5.0 provides separate emission data for each type of pollutant with each specific industry/sector, such as the power industry; energy and transition industries; gas; air; road traffic; railway, pipeline and off–road transportation operations; ship; build; fuel extraction…

The study utilizes emission data from road traffic sources that EDGAR calculated in 2015 for $PM_{2.5}$ and PM_{10}. In particular, monthly averages to consider the distribution as well as changes in values during the year. The data is available on the website: https://edgar.jrc.ec.europa.eu/dataset_ap50#sources. This is the data source for testing the emission estimation results of the WRF–CMAQ model system.

2.3. Methodologies

2.3.1. Estimating vehicle volume

Types of roads are divided into 04 categories: (i) main urban road; (ii) secondary urban road; (iii) main rural road; (iv) secondary rural road. Vehicles are divided into 05 categories: (i) motorbikes; (ii) cars (< 9 seats); (iii) cars (12–24 seats); (iv) light trucks (02 axles); (v) heavy trucks (> 02 axles). The CMAQ model manual [15] is used as the basis for the above classification work.

The research team measured traffic data at locations and routes with vehicular traffic representing each type of road corresponding to administrative regions. Survey frequency at each site is 03 times a day in the morning (07:00–08:00), noon (11:00–12:00) and afternoon (16:00–17:00). Regarding the measurement method, in each measurement, traffic activity is recorded through the smartphone's camera with appropriate resolution. The video files are then processed and the media counts are counted.

However, due to limitations in time and human resources and devices, the survey work of the research team could not be representative of all the roads in Ha Noi, the mean daily vehicle loads extracted from references [16–17] are used. However, this data is the average value of day and could not present the hourly distribution of vehicle load. Therefore, an integrated estimation is proposed to retrieve daily vehicle flow as follows:

Step 1: Count vehicle load in 1 hour at 3 durations in a day of roads from observed videos. The results are vehicle load distributions of roads in Annex Table 1.

Step 2: Extract vehicle load of roads from references [1615] and [17] as mentioned in Annex Table 2.

Step 3: For the roads where vehicle distribution and mean daily vehicle load are both estimated in Step 1 and Step 2, the hourly vehicle flow is interpolated.

Step 4: For the road where only the mean daily vehicle load is estimated, the vehicle flow is estimated using the hourly distribution of similar roads in terms of type and location.

2.3.2. Coupled model WRF–SMOKE

SMOKE model (Sparse Matrix Operator Kernel Emissions) was developed by the MCNC Environmental Modeling Center (EMC) to estimate emissions (manmade and biogenic) using sparse–matrix algorithms [18]. The model outputs contribute to air quality simulation and forecasting. The SMOKE model provides processes to estimate pollutant emissions such as CO, NO_x, NH_3, SO_2, PM_{10}, $PM_{2.5}$, and so on. The model transfers emission inventory data to emission loads that are inputs of air quality models.

The SMOKE model uses two approaches to compute traffic emissions. The first approach precomputes traffic emission before running SMOKE. The second approach run SMOKE with inputs of vehicle miles traveled (VMT), vehicle load (VPOP), meteorology and MOVES outputs. In which, MOVES is a module used to simulate bulk emission or emission rates of motor vehicle.

To couple WRF with SMOKE in gases pollutant emission, the meteorological outputs from WRF model (spatial and temporal temperatures and relative humidity) are processed using MCIP (Meteorology–Chemistry Interface Processor) output files. These meteorological inputs are then set up for MOVES to get the emission rate. This output will be used to compute the pollutant emission from mobile sources using processes of temporal and spatial allocation, chemical speciation and layer assignment.

2.3.3. Modelling method

The input data for calculation of emissions matters, specifically vehicles and road types, will be researched and classified to choose an appropriate emission factor. The emission estimation process using the combined model WRF–SMOKE allows the integration of

emission data processing methods by sparse matrix algorithms on a high–performance computer system based on variations in meteorological conditions.

Meteorological factors that affect the emission of vehicles are extracted from the output of the WRF model such as temperature, humidity and wind. The WRF model in the study was edited with the following parameters and implementation procedures:

- Domain coordinates: 104.3809–107.5417°E; 19.57395–22.14902°N;
- Number of grid points for the calculated domain: 84 – 84;
- Number of grid cells in each dimension: 83;
- Center of the domain: 21.02899°N–105.412°E;
- Size of grid cells: 2 km × 2 km;
- Vertical levels: 38.

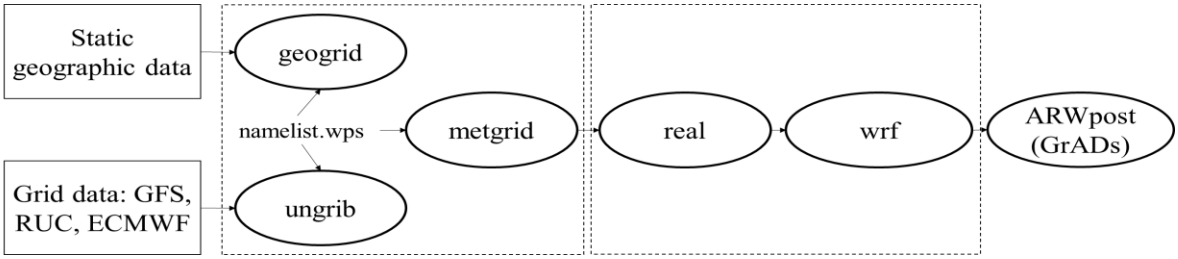

Figure 3. Processing stages of WRF model.

The formula for estimating PM emissions from vehicles will be implemented by multiplying the distance travelled data in each day of vehicles by the number of vehicles and the emission factor of the respective vehicle type. The input meteorological data for the SMOKE model will be downscaled in terms of the calculation domain for the Hanoi area using the WRF model from the GFS global data.

As regards the practice of national and international studies on the estimation of PM emissions from vehicles, it can be seen that an inventory or emission estimate can be made through the application of a variety of different modeling methods. Each type of model developed will be suitable for each specific parameter and research area. Studies on emissions inventory in Viet Nam have generally updated advanced technologies in the world. In which, modeling method is widely applied to calculate, estimate emissions or simulate, evaluate and forecast emissions distribution. Therefore, the use of modeling to estimate emissions of pollutants in the air is completely appropriate and has a solid reference base.

The transportation emission estimation can be made by simple calculation through the following formula [18]:

$$E = A * EF \quad (1)$$

where E is the emission level (tons/day); A is the active data of each type of vehicle (km/day); EF is the emission factor of each type of vehicle (tons/km).

Mathematical models also use the above formula to estimate emissions. Furthermore, the models also allow for estimating emissions according to defined calculation domains, thereby supporting post-processing to estimate and present in the form of maps and charts. Considering the research objectives, the combination of the weather forecasting and research model (WRF) with the sparse matrix emission model (SMOKE) has been applied in many research cases in Vietnam. Therefore, the use of the combined models above in the field of emission estimation for Viet Nam is appropriate and highly applicable.

2.3.4. GIS and remote sensing method

The input data of the SMOKE model require preprocessing stage using GIS and remote sensing technology. The administrative boundary data to be determined by GIS include coordinates, population, area, and district code. Data on cadastral boundaries and road

networks that need to be determined by GIS include generating and classifying road networks according to specific road types, lengths and corresponding road codes in each district.

A distributional map of PM emissions from traffic vehicles of Ha Noi will be created based on the combination of the output of the SMOKE model and the application of ArcGIS software together with the emission estimation results.

3. Results and discussion

3.1. Status of $PM_{2.5}$ and PM_{10} concentration in Hanoi

According to the air quality overview report in Hanoi released by the Ha Noi Department of Natural Resources and Environment, the local air quality has changed over time. In general, air quality usually improves between May and October (rainy season) and decreases from November to April (dry season) every year. Indicators of dust $PM_{2.5}$ and PM_{10} are always recorded with the highest number of days exceeding the standard, especially at monitoring stations near traffic areas. During the day, PM concentration tends to increase between 07:00–09:00 and 16:00–23:00. As regards types of monitoring (Monitoring types include: residential, countryside, craft village, urban and sub-urban, traffic), traffic monitoring witnessed the worst air quality condition [19].

The analysis results of the hourly average and 24–hour average of $PM_{2.5}$ monitoring data also show quite obvious changes over time. During the rainy months (May to October), the measured $PM_{2.5}$ concentration is usually lower than in the rest of the months. During this time, although the temperature is high, the humidity is maintained at a high level (above 85%) causing showers that help disperse PM in the air. At the same time, the period when the concentration of $PM_{2.5}$ exceeds the limit (average of 24 hours) of QCVN 05:2013/BTNMT gradually decreased over the years, but generally remained at a high level (Figure 4).

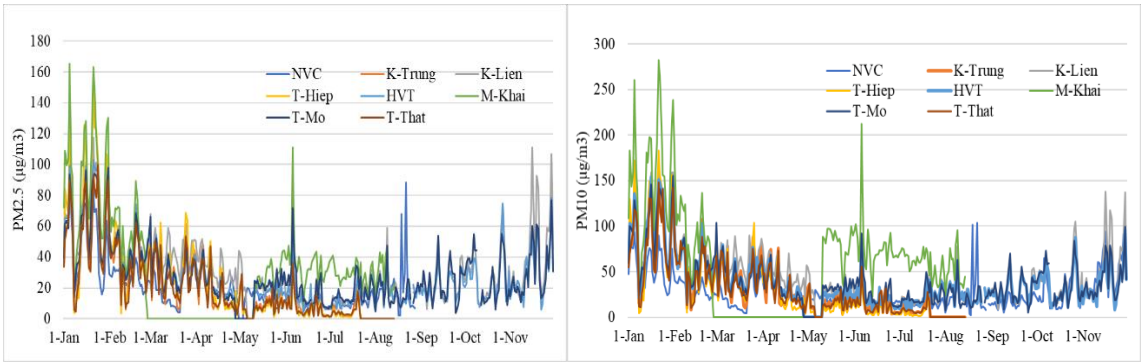

Figure 4. Average daily $PM_{2.5}$ (left) and PM_{10} (right) at some stations in Hanoi in 2021.

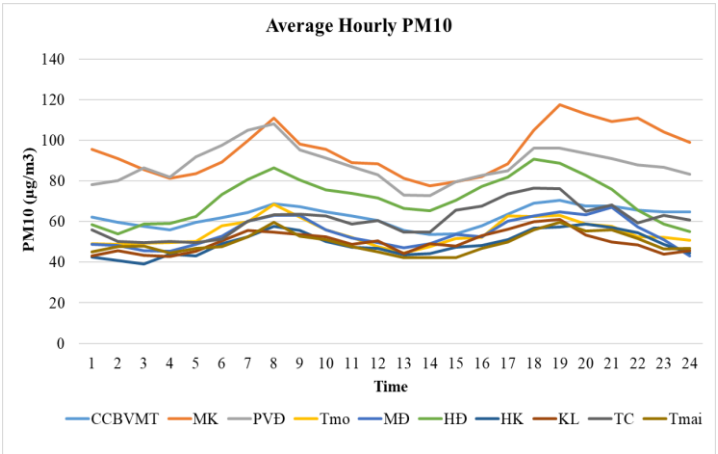

Figure 5. Variation curve of daily average PM_{10} concentration at 10 stations managed by Hanoi Department of Natural Resources and Environment (May 2017 – December 2018).

The assessment of PM_{10} observation showed that the hourly and 24–hour average concentrations at the stations changed significantly over time. During months with low precipitation and low temperatures (from July to October), the observed concentration of PM_{10} is usually lower than that of the dry season months with higher air temperature (December to June) (Figure 4). The general trend of the day (Figure 5), the concentration of PM_{10} usually peaks between 7:00–9:00 and 18:00–20:00. This is the rush hour with high traffic density.

3.2. Vehicles volume corresponding to road types

Measurement data show that the main urban road and the secondary urban road have a proportion of hundreds of vehicles participating on the road that are equivalent. Specifically, motorbikes are the main means of transport with the proportion accounting for over 70%. For the main rural road (highway), this figure is lower because vehicles operate at high speeds. However, the number of motorbikes is still quite large.

Considering the traffic flow, the traffic is usually high during the commute time and at the end of the day on main urban roads. These times are usually 07:00–09:00 and 17:00–19:00. In contrast, the period of reduced vehicle traffic usually falls around 1–2 hours in the afternoon, around 12:00–14:00, and then gradually increases. This trend is quite evident in motorbikes and cars (< 9 seats).

In the area of main rural roads, the number of motorbikes still accounts for the majority with a proportion of over 80%. Next are cars with less than 9 seats with a proportion of about 10%. Among the remaining vehicles, the proportion is small and there is no big difference in proportion. The proportion of means of transport of the main rural road as well as the daily flow variation is similar when compared with the urban road. Moreover, the traffic of motorbikes and cars with fewer than 9 seats increases significantly between 07:00 and 09:00 in the morning and 17:00. The types of trucks, including light trucks and vans, are not too large, but maintained with fairly even traffic throughout the day. Therefore, emissions from trucks of all kinds are still significant.

In the area of secondary rural roads, the proportion of motorbikes is lower than that of main rural roads, at 65%. Instead, there is an increase in cars under 9 seats as well as light trucks. The proportion of cars over 9 seats and heavy trucks is also higher than that on main rural roads. The secondary rural road variables are quite similar to other types of roads in terms of motorbikes and cars with fewer than 9 seats. However, the traffic of cars over 9 seats and trucks is higher and remains high throughout the day.

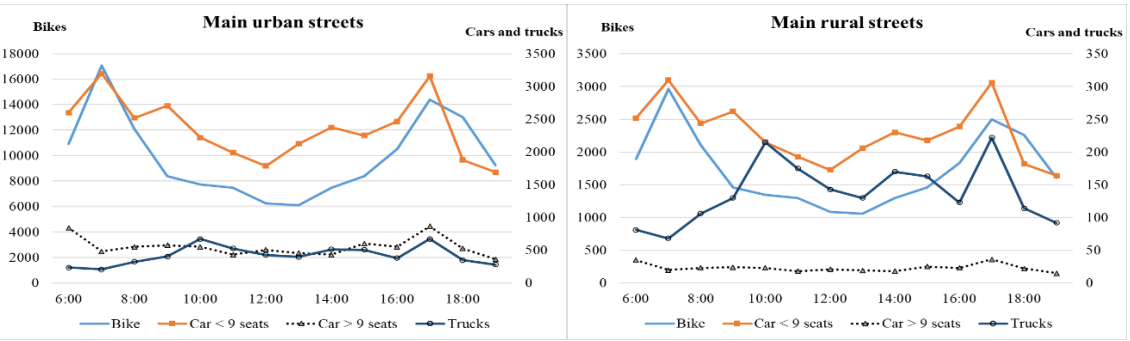

Figure 6. Vehicle loads on some types of roads in Hanoi.

3.3. Estimating results of $PM_{2.5}$ and PM_{10} emissions in Hanoi

Table 2 illustrates the estimated results of emissions of two types of PM from the traffic source in Hanoi by month in 2021. Total emissions in 2021 of vehicles in Ha Noi for $PM_{2.5}$ is 325,045.8 tons/year (average 27,087.2 tons/month) and for PM_{10} is 523,565.9 tons/year (43,630.5 tons/month).

Table 2. Estimated results of $PM_{2.5}$ and PM_{10} emissions from traffic sources in Ha Noi in 2021.

Month	$PM_{2.5}$ emissions (tons)	PM_{10} emissions (tons)
1	22,282.9	37,781.3
2	26,389.1	42,213.2
3	27,131.3	43,441.3
4	28,100.1	45,166.8
5	28,207.9	45,080.1
6	27,468.6	44,286.5
7	27,275.1	43,620.9
8	27,398.1	43,891.4
9	27,623.9	44,360.0
10	28,410.8	46,104.1
11	28,048.2	44,945.9
12	26,709.8	42,674.4
Total	**325,045.8**	**523,565.9**

The spatial estimation results show that the main emission areas of $PM_{2.5}$ and PM are concentrated in the citadel districts (Figure 7). This is an area with a large population density and many traffic vehicles. Furthermore, this area often happens to be congested at peak hours. In addition, areas with high emission levels are also the locations of highways, national highways, and provincial roads with a large number of vehicles such as cars over 9 seats along with trucks.

In terms of spatial distribution, in the central area, PM_{10} has wide coverage with a higher value than $PM_{2.5}$. Specifically, with an emission value of over 5 tons/month, the emission map of $PM_{2.5}$ only covers the area of Hai Ba Trung, Dong Da, Hoang Mai, and Thanh Xuan districts. PM_{10} covers a wider area to the west including the aforementioned districts along with Bac Tu Liem, Nam Tu Liem and Ha Dong. In contrast, $PM_{2.5}$ tends to cover more widely than PM_{10} in the south of the city, along National Highway 1A extending from Thanh Tri district to Ha Nam province. According to measured traffic data, this is the main rural road area with trucks participating in high volume and maintaining high volume during the day. In temporal distribution, the period with high emission levels is April – May and October – November, from June to September, emissions have decreased and maintained at a lower level. This variation is similar to the characteristics of $PM_{2.5}$ and PM_{10} in Ha Noi mentioned in Section 3.1.

3.4. Comparation between $PM_{2.5}$ and PM_{10} emissions estimating results with the global data EDGAR

The calculation from the EDGAR model shows that the main emission zones of both $PM_{2.5}$ and PM_{10} are in citadel districts including Bac Tu Liem, Nam Tu Liem, Tay Ho, Cau Giay, Ba Dinh, Hoan Kiem, Dong Da, Hai Ba Trung, Ha Dong, Thanh Tri, Hoang Mai (Figure 7). These areas have an average monthly $PM_{2.5}$ and PM_{10} emission values of 4–19 tons/month. In terms of temporal, the period of widespread emissions in both value and spatial remained from November to May with wider emission areas including Long Bien and Gia Lam to the East, and Hoai Duc to the west.

High–level emission areas are mainly in central districts, which is similar to EDGAR data. The variation in the area is not much. The most obvious increase can be seen in the southern region, including Thanh Tri and Phu Xuyen districts, with an increase in the months of the year. Besides, it can be seen that there is another high emission zone located in the northwest of the city, extending along route 32 starting from Bac Tu Liem district to the Son Tay area (adjacent to Vinh Phuc province). This is the area with the majority of motorbikes and cars with less than 9 seats, especially the traffic flow of cars over 9 seats as well as light trucks and large heavy trucks remain high during the day.

Even though there are some emission differences due to resolution, these spatial and temporal variations are quite similar to that obtained from EDGAR (Figure 8).

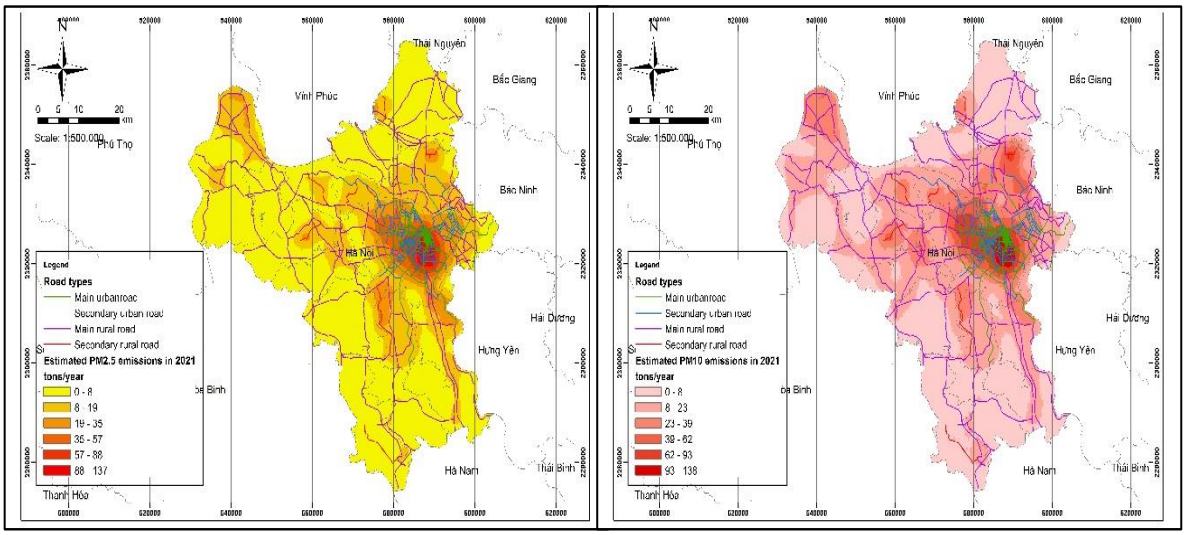

Figure 7. Estimated results of $PM_{2.5}$ and PM_{10} emissions from traffic sources in 2021.

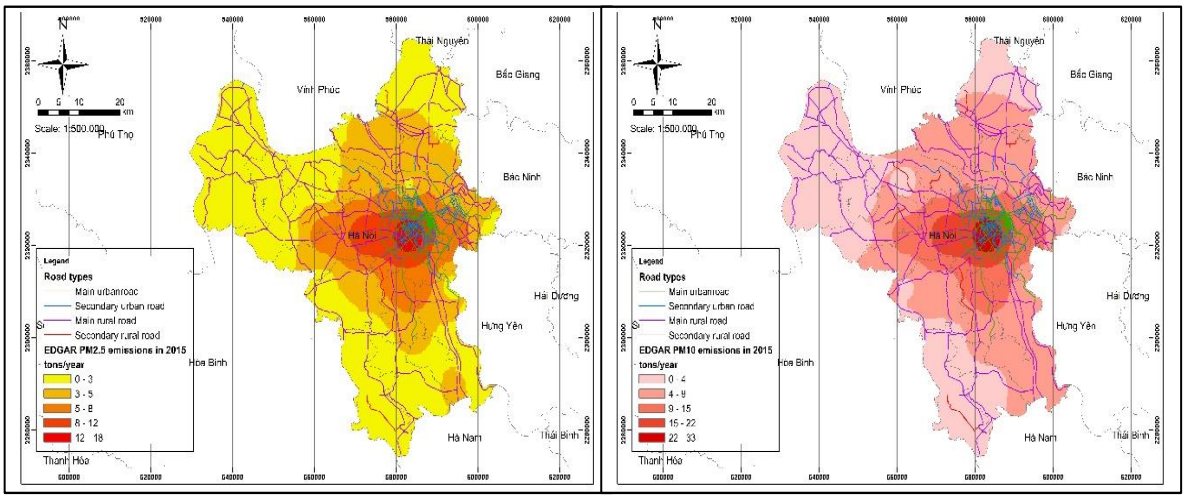

Figure 8. EDGAR $PM_{2.5}$ and PM_{10} global emissions data from transport sources.

Since there is no data on EDGAR in the same year as our study i.e., 2021, the ratio between $PM_{2.5}$ and PM_{10} emission in a year is used to be to be a reference for our calculation with the assumption that these two particular matters have a closed relationship [20]. The ratios are around 1.8 in EDGAR estimation and 1.6 in our calculation.

Table 3. Comparison of total $PM_{2.5}$ and PM_{10} emissions from transportation sources between estimated results and EDGAR.

No.		**$PM_{2.5}$ emissions (tons/year)**	**PM_{10} emissions (tons/year)**
1	WRF–SMOKE	325,045.8	523,565.9
2	EDGARv5.0	115,054.55	213,852.3

A comparison of monthly emissions of districts in Hanoi city is also conducted to see the spatial correlation between EDGAR and SMOKE estimations. The monthly emission of cells in a district is averaged to get a representative value. Figure 9 shows a close relationship between WRF–SMOKE model with EDGAR data in both $PM_{2.5}$ and PM_{10} emission estimation.

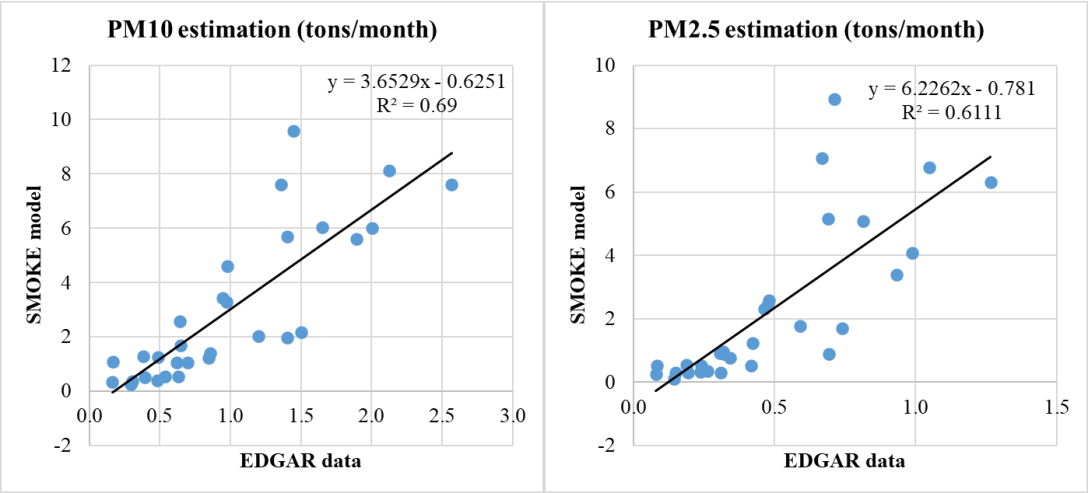

Figure 9. Correlation of EDGAR and SMOKE estimation for districts of Hanoi.

4. Conclusion

The study estimated $PM_{2.5}$ and PM_{10} emissions from transportation sources at 325,045.8 tons/year (averagely 27,087.2 tons/month) and 523,565.9 tons/year (averagely 43,630.5 tons/month). The results are relatively similar to the spatial scale of EDGARv5.0 as well as the correlation between the emission data of $PM_{2.5}$ and PM_{10}. The estimated data was higher than that of EDGAR data due to the difference in the time of calculation (the article calculated for 2021, the EDGAR calculated for 2015). Furthermore, the WRF–SMOKE combined model is suitable to estimate emission inventories for other provinces.

Since the study was implemented in 2021 when Hanoi experienced the COVID–19 pandemic, the emission inventory was retrieved containing several uncertainties in terms of traffic load and air pollution measurements. The vehicle countings might not be representative of the traffic status of Hanoi. The PM emission results, thus, may be biased values. Furthermore, the data source's limitation is one of the biggest challenges in air pollution simulation.

Author contribution statement: Provided human and financial sources for the survey; Designed the study, Revised the manuscript: N.T.T.; Wrote drafts, Did calculation: C.H.V.; Designed the study: P.V.S.; Designed the study and Revised the manuscript: T.V.T.; Contributed to SMOKE calculation: L.V.L.; Contributed to WRF simulation: T.B.K.

Acknowledgements: The study was supported by a grant from the project TNMT.2019.05.03 "Short–term air quality forecasting in Hanoi citadel area", funded by the Vietnam Ministry of Natural Resources and Environment (MONRE). The authors would also like to thank the members of the Water Resources Institute and the Climate Change Department for technical support and discussions that improved the quality of the publication.

Competing interest statement: The authors declare no conflict of interest.

References

1. Thomke, F.; Jung, D.; Besser, R.; Roder, R.; Konietzko, J.; Hopf, H.C. Increased risk of sensory neuropathy in workers with chloracne after exposure to 2,3,7,8–polychlorinated dioxins and furans. *Acta Neurol. Scand* **1999**, *100(1)*, 1–5.
2. Kagawa, J. Evaluation of biological significance of nitrogen oxides exposure. *Tokai J. Exp. Clin. Med.* **1985**, *10(4)*, 348–353.
3. Balmes, J.R.; Fine, J.M.; Sheppard, D. Symptomatic bronchoconstriction after short–term inhalation of sulfur dioxide. *Am. Rev. Respir. Dis.* **1987**, *136(5)*, 1117–1121.

4. Vermylen, J.; Nemmar, A.; Nemery, B.; Hoylaerts, M.F. Ambient air pollution and acute myocardial infarction. *Lancet* **2001**, *358*, 1602.
5. Sawicka–Kapusta, K. Damage to the liver, kidney, and testis with reference to burden of heavy metals in yellow–necked mice from areas around steelworks and zinc smelters in Poland. *Toxicology* **2003**, *186(1–2)*, 1–10.
6. Ghio, J.; Huang, Y.C. Exposure to concentrated ambient particles (CAPs): a review. *Inhal. Toxicol.* **2004**, *16(1)*, 53–59.
7. Marilena, K.; Elias, C. Human effects of air pollution. **2018**, *51(2)*, 362–367.
8. Bellinger, D.C. Teratogen update: lead and pregnancy. *Birth Defects Res. A Clin. Mol. Teratol*, **2005**, *73*, 409.
9. Kimbrough, R.D.; Carter, C.D.; Liddle, J.A.; Cline, R.E. Epidemiology and pathology of a tetrachlorodibenzodioxin poisoning episode. *Arch. Environ. Heal.* **1977**, *32*, 77.
10. Amann, M. et al. Future air quality in Hanoi and northern Vietnam, 2019.
11. London Councils. Demystifying Air Pollution in London, 2018.
12. Wangwongwatana, S. Air Quality Management: Thailand's experiences. 2013.
13. General statistic office, 2019.
14. Bang, H.Q.; Khue, V.H.N. Air emission inventory. 2019. (In Vietnamese)
15. CMAQ user's guide. Available online: https://github.com/USEPA/CMAQ/blob/main/DOCS/Users_Guide/README.md (accessed in 2021).
16. COMPASS TECH. 2021. Available online: https://compasstech.asia/traffic–luu–luong–tuyen–duong–tai–ha–noi
17. Nippon Koei Co., Ltd – Japan. Report of traffic survey "Road project overseas market cultivation in Vietnam", 2019.
18. The institute for the Environment – The University of North Carolina at Chapel Hill, SMOKE v4.7 User's Manual, 2019.
19. Hanoi Department of Natural Resources and Environment. Report No. 3252/STNMT–CCBVMT dated 11/05/2021 of Hanoi Department of Natural Resources and Environment on reporting and providing information and data for the development of the State of the Environment Country Report, 2021.
20. Sahanavin, N.; Prueksasit, T.; Tantrakarnapa, K. Relationship between PM_{10} and $PM_{2.5}$ levels in high–traffic area determined using path analysis and linear regression, *J. Environ. Sci.* **2018**, *69*, 105–114.

Annex

Annex Table 1. Observed vehicle load (in Oct 2021).

No.	Road type	Measured locations	Coordinates
1	Main urban road	Beltway 2 street – Cau Giay intersection	21,0308; 105,8021
2		Tay Son street	21,0072; 105,8232
3		Nguyen Chi Thanh street	21,0225; 105,8098
4		Tran Duy Hung street	21,0129; 105,8021
5	Secondary urban road	Kim Ma street	21,0308; 105,8179
6		Doi Can street	21,0368; 105,8155
7		To Huu street	20,9911; 105,7838
8	Main rural road	Upper Beltway 3 street – Tran Duy Hung intersection	21,0178; 105,7821
9		Provincial road 427, Ha Hoi ward, Thuong Tin district	20,8712; 105,8733
10	Secondary rural road	Tam Hiep gas station, Tam Hiep ward, Phuc Tho district	21,0854; 105,6271

Annex Table 2. Vehicle loads extracted from references [16–17].

No.	Road type	Measured locations	Coordinates
1	Main urban road	Vinh Tuy bridge	21,0037; 105,8753
2		Chuong Duong bridge	21,0377; 105,8605
3		Nhat Tan bridge	21,0895; 105,8193
4		325 Nguyen Van Cu street	21,0467; 105,878
5		95 Giang Vo street	21,0311; 105,8294
6		83 Lang Ha street	21,0182; 105,8162
7		210 Xa Dan street	21,0159; 105,8324
8		72 Nguyen Trai street	21,0012; 105,8173
9		129 Giai Phong street	21,0018; 105,8414
10		Au Co street	21,0611; 105,8327
11		Mai Dong street	20,9964; 105,8622
12		O Cho Dua street	21,0183; 105,8294
13		Nguyen Thai Hoc street	21,030; 105,8367
14		Le Van Luong street Tran Duy Hung street	21,0018; 105,7998
15		Tran Khat Chan street	21,0092; 105,8578
16		Ho Tung Mau street	21,0404; 105,7654
17		Nguyen Huu Tho street	20,9709; 105,8382
18	Secondary urban road	Yen Phu street	21,0511; 105,839
19		Tran Dien street	20,9886; 105,8294
20		Le Trong Tan street	20,9984; 105,8287
21	Main rural road	Thang Long bridge	21,098; 105,7864
22		Phap Van – Thanh Tri bridge	20,9578; 105,8499
23		Thanh Tri bridge	20,9938; 105,9019

VIETNAM JOURNAL OF HYDROMETEOROLOGY

Research Article

Calculation of hydrological features for serving the exploitation and use of surface water of Dakbla Thuong hydropower plant

Le Thi Thuong[1*], Nguyen Tien Quang[1], Tran Thi Hong Minh[1]

[1] Hanoi University of Natural Resources and Environment; ltthuong.kttv@hunrre.edu.vn; ntquang@hunre.edu.vn; tthminh@hunre.edu.vn

*****Corresponding author: ltthuong.kttv@hunrre.edu.vn; Tel.: +84–968672336

Received: 7 August 2022; Accepted: 15 September 2022; Published: 25 September 2022

Abstract: The construction of hydroelectric power plants to develop electricity sources is one of the critical factors of the economic development in Kon Tum Province. Investing in the construction of hydroelectric work contributes to the national electricity source. It also actively contributes to the local irrigation by providing water in the dry season and reducing floods in the wet season. Dak Bla Thuong hydropower plant is in line with the master plan of the Dak Bla river basin, and will optimally exploit energy for the planned river section without affecting neighboring systems in the Dak Po Co river system. Besides, it will contribute to adding a significant energy source to the national power system with a total installed capacity of 9.0 MW and an annual electricity output of about E_o = 31.85 million KW. This paper used a purely statistical method based on a series of hydrological data from 1977 to 2019 to calculate some hydrological features such as standard volumetric flow rate, the minimum monthly flow, the design of flood discharge maximum, etc to serve the licensing of exploitation and use of surface water, ensuring that the work implements well the task of generating electricity while ensuring the minimum flow to the downstream to diminish the risk which is caused by the operation process of electricity generation.

Keywords: Dakbla Thuong hydroelectricity; Exploitation and use of surface water; Hydrological features.

1. Introduction

According to the report of the World Hydropower Association (IHA) in 2018, the installed capacity of hydropower plants in the world has reached 1,267 GW (accounting for 20% of the world's electricity production). China is a rapidly developing country in the construction technology of hydroelectric dam, especially large hydroelectric dams. The Chinese government has implemented a series of hydropower management solutions such as, using the integrated Meta management approach for large hydropower projects; applying the principle of optimizing water resource allocation, planning in case of flood discharge...

Energy is a critical factor in developing countries for economic growth as well as for social development and human welfare. Hydropower is a renewable source of energy, which is economical, non–polluting and environmentally benign among all renewable sources of energy. For the efficient operation of hydropower plants, the hydro energy is stored either in reservoirs for dam based schemes or settling basins for run–of–river schemes. These reservoirs or settling basins are filled with sediments over a period of time. This problem must be taken care of by sediment settling systems in power plants. However, several unsettled sediment pass through the turbines every year and turbine parts are exposed to severe erosion. The erosion of hydro turbine components is a major problem for the efficient

operation of hydropower plants. These problems are more commont in power stations which are of run–of–river types. The problem is exacerbated if the silt contains higher percentage of quartz, which is extremely hard [1].

According to the study [2], a wide range of literature streams and methods were examined for this research, including sustainability, integrated resource planning, and construction of portfolios of electricity generation technologies. The research then focused on current and emerging HPSTs (hydropower generation and storage technologies), and technical, economic, social, and environmental sustainability objectives associated with those technologies in the PNW (Pacific Northwest) region of the United States. Candidate technologies obtained from the literature were examined using the Delphi Method, and then rated according to their perceived impacts using the AHP (Analytical Hierarchy Process). GP (Goal Programming) was then used to determine an optimal mix of technologies to achieve sustainability objectives, and used these weightings and assumptions related to specific scenarios regarding technology development, adoption, and availability. This research is important because few previous studies have systematically considered multiple objectives and criteria from multiple stakeholder experts for creating portfolios of sustainable electricity generation. Previous research has also not comprehensively investigated the manner in which changing scenarios of technology development and availability rates may lead to various technological, economic, environmental, and social impacts with regard to planning of regional electrical generation and storage systems.

Nepal has 83,000 MW (megawatts) of exploitable hydropower resources. Yet the country has tapped less than 650 MW of this potential and hydroelectricity meets less than 1% of total national energy consumption, which is explained through the paper. Using a mixed methods approach consisting of semi–structured research interviews, site visits, and a literature review, it explores the various factors impeding the use of small–scale and medium–sized hydroelectric power stations in Nepal. It begins by laying out the research methods for the study along with a concept known as the social science systems approach, or socio–technical systems theory. This theory supposes that the barriers to any technology from reaching commercialization consists of values, attitudes, regulations, and price signals, as well as technical. The study then evaluates a “seamless web” of these types of barriers facing hydropower systems in Nepal. It concludes lessons for policymakers and scholars concerned about Nepal as well as energy policy more generally [3].

[4] shows that this study examines the climate change impacts on 132 US federal hydropower plants; A runoff–based approach is adopted to associate runoff and annual generation; A series of hydro–climatic models is used to project future runoff and generation; and seasonal runoff changes are projected in the future.

The need to improve Nigeria’s power generation has emphasized the importance of improving the country’s hydropower generation output [5]. However, the development of hydropower resources is currently being hampered by a hydrological data shortage due to large ungauged river channels. Data extension techniques with empirical rainfall–runoff models are used to overcome this challenge [6]. A recent study [7] developed a new hybrid biogeography–based optimization (BBO) technique to achieve a better capability to predict daily stream flow. The study referenced to [8] regression analysis to give excellent results in the data analysis and forecasting of hydrological runoff; the study referenced in [9] also used the regression tree ensemble approach to develop a model with good accuracy for runoff prediction. Ramana confirmed the adequacy of regression analysis for runoff prediction with the formulation of a model with three hydrological modules [10]. The methods of modeling surface runoff involve complex evaluation processes with many interconnecting variables [11] that are not available for most river basins in Nigeria.

[12] presents a model to carry out a short–term flow data extension for a minimum of 30 years using the Gauss–Newton Empirical Regression Algorithm (GNRA) for the

determination of the hydropower generation capacity of rivers in ungauged channels. An averaged 2 years of precipitation, observed experimental discharged data, and 30 years of historical and predictive precipitation data were used to generate a regression model equation after authentication analysis. A minimum, average, and maximum of 30 years of historical discharge data and power characteristics of the river were generated. A discharge predictive accuracy of 96.71% and a Pearson Correlation Coefficient of 0.954 were established between the experimental and model results. The river has minimum, average, and peak power potentials of 5 MW, 10 MW, and 20 MW, respectively, and is capable of yielding power throughout the year.

Cambodia is a country with a special network system and access to many countries. Cambodia has cooperated with surrounding countries to research and develop hydropower. Cambodia has cooperated with China to build the Sesan II hydropower plant, operating since November 2017 on the Sesan River – a tributary of the Mekong River in Northeastern Cambodia. Facing the current situation of massive hydropower development in the Mekong basin, the International Mekong River Association has implemented the project "Initiative Hydropower (ISH)" with the main tasks of: Strengthening communication and cooperation between member countries and stakeholders in hydropower development in river basin; build a knowledge base (data and information) about hydropower; provide technical assistance to the linkages of member countries and develop measures to enhance the sustainable of projects. In particular, the project provided a quick assessment tool of the hydropower company.

This is also one of the tools that Vietnam is using to appraise and evaluate the sustainable development of hydropower projects. In addition, a number of case studies assess the impact of renewable energy construction including hydropower on the socio–economic environment in France. Research has shown that the environmental impacts of hydropower projects vary widely, depending on site–specific mitigation measures and production strategies: if poorly managed, Hydropower production can reduce biodiversity and can significantly degrade alluvial ecosystems and related services [13].

From 2006 to now is an important development period in the exploitation of hydroelectric power of the country. The largest hydropower projects built and completed during this period are: Son La Hydropower (2400 MW), Lai Chau Hydropower (1200 MW) and Huoi Quang Hydropower (560 MW). Hydropower development began to deepen.

At present, the inter–reservoir operating reservoir for hydropower cascades has been established and signed by the Prime Minister to issue a decision for all river basins with hydropower ladders. As of 2018, a total of 80 large and new hydropower projects have been put into operation with a total installed capacity of 15,999 MW. It can be said that up to now, large hydropower projects with a capacity of over 100 MW have almost been fully exploited. Projects with favorable locations and low investment costs have also been implemented. Some hydropower plants are under construction and expansion and storage hydropower plants will be invested to match the structure of power sources in the national power system.

[14] has determined that the construction of Cam Thuy 1 hydropower plant does not affect the exploitation of Cam Luong fish stream tourism because there is no connection between the water of Cam Thuy 1 hydropower reservoir and the water level of Cam Luong fish spring in the year both the flood season and the dry season. [15] studied on "Research on calculating and regulating reservoirs to improve operation efficiency of A Vuong hydropower plant" with the following objectives: (1) Surveying and studying the current status of reservoir water use in order to provide operational solutions that can be applied and increase the efficiency of water use for power generation for A Vuong Hydropower Plant; (2) The solution to calculate the optimal operation of the reservoir water source, if successfully applied, will contribute to improving the environment, reducing the pressure of electricity shortage, thereby contributing to ensuring the country's energy security.

The study [16] has focused on giving two suitable operating options for daily regulating reservoirs. Therefore, the algorithm is built and applied to the Krong No 2 and 3 hydroelectric ladders on the Krong No river. Simulation results show that both lakes operate under the plan of operating at maximum capacity during peak hours, but when the flow is low, the amount of water from the lake is used to generate electricity until the water level is dead. Thus, in the next day, the water level of the lake may not reach the average lever before 9:30 a.m if the amount of water is small. This option will bring high efficiency to the ladder system than when considering independent lakes. [17] studied "Building algorithms and programs to calculate hydroelectricity, economic efficiency of stored hydroelectric power stations in Vietnam". This paper presents the initial research results on the possibility of building stored hydroelectric power plants in Vietnam, builds algorithms, writes programs to calculate hydroelectricity and analyzing energy economy of hydropower Tay Nguyen projects. The program has been piloted for Phu Yen Dong Hydroelectricity project, Son La province.

[18] studied on "Determined the parameters of small and medium hydropower stations regulating working days in flooded dam". The article used a combination of simulated hydrological calculations for the stairs, and at the same time considered the construction cost factor when other parameters changed, within the scope of the article, it was limited to only two small hydroelectric projects with day–regulating lakes. From there, the calculation is applied to the Thuong Son Tay project on the Dak Dring river in Quang Ngai province. The paper used computational methods to simulate hydroelectricity combined with economic analysis to select the optimal discharge channel bottom elevation and dead water level when these stations work in steps and ladders in flood dam. For downstream hydropower plants, when the upstream reservoirs participate in regulation, the dead water level can be raised to ensure the most efficient operation. For hydropower plants in the upstream where the working mode depends on the upstream water level of the downstream hydropower plant, the bottom elevation of the discharge channel cannot be selected according to the dead water level of the lower lake (when designing). but need to rely on the operating dead water level of the lake below. When being applied to Thuong Son Tay and Son Tay, it shows that the dead water level of Son Tay Lake is about 6 m higher than the dead water level during the engineering design process while the bottom elevation of the Thuong Son Tay hydropower discharge canal (189.5 m) is approximately equal to that of the Thuong Son Tay hydropower plant. Optimal dead water level.

The above studies have shown different approaches in the process of calculating hydrological characteristics such as discharge, water level, serving different stages before and after the plant construction and put into operation. However, new studies only focus on calculations for plant operation. On the basis of analysis of studies related to hydroelectricity and methods of calculating hydroelectricity for design and construction of hydropower projects. Thereby, the researches mostly calculate related issues such as calculation of lake regulation to improve operational efficiency or calculate to improve economic efficiency... These studies mainly focus on the calculation of hydropower to improve the operating efficiency of the hydropower plant. In other ways, the calculation is done at the stage after the plant has been put into operation. The calculation of hydroelectricity for the design at the pre–feasibility stage has not been mentioned much. In fact, the calculation of the initial hydrological characteristics is an indispensable step for the calculation and design of hydropower plants. Thus, the main purpose of the paper is to calculate hydroelectricity to determine the basic hydrological characteristics of flow, water column... and propose some solutions to minimize negative impacts on the environment when building DakBla Thuong hydropower plant.

2. Materials and Methods

2.1. Description of study site

Dak Bla Thuong hydropower plant is located in the territory of two communes Dak Ruong and Tan Lap in Kon Ray district, Kon Tum province. The construction of the Dak Bla Thuong hydropower plant aims to exploit the energy source on the Dak Bla River to generate electricity, contributes to increasing more power to the regional power netwok, and taking the initiative in power when a problem occurs with the national grid. Dak Bla Thuong hydropower work is a transverse dam–type hydroelectric work. River basin to dam route Dak Bla Thuong hydroelectric is located in the upper and middle areas of the Dak Bla river. The topography of the studied basin is a high mountainous area and the basin tends to tilt from North to South. The watershed of the West and Southwest basins (passing through the 1600–2066 m high mountains) is slightly higher than the East and the Northeast (passing the 1500–1800 m high mountains). The highest point of the basin is the Ngoc Linh Mountain at 2066 m, the lowest point in the dam route is the river bed with an elevation of about 585 m. Regarding hydrological measurement: In the DakBla river basin, there are two basic hydrological measurement stations, namely the Kon Tum hydrological station that fully monitors all factors (Q, X, flood extraction, Mud and sand) from 1977 to 2019 and Kon Plong station from 1994 to 2019. The measurement stations of related hydro–meteorological factors are listed in Table 1.

Table 1. Network of hydrometeorological stations related to the study area.

No.	Station	Measurement factors	Times	
			From	To
I		Meteorological Station		
1	Dak To	Rainfall	1977	2019
		Evaporation	1977	2019
		Average wind	1977	2019
		Wind max 8 directions, no direction	1977	2019
		Sunshine hours	1977	2019
		Humidity	1977	2019
		Temperature	1977	2019
2	Kon Tum	Rainfall	1977	2019
		Evaporation	1977	2019
		Average wind	1977	2019
		Wind max 8 directions, no direction	1977	2019
		Sunshine hours	1977	2019
		Humidity	1977	2019
		Temperature	1977	2019
3	Dak Glei	Rainfall	1977	2019
4	Tra My	Rainfall	1960	2019
5	Kham Duc	Rainfall	1978	2019
6	Po Re Me	Rainfall	1977	2019
7	Gia Vuc	Rainfall	1977	2019
8	Pleiku	Rainfall	1977	2019
9	Sa Thay	Rainfall	1982	2019
10	Son Ha	Rainfall	1977	2019
II		Hydrology stations		
1	Trung Nghia	Discharge, water level, alluvium	1978	1998
2	Dak Mot	Discharge, water level, alluvium	1994	2019
3	Kon Tum	Discharge, water level, alluvium	1960	2019
4	KonPlong	Discharge, water level	1994	2019
5	Dak To	Discharge, water level	1978	1978

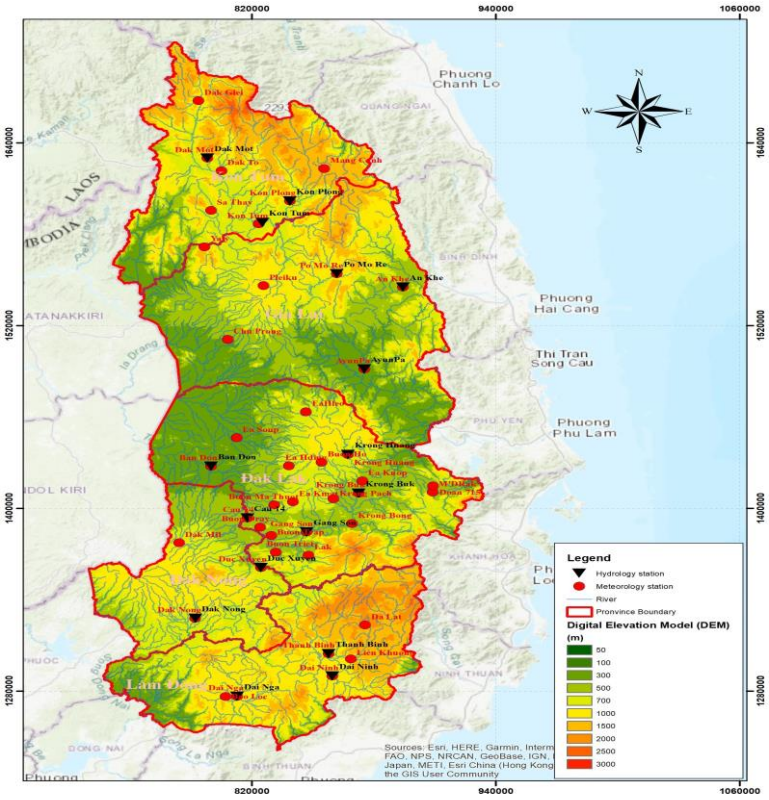

Figure 1. Network of hydrometeorological stations related to the works.

2.2. Flow regime to DakBla Thuong construction line

2.2.1. Average annual rainfall

Dak Bla River Basin belongs to a rainy area, the distribution of rain in the study basin is uneven, tends to increase gradually in the direction of southwest and northeast (increasing towards upstream), the average annual rainfall is the area fluctuates with a fairly large amplitude from 2800÷3800 mm in the northern region adjacent to Quang Nam province, while the average rainfall in Kon Tum–Trung Nghia valley is only about 1700÷1900 mm. A year is divided into 2 seasons, the rainy season from May to October and the dry season from November to April in which the rainfall in the rainy season accounts for 80÷90% of the annual rainfall. The number of rainy days in the year is about 160 days in the regions with heavy rainfall, about 110 days in small rain areas, and about 90% of rainy days fall in the months affected by the southwest and west monsoons.

- Determining the average rainfall in the basin for the hydrological station Kon Tum: Using rainfall data from Son Ha, Dak Glei, Dak To, KonPlong, Kon Tum, Gia Vuc, Pleiku, Po Mo Re, Sa Thay stations, calculated is $X_{0tvKonPlong}$ = 2487.1 mm.

- Determining the average rainfall in the basin for the basin between Dak Bla Thuong – Thuong Kon Tum: Using rainfall data from Dak To, KonPlong, Kon Tum, Gia Vuc, Po Mo Re stations, calculated is $X_{0Dak\ Bla\ Thuong\ –\ TKT}$ = 2417.0 mm.

- Using the maximum daily rainfall of 4 stations Kon Tum, KonPlong, Dak To and Dak Glei to calculate the rainfall causing floods for the construction route. Calculation results of rainfall causing floods according to design frequencies are shown in Table 2.

Table 2. Rainfall causes floods according to the frequency at the construction route (mm).

P%	0.1%	0.2%	0.5%	1%	1.5%	2%	5%	10%
X(mm)	456	417	364	325	302	286	234	196

2.2.2. Annual flow

a) Calculation method

The study basin includes the basin of the Thuong Kon Tum dam (374 km^2) and the part from the Thuong Kon Tum dam to the DakBla 2 dam (1098.5 km^2). Because the Upper Kon Tum reservoir was built with the task of transferring water to another basin, the problem of calculating annual flow is mainly related to the area (F = 1098.5 km^2).

To calculate the annual flow for the DakBla Thuong hydropower work, hydrological calculation methods are used for the basin, then the results are analyzed and compared to choose the appropriate method.

In hydrological calculations, the following methods are commonly used to calculate annual flows.

Method 1: Using the formula in the norm to determine the average annual discharge of the basin from daily rainfall, potential evaporation of the basin and research parameters on the morphology of each hydrological region, this method is usually used in case there is no hydrographic data in the basin. However, using this method means only the average annual discharge can be calculated (Q_0). The simulation of the daily and monthly average flow of the study route must be based on several hydrological stations in the vicinity of the study area.

Method 2: Using the same hydrological station (same or located on the same river system), this method when calculating will use correction factors such as area ratio, and rainfall rate to determine the Q_0. To determine the average daily and monthly discharge, it is possible to use the average daily and monthly discharge of the same catchment as zoomed in for the study route. This method has the disadvantage of the dependency on the quality and length of the same hydrological station.

Method 3: Using mathematical models such as NAM, TANK, etc the common feature of these models is to find a hydrological station with a moderate area, with a measurement time of about 7 years or more. Determine the average rainfall in that basin and the distribution of rain from a relatively typical rain station, suitable for the basin, then detect the coefficients included in the program to simulate the incoming flow of the hydrological station to suit reality (detecting the set of parameters). After completing the model's set of parameters, borrow the model's parameters to calculate the daily, monthly and yearly flow for the study basin. The characteristic of this method is that it can be applied to small watersheds (only one rain station is affected) and can extend the document to only the length of the rain monitoring document. However, the limitations of this method are: (i) the calculated coefficients for the hydrological station are not necessarily suitable for the study route without 3–5 years of testing with real measured data of the river the study area (program test) and (ii) it is not possible to adjust the diurnal flow in the dry season when there are long periods of no or negligible daily rainfall. This results in the dry season months; the average daily discharge is almost unchanged and is taken as a fixed value from the point of view of the programmer. With the above analysis and arguments, the study basin has an area of 1098.5 km^2; there are hydrological stations like KonPlong, Kon Tum also has a moderate area (approximately the study basin) and have long and continuous measurement documents, especially belonging to the system of hydrological stations managed by the State, so data ensures reliability for calculation. It is recommended to use method 2 only to calculate incoming flow for the route of the DakBla Thuong hydropower plant.

b) Determine the annual flow to the construction route from the same catchment method

The flow chain of the construction route is calculated from the KonPlong station according to the ratio of the area with the correction factor: K_F = 1.16 (1098.5/943). The flow sequence of the construction route is calculated from KonPlong station according to the ratio of the area with correction factor: K_F = 1.16 (1098.5/943) and calibration according to the average rainfall of the basin etween DakBla Thuong basin and KonPlong hydrological station with coefficient K_X = 2417.0/2487.1 = 0.97.

Discharge conversion calculation formula:

$$Q_{Work} = Q_{KonPlong} \times K_X \times K_F \quad (1)$$

Calculation results of hydrological features at specific construction routes as shown in Table 3.

Table 3. The hydrological features of the DakBla Thuong dam route by the same method.

Basin	F (km^2)	X_0 (mm)	α_0	Y_0 (mm)	W_0 ($10^6 m^3$)	Q_0 (m^3/s)	M_0 ($l/s.km^2$)
Dakbla Thuong	1098.5	2417	0.603	1457	1601.4	50.8	46.2

Annual flow of the construction route taking into account the environmental flow discharged from the Thuong Kon Tum reservoir

According to the Decision No. 1182/QD–TTg dated July 17, 2014 of the Prime Minister on promulgating the process of inter–reservoir operation in the Se San River Basin [19], Thuong Kon Tum reservoir must discharge water continuously to the downstream of Dak Nghe river not less than 5.8 m^3/s for the months of February, March and April; not less than 3.3 m^3/s for the months of December, January, May and June. In other months, there are no specific regulations on the amount of water required to be discharged through the dam into the Dak Nghe River, but only on unscheduled requests of the People's Committee of Kon Tum province. Thus, the average discharge water volume (environmental flow) from Thuong Kon Tum reservoir for the whole year is addition to the DakBla Thuong hydropower plant as shown in Table 4.

Table 4. Discharge water volume from Thuong Kon Tum hydropower plant.

Months	I	II	III	IV	V	VI	VII	VIII	IX	X	XI	XII	Average
$Q_{discharge}$ (m^3/s)	3.3	5.8	5.8	5.8	3.3	3.3	0.0	0.0	0.0	0.0	0.0	3.3	2.55

Consequently, the features of annual flow and design annual flow to the construction route should be taken into account, and the environmental flow entering from the Thuong Kon Tum reservoir are determined as in Tables 5 and 6.

Table 5. Hydrological features to the Dak Bla Thuong dam route.

Catchment	F (km^2)	X_0 (mm)	α_0	Y_0 (mm)	W_0 ($10^6 m^3$)	Q_0 (m^3/s)	M_0 ($l/s.km^2$)
Dak Bla Thuong	1098.5	2417	0.633	1530	1681.8	53.3	48.5

Table 6. Annual flow rate corresponding to design frequencies.

Route	Statistical features			Flow for design frequency				
	Q_0	C_v	C_s	75%	80%	85%	90%	95%
DakBla Thuong	53.3	0.18	0.43	46.5	45.09	43.5	41.6	38.9

2.3. The discharge–frequency curve

This study used observed data to measure the average daily and monthly flow of the KonPlong hydrological station (1977–2019) according to the following steps:

+ Build flow retention curve average daily and monthly of KonPlong hydrological station;

+ Build flow retention curve average daily and monthly at DakBla Thuong route;

+ Calculate to convert flow retention curve average monthly of DakBla Thuong route become flow retention curve average daily of the route according to the ratio between the coordinates of the daily average flow and the monthly average of the KonLong hydrological station.

Coordinates of the daily discharge and probability curve and the daily discharge and probability curve in the wet season at the constructions as shown in Figures 2a–2b.

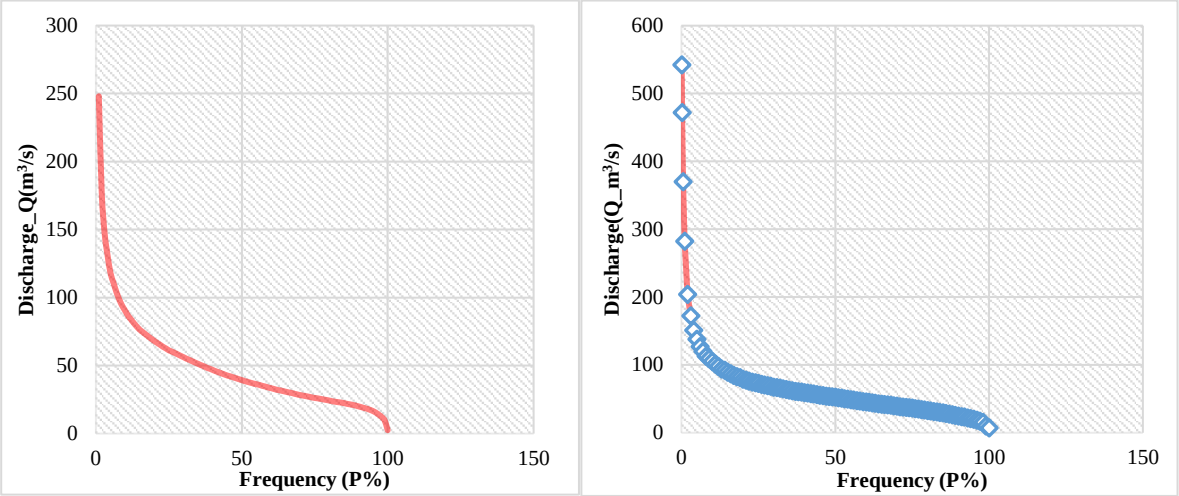

Figure 2. (a) The discharge–frequency curve daily; (b) The discharge–frequency curve wet season at the constructions.

3. Results and discussion

3.1. Design flood flow

To calculate the design flood peak flow for the Dak Bla Thuong construction route, two cases need to be considered: under natural conditions; and when there is Thuong Kon Tum reservoir in the upstream flood discharge.

3.1.1. Calculation of design flood peaks according to real documents measured according to natural conditions

From the actual flow data of the KonPlong station, the flood flows corresponding to the design frequencies can be calculated. The results of flood calculation from the KonPlong hydrological station are shown in Table 7.

Table 7. Floods by frequency at KonPlong and Kon Tum hydrological stations (m^3/s).

Flood frequency at KonPlong station (m^3/s)								
P%	0.1%	0.2%	0.5%	1%	1.5%	2%	5%	10%
Q(m^3/s)	7269	6369	5202	4342	3850	3507	2458	1728
Flood frequency at Kon Tum hydrological station from 1995 to present (m^3/s)								
P%	0.1%	0.2%	0.5%	1%	1.5%	2%	5%	10%
Q(m^3/s)	15876	13940	11425	9565	8500	7755	5470	3864
Calculation of design flood peak according to actual data of Kon Tum station (long series from 1977 to present)								
P%	0.1%	0.2%	0.5%	1%	1.5%	2%	5%	10%
Q(m^3/s)	8980	8049	6828	5913	5383	5009	3836	2974

3.1.2. Calculating the design flood peak at the construction route

Using the reduction formula to determine the design flood at the construction route

$$Q_{CT} = Q_{TP} \times (F_{CT}/F_{TP})^{1-n} \quad (2)$$

where Q_{CT} is the flow calculation for the construction; Q_{TP} is the flow calculation at the zoom station; F_{CT} is the basin area of calculation construction; F_{TP} is the basin area of zoom station; nis the reduction coefficient.

Calculated results of flood discharge for the construction route as shown in Table 8.

Table 8. The results of design flood at the construction route according to the reduction formula (m^3/s).

Design flood at the construction route according to the reduction formula from KonPlong station (m^3/s)								
Catchment	0.1%	0.2%	0.5%	1%	1.5%	2%	5%	10%
Dak Bla Thuong	8130	7124	5819	4856	4306	3922	2749	1932
Design flood at the construction route according to the reduction formula from Kon Tum station from 1995 to present (m^3/s)								
P%	0.1%	0.2%	0.5%	1%	1.5%	2%	5%	10%
Q(m^3/s)	7996	7021	5754	4818	4281	3906	2755	1946
Design flood at the construction route according to the reduction formula from Kon Tum station for a long period from 1977 to present (m^3/s)								
P%	0.1%	0.2%	0.5%	1%	1.5%	2%	5%	10%
Q(m^3/s)	4523	4054	3439	2978	2711	2523	1932	1498

Analyze and select the results: The design flood calculation results from KonPlong station and Kon Tum station in the same period (from 1995 to the present) are not much different. However, the results of flood calculation in 2 short and long periods from Kon Tum station are not much different. This calculation result is also consistent with the analysis results of rain causing floods between short and long periods of stations related to the study area. The results of the short–term design flood calculation does not fully reflect the flood situation of the study area. The Central Highlands region in general and Kon Tum province in particular usually do not have large floods (only the 2009 flood) has occurred. This flood is considered particularly large, which dramatically changes the flood regime in the Se-san River Basin.

3.1.3. Calculation of the design flood peak to the construction route in the condition of flood discharge from the Thuong Kon Tum hydropower plant

According to the National Technical Regulation of Irrigation Works – Major Design Regulations (QCVN 04–05: 2012/BNNPTNT): in the ladder operation diagram, if the grade of the reservoir work is under consideration investment is lower than the level of the work being exploited at the upper level, the design calculation must ensure that the flood discharge capacity of the lower level works is equal to the flood discharge volume (design flood flow and check flood flow) of the upper–level systems and the flood volume in the middle area according to the grade of the lower level works.

Dak Bla Thuong hydropower construction is located at the downstream of Thuong Kon Tum hydropower plant, so when this hydropower plant comes into operation, the flood flow to Dak Bla Thuong dam will be discharged from Thuong Kon Tum lake and midstream flood flow.

Therefore, this study used the design flood discharge already issued in the inter–reservoir operation process in the Sesan river basin with the design and check flood peak flow as follows:

- The peak flood flow corresponding to the design frequency is: $Q_{tk(0,1\%)} = 2172$ m^3/s;
- The peak flood flow corresponding to the check frequency is: $Q_{kt(0,02\%)} = 3320$ m^3/s,

The design and check flood process to the Thuong Kon Tum dam route and the area between Thuong Kon Tum–Dak Bla Thuong was calculated by the same frequency method according to the actual flood model measured at Kon Tum station. Through the study of many actual flood models of the Kon Tum hydrological station, it was determined that the 2009 flood was likely to cause the most adverse effects to the construction. The results of the calculation of the flood process to the Thuong Kon Tum dam line are shown in Figure 3, and the results of the calculation of the middle area flood processes of the Thuong Kon Tum – Dak Bla dam route are shown in Figure 4.

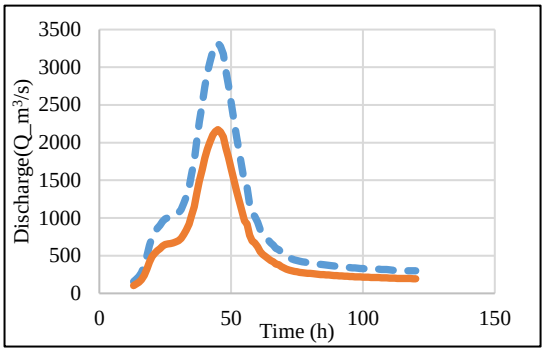

Figure 3. Design flood process according to frequency P = 0.02% (dashed line) and P = 0.1% (solid line) at Thuong Kon Tum dam route.

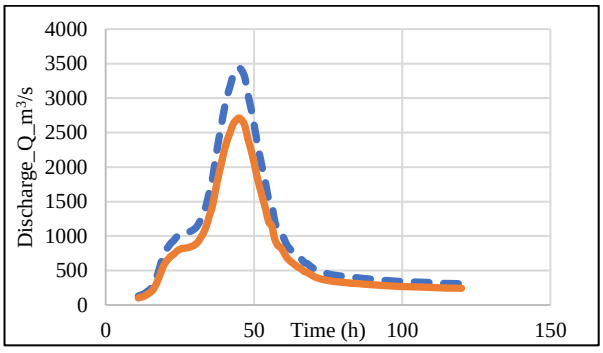

Figure 4. Design flood process according to frequency P = 0.5% (dashed line) and P = 1.5% (solid line) at Thuong Kon Tum dam route.

From the flood process curve to Thuong Kon Tum lake, considering the transmission flow time combined with the flood process curve in the middle zone, the flood process curve to the Dak Bla Thuong dam route can be determined. The results of the calculation of the check flood process to dam route is shown in Table 9 (Thuong Kon Tum check flood combination P = 0.02%; Middle area P = 0.5%) and Table 10 (Thuong Kon Tum design flood complex P = 0.1%; Middle area P = 1.5%).

Table 9. Design flood process by check frequency combination to Dak Bla Thuong dam.

T (hours)	Thuong Kon Tum	Middle area	Total	T (hours)	Thuong Kon Tum	Middle area	Total
1	0	97.2	97.2	61	1472	879	2350
2	0	95.6	95.6	62	1410	820	2231
….	….	….	….	….	….	….	….
59	1888	1059	2947	119	305	309	614
60	1691	978	2668	120	303	308	611
Max	3320	3439	6215				

Table 10. Design flood process by design frequency combination to Dak Bla Thuong Dam.

T (hours)	Thuong Kon Tum	Middle area	Total	T (hours)	Thuong Kon Tum	Middle area	Total
1	0	76.6	76.6	61	963	693	1656
2	0	75.4	75.4	62	922	647	1569
….	….	….	….	….	….	….	….
59	1235	835	2070	119	199	244	443
60	1106	771	1877	120	198	243	441
Max	2172	2711	4507				

3.2. Determine the minimum flow downstream of the work

In order to limit the impact due to the decrease in flow after the downstream of the hydroelectric dam and after the plant, the Law on Water Resources No. 17/2012/QH13 was approved by the National Assembly of the Socialist Republic of Vietnam on June 21. /2012 [20] and Decree No. 201/2013/ND–CP dated November 27, 2013 of the Government detailing the implementation of a number of articles of the Law on Water Resources stipulated, DakBa Thuong hydropower works must be discharged downstream to maintain the minimum flow.

The minimum flow that needs to be maintained downstream of the work is analyzed and determined on the basis of an assessment of the current situation of water sources, the demand for water use and consideration of the possibility of flow fluctuations downstream of the

work. At the same time, the selection of the minimum discharge volume should be consistent with the actual conditions, harmonizing the exploitation of resources for socio–economic development, environmental protection and investment efficiency of the work.

The determination of the location and minimum flow value is carried out according to the guidance in Circular No. 64/2017/TT–BTNMT dated December 22, 2017 of the Ministry of Natural Resources and Environment [10] regulating the determination of minimum flow on rivers, streams and downstream of reservoirs and dams. According to the provisions of Article 6, Circular No. 64/2017/TT–BTNMT, the location to determine the flow ensures downstream of the DakBa Thuong hydropower work is right after the dam.

Analysis of the basis for choosing the minimum flow value to maintain the Dakla Thuong hydropower work: In order to have a basis for determining the minimum flow that needs to be maintained downstream, it is necessary to know the information about the current status nature, flow regime, ecosystem characteristics, as well as demand for water use in DakBla river downstream of DakBla Thuong hydropower work.

- About the current status and demand for water exploitation and use on both sides of the DakBla river from the downstream of the DakBla Thuong dam to the DakBla 1 hydropower work.

+ About water demand for domestic and agriculture: the area from downstream of the DakBla Thuong dam to DakBla 1 hydroelectric work has a terrain of rocky mountains, the vegetation here is mainly shrubs and do not have economic value, poor ecosystem, sparse population. Currently, in the planning, there are in no exploitation works and water used on the main river Ma for domestic and industrial purposes and the water source for people's daily life is not taken directly from the DakBla river but is supplied by from rain and water from small creeks.

+ On the section of DakBla river in the downstream area of DakBla Thuong hydropower work, there are no aquaculture and water transportation activities;

+ The aquatic ecosystem is poor, there are no rare and valuable aquatic species, only a few fish species of low economic value live.

- Regarding the regulation of the minimum flow value according to Circular 64/2017/TT–BTNMT dated December 22, 2017, of the Ministry of Natural Resources and Environment [21]: According to Clause 2, Article 4 of Circular 64/2017/TT–BTNMT (stipulating objectives, requirements and bases for determining minimum flow) “Minimum flow in rivers, streams and downstream of reservoirs is determined must be in the range from the minimum monthly discharge to the average discharge of the smallest 3 months (m^3/s)”.

From the series of monthly average flow data to the DakBla Thuong hydropower dam route, the flow characteristics are determined:

+ Minimum monthly flow: $Q_{month\ min}$= 5.29 m^3/s (III/2016);

+ Minimum 3–month average flow: $Q_{averge\ 3\ tháng\ min}$ = 6.83 m^3/s;

According to the Circular, the minimum flow value can be determined within the range of:

$Q_{month\ min}$= 5.29 m^3/s $\leq Q_{minimum} \leq Q_{average\ 3–month\ min}$ = 6.83 m^3/s

- Recommendation: As analyzed above, there is no need to exploit and use water from the DakBla river downstream. Demand for water for drinking and domestic, people often use water from small streams. Therefore, the purpose of maintaining a minimum flow downstream of the dam is to ensure the continuity of the flow, the environment of the stream and the normal development of the aquatic ecosystem. However, in order to match the capacity of the water source to the lake and harmonize the benefits of power generation and other benefits, it is recommended to maintain the minimum flow after the DakBla Thuong dam equal to 50% of the minimum monthly flow value. Therefore, the minimum flow value is: Q_{tt} = 2.65 m^3/s.

3.3. Calculation of sediment flow to the construction route

The determination of suspended sediment with Dak Bla Thuong route in this period is based on the suspended turbidity at Kon Tum and Kon Plong stations: ρ_o = 145 (g/m^3),

The amount of suspended sediment to the dam is calculated by the formula: $M_1 = \rho_0 \times Q_0 \times T$

With the density of suspended sediment taken as 1,182 tons/ m^3, the annual volume of suspended sediment to the construction route is: $W_1 = M_1/1{,}182$.

The content of bottom sediment transport in the lake is taken empirically by 40% of the suspended sediment volume, with the density of bottom sediment transport taken as 1,554 tons/m^3 of the bottom sediment transport capacity is determined: $W_2 = M_1 \times 40\% /1{,}554$.

The deposition capacity of the work: $W = W_1 + W_2$

The annual volume of sediment deposited to the work route is shown in the following Table 11.

Table 11. Annual amount of sediment to the dam site.

Factors	Unit	Dam route
Average annual flow	m^3/s	51.6
Suspended sediment content	kg	0.145
Annual volume of suspended sediment to the dam route	tons	235952
The density of suspended sediment	tons/m^3	1,182
Mass of bottom sediment transport (40% suspended)	tons	94381
The density of bottom sediment transport	tons/m^3	1,554
The volume of sediment suspended	10^{3}m^3	199,621
The volume of bottom sediment transport	10^{3}m^3	60,734
The total volume of sediment to the lake annually	10^{3}m^3	260,355

3.4. Flow–water level relationship downstream of the dam route

Calculation results of the flow, and water level downstream of the factory route are shown in Table 12.

Table 12. Z~Q relationship downstream of the factory route.

Z (m)	0	19.65	118.70	331.75	626.30	586.20	586.70	587.20	587.70
Q (m^3/s)	583.50	584.54	584.70	585.20	585.70	992.36	1425.47	1920.9	2472.0
Z (m)	588.20	588.70	589.20	589.70	590.20	590.70	591.20	591.70	592.20
Q (m^3/s)	3084.6	3689.4	4352.0	5113.7	6013.9	6968.3	7875.1	8828.2	9790.9

3.5. The impact assessment of the work on the environment–society

3.5.1. Migration and resettlement work

The investor commits to the households that are obligated to the arable land of the households to be compensated in cash at the price prescribed by the State. Because there are no households in the lake bed and the work area, there is no resettlement. On the basis of actual survey measurements with the witness of households, commune authorities, measurement data and self–declaration of damage and collecting opinions of households on compensation for damage when the State recovers land for construction, the investor will coordinate with the district's compensation and site clearance board to implement.

3.5.2. Impact of the construction on the environment and mitigation measures

Treatment of domestic and production waste: Domestic waste is generated mainly from workers' housing quarters. To treat this amount of waste, it is necessary to build landfills in the work area. The locations of these dumps need to be located outside the lake bed and

flood–affected areas to avoid becoming a source of pollution after the reservoir is formed. Solutions for collection and treatment of domestic wastewater: workers' quarters need to have a standard domestic waste collection and treatment system before discharging into rivers and streams. For toilet areas, septic tanks should be used to settle solid waste before discharging water into the treatment system.

Solution for material storage yards: One of the main causes of increasing turbidity in river water is rainwater washing away the concentrated soil in the storage yard. To reduce turbidity from this source, it is possible to apply the method of digging ditches to gather around the landfill to collect rainwater that overflows on the surface of the landfill, and then settle it before discharging into the river.

Measures to reduce air pollution: To reduce air pollution around the construction site, the following measures should be applied: all vehicles transporting construction materials must be covered when shipping; apply moisture spray during the levelling process in the time of strong sunshine and wind; spraying water on roads near residential areas where motorbikes often pass through, spray cycle at least once a day; there is a suitable vehicle regulation mode to avoid increasing the vehicle density too high; levelling of materials right after pouring into the dump and spraying with moisture to reduce dust diffusion due to the effect of wind; equip hats for workers operating machines that cause loud noise.

Ecological protection measures: Educating people and workers to build awareness of ecological protection. In order to minimize the adverse impacts of project construction on wildlife, some additional measures should be applied: manage construction workers, completely ban hunting wild animals and indiscriminate deforestation; Regulations for contractors to standardize machines used in construction to ensure that they do not cause noise as well as discharge dust and smoke in excess of the permitted standards of Vietnam; Search and organize mines for mining construction materials far from the less affected forests in the area.

Measures to protect the health of workers and people in the project area: Build a water treatment station to provide clean water for workers; Build at least 1 medical station (separately for construction workers) in the area; Training and guidance for workers on occupational safety measures and common disease prevention.

Measures to minimize negative impacts during water storage and reservoir operation

Clearing the reservoir: To minimize the pollution of reservoir water, it is necessary to clean up the lake bed before blocking the flow.

Plants and trees in the lake bed need to be cleaned and cut down. The rest of the plant should not be more than 50 cm tall. The cut stems and branches are used as fuel, and the leaves are spread evenly on the ground. For existing toilets and barns in the area to be demolished, it is recommended to fill them with clean soil before filling the lake with water.

To clean up the lake, according to the above standards, the investor can apply some solutions commonly used in other reservoirs such as: financial support for households to clean up their own gardens and residences before moving out of the lakebed area. This is a practical measure because people also want to take advantage of the trunks and branches to make wood and firewood. Contract with local authorities (such as Forest Protection Department, Forest Enterprises, etc.) to clean up on public land.

4. Conclusion

The paper research overviews about the construction area and study problems related to the calculation of hydrological characteristics for the DakBla Thuong hydropower. The paper also calculates of some hydrological characteristics such as: average annual flow rate, peak flow corresponding to the design flood, check flood... and especially the determination of the minimum flow value to discharge after the DakBla Thuong hydropower is one of the important bases for considering the operation, exploitation and use of surface water on the

DakBla river in the area of construction of the work route. In addition, the paper assessed the impact of hydropower projects to the environment, economic and society in the vicinity or the project and proposed mitigation solutions. However, the study has not evaluated the hydro–hydraulic interaction of hydropower project in the system river. This will be content that needs to be studied in the next paper.

Author contribution statement: Developing research ideas: L.T.T.; Selection of research methods: L.T.T.; Data processing: L.T.T.; Determination of hydrological features: L.T.T., N.T.Q., T.T.H.M.; Writing draft articles: L.T.T., N.T.Q., T.T.H.M.

Acknowledgements: This study was carried out under the sponsorship of the provincial scientific research project under the Truong Giang Hydropower Joint Stock Company and International Environmental and Power Construction Consulting Joint Stock Company (IPCEC) on Preparation of Pre–Exam Study Report, Planning Supplement Report, Preparation of Capability Study Report construction competition, setting up Technical Design – Total costing and making construction drawings of Dak Bla Thuong Hydropower Project.

Competing interest statement: The authors warrant that this article is the work of the authors, has not been published anywhere, and has not been copied from previous studies; there is no conflict of interest in the author group.

References

1. Vineet, K.S.; Neha, S.C.; Kushwaha, D. An overview or hydro – electric power plant. *ISST J. Mech. Eng.* **2015**, *1*, 59–62.
2. Cowan, K.; Daim, T.; Anderson, T. Exploring the impact of technology development and adoption for sustainable hydroelectric power and storage technologies in the Pacific Northwest United States. *Energy* **2010**, *35(12)*, 4771–4779.
3. Benjamin, K.S.; Dhakal, S.; Gippner, O.; Bambawale, M.J. Halting hydro: A review of the socio–technical barriers to hydroelectric power plants in Nepal. *Energy* **2017**, *36(5)*, 3468–3476.
4. Kao, S.C.; Sale, M.J. Projecting changes in annual hydropower generation using regional runoff data: An assessment of the United States federal hydropower plants. *Energy* **2015**, *80*, 239–250.
5. Abdulkadir, T.; Salami, A.; Anwar, A.; Kareem, A. Modelling of Hydropower Reservoir Variables for Energy Generation: Neural Network Approach. *Ethiop. J. Environ. Stud. Manag.* **2013**, *6*, 310–316.
6. Pechlivanidis, I.G.; Jackson, B.M.; Mcintyre, N.R.; Wheater, H.S. Catchment Scale Hydrological Modelling (2011): A Review of Model Types, Calibration Approaches and Uncertainty Analysis Methods in the Context of Recent Developments in Technology and Applications. *Glob. NEST J.* **2011**, *13*, 193–214.
7. Roy, B.; Singh, M.P. An Empirical–Based Rainfall–Runoff Modelling Using Optimization Technique. *Int. J. River Basin Manag.* **2020**, *18*, 49–67.
8. Mishra, S.; Saravanan, C.; Dwivedi, V.K.; Shukla, J.P. Rainfall–Runoff Modeling Using Clustering and Regression Analysis for the River Brahmaputra Basin. *J. Geol. Soc. India* **2018**, *92*, 305–312.
9. Zhang, Y.; Chiew, F.H.S.; Li, M.; Post, D. Predicting Runoff Signatures Using Regression and Hydrological Modeling Approaches. *Water Resour. Res.* **2018**, *54*, 7859–7878.
10. Ramana, G.V. Regression Analysis of Rainfall and Runoff Process of a Typical Watershed. *Int. J. Sci. Appl. Inf. Technol.* **2014**, *3*, 16–26.
11. Sitterson, J.; Knightes, C.D.; Parmar, R.; Wolfe, K.; Avant, B.; Muche, M.E. An Overview of Rainfall–Runoff Model Types. In Proceedings of the 9th International

Congress on Environmental Modelling and Software, Fort Collins, CO, USA, 2018, pp. 24–28.

12. Audu, L.M.; Musa, N.A. Model Development for Discharge Data Extension for Ungauged Rivers Channels: A Case Study of the Proposed River Orle Hydropower Plant. Proceeding of the 2nd International Conference on Advances in Mechanical Engineering (ICAME–22), Islamabad, Pakistan, 25 August 2022.
13. Pontoni, F.; Creti, A.; Joëts, M. Economic and Environmental Implications of Hydropower Concession Renewals: A Case Study in Southern France. *Revue Économique* **2018**, *69(2)*, 241–266.
14. Sung, T.V.; Bang, N.T. Evaluation of impacts of Cam Thuy 1 hydropower project on Cam Luong fish stream and water transport on Ma river. *J. Constr. Sci. Technol.* **2012**, *8*, 73–83.
15. Thai, N.Q. Research on calculation and regulation of reservoirs to improve operation efficiency of A Vuong hydropower plant. Master's thesis in Engineering, University of Danang, 2013.
16. Nghia, N.V. Study on selecting a reasonable power generation operation process for the Krong No 2 and 3 hydroelectricity ladders. *J. Constr. Sci. Technol.* **2017**, *41*, 1–9.
17. Bang, N.T.; Cuong, P.D. Building algorithms and programs to calculate hydroelectricity, economic efficiency of stored hydropower stations in Vietnam. *J. Constr. Sci. Technol.* **2010**, *2*, 31–41.
18. Nghia, N.V. Determining parameters of small and medium hydroelectric power stations regulating working days in flooded dam. *J. Water Resour. Sci. Technol.* **2019**, *54*, 1–9.
19. Prime Minister. Decision No. 1182/QD–TTg dated July 17, 2014 promulgating the process of inter–reservoir operation in the Sesan river basin, 2014.
20. Law on Water Resources. No.: 17/2012/QH13, June 21, 2012.
21. Ministry of Natural Resources and Environment. Circular 64/2017/TT–BTNMT dated December 22, 2017 Regulations on determining minimum flows in rivers, streams and downstream of reservoirs and dams, 2017.

VIETNAM JOURNAL OF HYDROMETEOROLOGY

Rerearch Article

The method of Analytic Hierachy Process AHP in selecting solution for sustainable exploitation and use to ensure domestic water source and agriculture for water shortage areas in Son La Province

Son Phung Kim[1], Hue Ha Nhu[2], Hang Le Thi Thu[1], Duong Tran Thuy[1], Tuan Nguyen Viet[1], Lan Pham Thi Huong[3*], Thuy Nguyen Thanh[3]

[1] Son La Department of Natural Resources and Enviroinment; Phungkimson@gmail.com; hangtnmtsl@gmail.com; Duongthuymt@gmail.com; TuanNV593@gmail.com
[2] Son La Department of Agriculture and Rural Development; huehn.snnptnt@sonla.gov.vn
[3] ThuyLoi University; lanpth@wru.vn; thanhthuy_rt@tlu.edu.vn

*****Corresponding author: lanpth@wru.vn; Tel.: +84–912537042

Received: 7 August 2022; Accepted: 20 September 2022; Published: 25 September 2022

Abstract: Analytical Hierarchy (AHP) method is a quantitative analysis method and it is widely used to compare alternative options especially in water resources sector. Instead of requiring a large amount of data, this method uses expert opinion and does not require too much numerical data. Therefore, it is suitable for the selection and determination of criteria on water sources, exploitation conditions, socio–cultural, environmental, economic, technical and technological, management and environmental criteria. exploiting and ensuring water supplement for domestic use and agriculture in the water shortage areas of Son La province. This paper introduces the method and apply the method to ensure which explotation solutions are sustainable and suitable for each region with different conditions in Son La province, evaluate the The criteria then serve as a basis for proposing solutions for exploitation and use for each water source.

Keywords: Method of hierarchical analysis; Decision making; Sustainable use of buildings.

1. Introduction

Nowadays, the interrelationship between water resources and social and economic and technical conditions are considered when selecting water exploitation solutions in the world as well as in Viet Nam. The method to assess the sustainability of the solutions that use water sources directly or indirectly, simple or complex, is choosen due to the availablity of data. Normally, the sustainable exploitation of water–using solutions is composed of three factors: water source; socio–economic and technical conditions. For exploitation works use water sources sustainably on economic–financial aspects when the investment rate of the project is low, the cost per cubic meter of water is low and the management, operation and repair and upgrade costs ensure the balance between income and expenditure.

Sustainability in technology is achieved when the local community or the project management unit exploiting and using the water source can master the technical operation of the works and resolve the technical problems of the works on time. Financial, social and technical aspects of sustainability are interrelated. Analytical Hierarchy Process (AHP) is one of the multi–objective decision making methods proposed by [1] a mathematician from Iraq. AHP is a quantitative method, used to sort decision alternatives and select an

alternative that satisfies given criteria. The AHP method was created to help to solve complex decision problems [2]. The AHP method has been widely applied to many fields, especially in the field of natural sciences. AHP is used as a flexible tool for decision analysis with multiple criteria, allowing decision criteria based on multiple attributes, which refers to a quantitative technique. Multicriteria methods are used to make decisions of problems composed of intangible aspects or with qualitative variables to evaluate. These methods do not consider the possibility of finding an optimal solution to a problem, but the solution depends on the predefined objective (s) [3]. The AHP provides the feasibility of including quantitative and qualitative data that in a "normal" analysis are left out because of their difficulty in measuring but relevant in obtaining the objective [4]. [5] applied AHP to deal with economic, political, social and engineering design problems, architectural pattern selection, pricing strategy, technology selection, planning, conflict resolution, benefit/cost analysis and resource allocation, etc. Currently, the AHP method is becoming more and more popular with the support of specialized software Expert Choice. Although the AHP method is used in water sustainability assessment, it is better to consult a group of experts to avoid bias and groups make better decisions than individuals, because groups are accepted to be more knowledgeable than individuals [6]. Hence, the standard AHP has been extended as group AHP in group decisions [7–9]. [10] used linear mixed models based on the regression approach to estimate the decision weights of AHP instead of using the geometric means for aggregating experts' judgments.

Some studies on the application of AHP are as follows: [11] has applied the utilizing analytic hierarchy process (AHP) for decision making in water loss management of intermittent water supply systems. [12] was used the AHP (Analytical Hierarchy Process) to highlight the distribution of groundwater recharge areas in the Moldavian Plain area by assigning weight factors to each thematic layer. In the realization of the study were used thematic layers such as drainage density, slope, land use, precipitation distribution, groundwater level, soils, lithology. For the final map, we used the weighted overlay toolbox from the ArcGis software, giving the weight factor for each thematic layer. PIM Consulting Center - Vietnam Institute of Irrigation Science [13] has applied the analytic hierarchical method (AHP) in the selection of design options for Irrigation projects. [14] used an Analytic Hierarchy Process (AHP) to select construction method alternatives. Use of AHP Method in Efficiency Analysis of Existing Water Treatment Plants. [15] has been evaluation model of regional water supply capacity based on AHPCRITIC method. This paper aims at evaluating the ability of a region to provide clean water to meet the needs of its population by establishing a multi-index comprehensive evaluation model. According to the UN water scarcity map, Australia was selected as the representative region to be evaluated by the model in order to analyze the reason of its water shortage. [16] presents the application of the Analytic Hierarchy Process (AHP) related to the operation of the drinking water supply network of the city of Chihuahua, Mexico, where two possible alternatives are delineated with the objective to optimize the service. [17] has been undertaken with an objective to delineate the groundwater potential of a small tropical river basin located in the western side of the Western Ghats in India as an example. A combination of geographical information system and analytical hierarchical process techniques (AHP) was used in the present study.

With the available information of each technical option for exploitation and use of water in extremely difficult areas (information about water sources, information on social and environment, information on economic and technical...), the AHP hierarchical analysis method will be applied in this study. This method is useful to select and determine criteria on water sources, exploitation conditions, socio–cultural, environmental, economic, and social aspects, technology, management and exploitation to ensure water supplement for domestic use and agriculture in water shortage areas of Son La province. AHP hiearchical

analysis limits subjectivity and ensures the suitability and harmony among specific objectivess of each project.

2. Materials and Methods

2.1. Study area

Son La is a mountainous province in the Northwest with dangerous terrain, very complex and strongly divided. As a consequence, the water distribution is temperally and spacially variable, i.e., the exceed water causes floods while the water shortage derives drought, some areas have the abundant water sources while water in other areas is very limited. The water scarecity leads to many difficulties for productions and lifes of local people. According to Decision No. 900/QD–TTg of the Prime Minister dated June 20, 2017 approving the list of extremely difficult communes, border communes, and safe zone communes into the investment category of the 135 program. From 2017 to 2020, Son La province had 118 extremely difficult communes eligible for investment, including 7 communes in Yen Chau district, 15 communes in Phu Yen district, 7 communes in Sop Cop district, 10 communes in Van Ho district, 14 communes in the district. Bac Yen, 13 communes in Muong La district, 22 communes in Thuan Chau district, 8 communes in Mai Son district, 5 communes in Moc Chau district, 15 communes in Ma river district, 2 communes in Quynh Nhai district. Among the above–mentioned extremely difficult communes, there are 20 special water shortage communes in Bac Yen districts (Hong Ngai, Chim Van, Hua Nhan, Lang Cuu), Muong La (Chieng Muon, Chieng Lao, Hua Trai, etc.) Nam Gion, Pi Toong, Ta Bu), Phu Yen (Huy Tan), Quynh Nhai (Muong Sai), Ma River (De Mon, Nam Ty), Sop Cop (Sam Kha), Thuan Chau (Bo Muoi, Co Tong) and Yen Chau (Chieng Dong, Chieng Tuong), Van Ho (Long Luong). According to the report of the Department of Agriculture and Rural Development of Son La province [3], the total number of concentrated water supply works in the province is currently 1548 works; the number of rural households granted from the concentrated works is 109,449.0 households; there are 54 sustainable works, 226 relatively sustainable works, 852 unsustainable works and 443 inactive works. The works stop working because (i) the inefficient operation management model led to the highrate of water loss; (ii) flood and rain washed away the main items of the works but; (iii) water sources for the works are gradually reduced and exhausted, the incoming flows are polluted due to cultivation and agricultural production by people in the region.

2.2. Research framework

The proposed technical solution includes a group of solutions for exploitation solutions using rainwater, surface water, and underground water sources. The sustainability of a solution to exploit and use water is considered as a function of the criteria of water sources (NN), social criteria (social) and economic and technical criteria (KT) according to the following formula:

$$E = f(NN, XH, KT) \quad (1)$$

where E is the sustainability index of the solution to exploit and use water; NN is the criterion of water source; Social is the criterion of society; KT is the economic and technical criteria.

Results of the project “Research to identify water sources and solutions for domestic and agricultural water supply for water shortage areas in Son La province” [3] identified areas with scarcity level of surface water in Son La province (Figure 1).

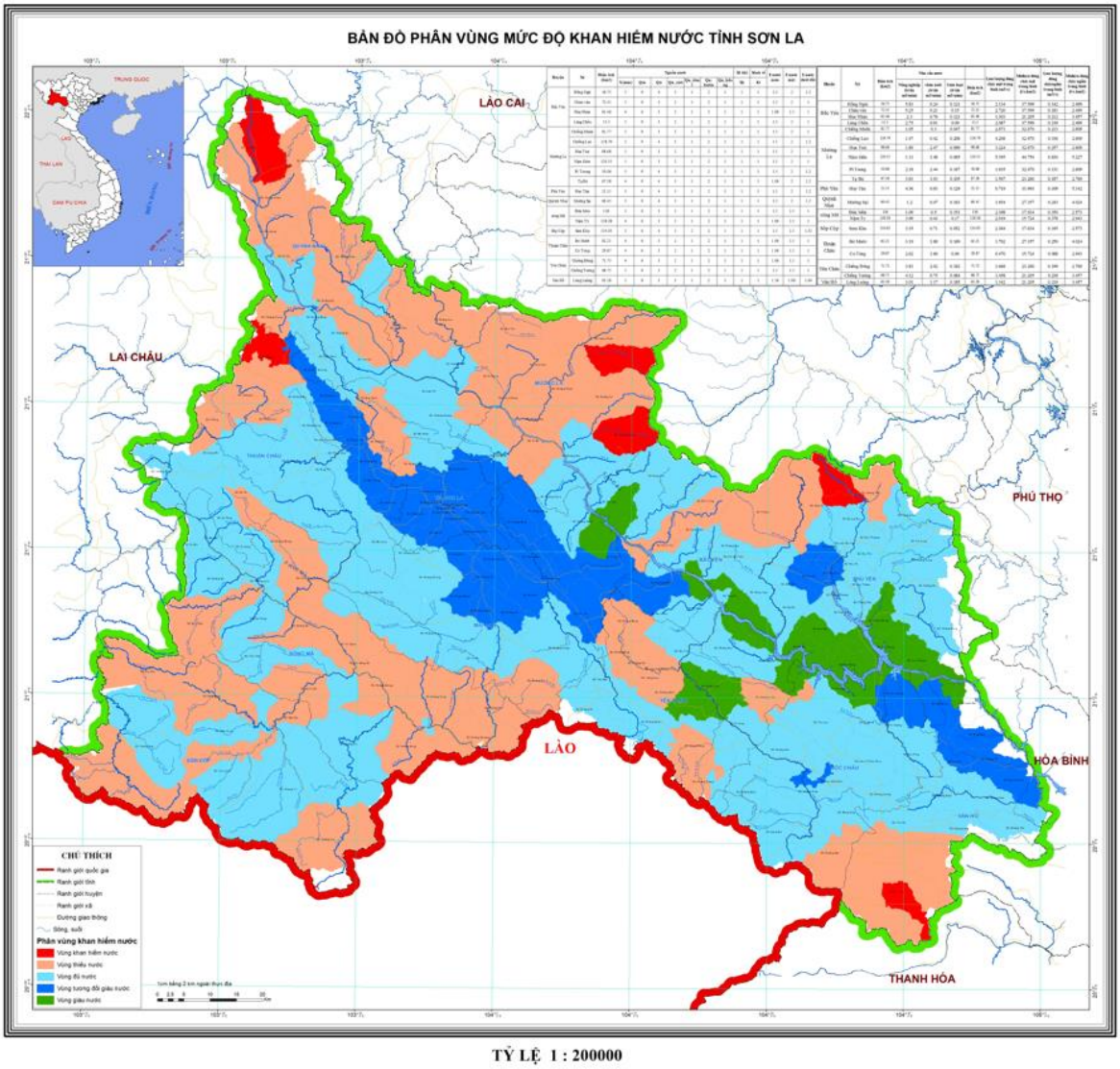

Figure 1. Map of location of communes with special difficulties in water scarcity in Son La province La.

The analysis and assessment of natural, socio–economic, and cultural norms on using water as well as the current status of water exploitation solutions in mountainous areas and especially difficult communes show that the water source criteria is the most important and followed by the social criteria to meet social security. After consulting experts, the weight of each criterion is determined as follows: WNN = 0.5; WXH = 0.3 and WKT = 0.2. Specifically, the criteria are determined as follows [18]:

Criteria on water sources

- For rainwater: high potential with average rainfall $X_0 > 2,500$ mm/year); medium potential with $1,200 < X_0 \leq 2,500$ mm/year); small potential with $X_0 \leq 1,200$ mm/year)

- For surface water: Average surface flow module is from 60 l/s–km^2 to 80 l/s–km^2 in the area for additional water supply; Average surface flow module is from 40 l/s–km^2 to < 60 l/s–km^2 in the area for additional water supply; Average surface flow module is from 30 l/s–km^2 to < 40 l/s–km^2 in the area for additional water conveyance; Average surface flow mode is from 20 l/s–km^2 to < 30 l/s–km^2 in the area for additional water supply; Average surface flow module is < 20 l/s–km^2 in the area for the additional water supply.

- For underground water sources: Potentially rich ($M_d \geq 500$ m^3/day/km^2) water source (exploitable reserve); Potentially median (reservable reserves) water source ($200 \leq M_d <$ 500 m^3/day/km^2); Potential poor (exploitable reserve) water sources (Md < 200

m^3/day/km^2); There are results of research, investigation and assessment of underground water resources by hydrogeological research boreholes with water flow and quality that ensure sufficient exploitation conditions, or have drilled wells being exploited for concentrated water supplycentral; There are results of research, investigation and assessment of underground water resources by hydrogeological research boreholes, but the flow and quality of water have not yet met the conditions for exploitation; There are no results of research, investigation and assessment of underground water resources by hydrogeological research boreholes; There are results of research, investigation, assessment of underground water resources and identification of a route with a flow and quality that meets the conditions for concentrated water supply exploitation (> 1 l/s), and an important route. at least 1 year of hydrology or water injection testing at the piezometers; There are results of research, investigation, assessment of underground water resources and identification of an piezometer with a flow and quality that meets the conditions for concentrated water supply exploitation (Q = 0.1–1 l/s) , the spring has not been observed for at least 1 hydrological year or has not been pumped for testing at the piezometers; There are results of research, investigation and assessment of underground water resources, and it is determined that there is an spring with a flow that ensures a single water supply for a small population cluster (Q < 0.1 l/s), and the spring has been observed less than 1 hydrological year or pumped to test water at the piezometers; There are results of research, investigation, assessment of underground water resources and determination of groundwater level in shallow areas (Ht < 10 m), results of research on water extraction from dug wells; There are results of research, investigation, assessment of underground water resources and determination of groundwater level in shallow areas (Ht < 10 m), but no results of research on water extraction from dug wells; There are results of research, investigation, assessment of underground water resources and determination of groundwater level in relatively deep areas (Ht > 10 m), but no results of research on water extraction from dug wells; There are results of cave investigation, detailed study and assessment that it is capable of exploitation but has not yet been invested in exploiting or is being exploited effectively; There are preliminary investigation and research results, but there are works being exploited; No investigation, preliminary research and no exploitation works.

Social criteria

- The center of a township is an area with high population density, ability to construct works for concentrated water supply, economic conditions affordable to pay for water supply services to make the works operate regularly.

- The center of the communes is an area with relativehigh population density, ability to construct works for concentrated water supply, and economic conditions affordable to pay for water supply services to make the works operate regularly.

- The villages and hamlets in communes, townships and townships have low population density and scattered population, is unable to exploit the works for centralized water supply, and economic conditions not affordable to pay for water supply services.

Economic technical criteria

- The center of a town or township is an area with good technical infrastructure conditions, which is very convenient for investigation as well as exploitation and operation of water supply works. The method of exploitation and use of water has an investment rate (calculated for 27 years) of less than 500 VND/m^3.

- The center of communes with relatively good technical infrastructure conditions makesinvestigation, exploitation and operation of water supply works convenient, Models and solutions for exploitation and use of water with high investment rate (calculated for 27 years) reaches 500–1000 VND/m^3.

- Villages in communes, townships and townships have less favorable technical infrastructure conditions for investigation as well as exploitation and operation of water supply works, Exploitation models and solutions using water with investment rate (calculated for 27 years) greater than 1,000 VND/m^3.

2.3. *The method of hierarchical analysis in AHP in the selection of AHP technical solution options by [19] researched and then developed in the 80s. This method calculate weights to apply for multi–criteria decision problems*

The calculation process consists of six main steps:

1. Decompose an unstructured situation into small pieces.
2. Build the AHP hierarchical tree.
3. Assign numerical values to subjective comparisons of the importance of criteria in decision making.
4. Calculate the weight of the indicators.
5. Consistency check
6. Aggregate results to make final rating

a) Build AHP hierarchy tree

After going through step 1, decompose the problem into small components, hierarchical tree AHP will be built around selection criteria and possibilities.

Based on the pairwise comparison principle, the AHP method can be described with 3 main principles, namely analysis, evaluation and synthesis. AHP answers questions like "Which option should we choose?" or "Which option is best?" by selecting the best alternative that satisfies the decision maker's criteria on the basis of comparing pairs of alternatives and a specific computational mechanism. Suppose we have a problem to make a decision (called an objective), which must be based on many criteria (Criterion C_1, Criterion C_2, ..., Criterion Cn). The alternatives that can be compared are PA_1, PA_2, … PA_m. The problems of the problem are modeled in Figure 2.

The method of hierarchical analysis to calculate the weights (importance coefficients) and the impact intensity hierarchy of the component factors is used by the American mathematician Saaty and a number of authors in the world as well as in Vietnam to quantitatively evaluate the intensity of the processes. This theory divides impact intensity (j) into 5 levels: 1, 3, 5, 7, 9 and provides a scale to compare the importance of impact factors. Saaty used the expert method to compare more than 5 levels of impact factors (1, 3, 5, 7, 9) and compare losses at 5 levels (1, 1/3, 1/5, 1/7, 1/9) on a square matrix of order n (n is the number of impact drivers used for comparison) (Table 1). In which, Saaty prescribes that the principal diagonal of the square matrix has a value of 1. This matrix shows that if the important index of factor A to B is n, then vice versa the importance ratio of B to factor A is 1/n. Based on the scale, a comparison matrix between the influencing factors can be established. After that, the weights for each component class is calculated by using the Eigen principle vector (the Eigen principle vector can be approximated by dividing each value of each column by the total number of values in that column to establish a new matrix, then the average value per row of the new matrix is the weight of the influencing factor with values from 0 to 1).

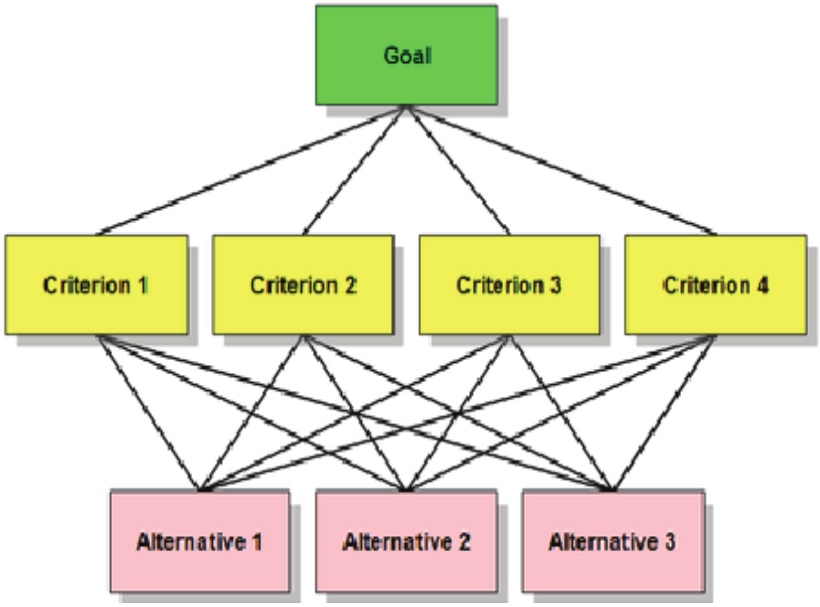

Figure 2. The diagram describes the hierarchical analysis problem [1].

Saaty's AHP method [1] compares two factors according to the principle that if factor A is more important than factor B, then A/B > 1 and vice versa, A is less important than B, then A/B < 1. If A and B are equally important, then A/B = 1. And the importance of A over B increases as the A/B ratio increases. And conversely, the smaller the A/B ratio, the lower the importance of A relative to B. Saaty offers the following scale for a "smart pairwise comparison".

Table 1. AHP's smart pairwise comparison table.

<< Less important						**More important >>**		
1/9 Less important many times	1/7 less important Much	1/ 5 less important Much less important Much	1/3 less important	1 Equally	3 important	5 More important Much more	7 important Much more important Much more	9 important many times

With the above comparison principle, a matrix of comparison pairs is created. And from this matrix, according to the Eigen Principle Vector, a "set of best–fit weights" can be calculated. Calculate the weight for each factor J in the factor in the set of factors using the Eigen principle vector method by dividing each value in each column by the total value in that column to establish the matrix, the average value on each row of the matrix is the weight of the influencing factors with values from 0 to 1.

The "Smart Pairwise Comparison" method can be clearly analyzed through the following example (5 factors) with the corresponding scores of 1, 3, 5, 7 and 9): Give the factors affecting the occurrence of hazards: A, B, C, D, E and build a matrix to compare smart pairs as in Table 2.

Table 2. Matrix of factors comparison.

Factors	**A(1)**	**B(3)**	**C(5)**	**D(7)**	**E(9)**
A(1)	1	3	5	7	9
B(3)	1/3	1	1.67	2.33	3
C(5)	1/5	1/3	1	1.4	1.80
D(7)	1/7	1/5	1/3	1	1.29
E(9)	1/9	1/7	1/5	1/3	1

Calculations of the Eigen principle vector can be approximated manually when dividing the value of the column by the total value of the scores in this column. This gives a matrix with new values between 0 and 1 when the sum of the column values equals 1. The mean of the rows in this matrix corresponds to the weights for that criterion [1]. Based on this matrix, following the Eigen Principle Vector with Jones's weighting method [18], the following combination of appropriate weights can be calculated: A = 0.59; B = 0.20; C = 0.11; D = 0.07; E = 0.04.

The comparison of the criteria in pairs and their importance is implemented. The priorities (aij values, with i running in rows, j running in columns) in pairs of criteria have positive integer values from 1 to 9 or the reciprocal of these numbers we get a matrix square (n × n) as Table 1. The coefficient of the matrix is obtained from the score of the pairwise comparison between components, factors or criteria. Value pairwise comparisons are made through expert opinion. The value of the correlation matrix coefficient is completely dependent on the subjectivity of the researcher in quantifying the weights for the objectives, which is a drawback of this method.

b) Building a matrix to compare indicators

This comparison is made between pairs of indicators and aggregates them into a matrix of n rows and n columns (n is the number of indicators). The element *aij* represents the importance of the index row *i* compared to the index column *j*.

$$A = (a_{ij})_{n\times n} = \begin{bmatrix} 1 & a_{12} & \dots & a_{1n} \\ a_{21} & 1 & \dots & a_{2n} \\ \vdots & \vdots & \vdots & \vdots \\ a_{n1} & a_{n2} & \dots & 1 \end{bmatrix}$$

The relative importance of indicator i to j is calculated by the ratio k (k from 1 to 9), vise versace importance of indicator j to i is i is 1/k. So $a_{ij} > 0$, $a_{ij} = 1/a_{ji}$, $a_{ii} = 1$.

c) Summarizing results

After calculating the weights of the criteria as well as of the options for each criterion, the above values will be summed up to obtain the appropriate index of each option according to the following formula:

$$Wis = \Sigma wijs * wjamj = 1,\ i=1,\ldots n$$

where wijs is the weight of option i corresponding to the criterion j; wja is the weight of indicator j; n is the number of alternatives; m is the number of indicators.

3. Results and discussion

3.1. Determin and estimate weigh factors

a) Create the matrix of importance among factors

To determine the weight W for each influencing factor or the importance of each factor, it is necessary to build a matrix of importance for the influencing factors. Comparison of importance between pairs of factors is carried out qualitatively based on expert consultation, previous studies to determine which factor's influence is more important, collected data and documents to verify the results. The estimated importance matrix for the factors are as shown in Table 3.

Table 3. Matrix of importance for the factors [A].

No.	Factor	KH	Surface water	Flow Under ground flow	Rainfall	Rate underground flow volume exploited through centralized water supply works	Underground flow volume exploiting the main road	Flow rate undergroun d flow for testing	Water exploitation underground flow rate of cave mining	Society	Economy
1	Surface water volume	Qm	1	2	3	4	5	6	7	8	9
2	Rainfall	X	0.5	1	3	3	5	5	7	7	9
3	Underground flow rate	Qn	0.33	0.33	1	3	3	5	7	7	Underground
4	Flow discharge concentrated water	Qn_cntt	0.25	0.33	0.33	1	3	3	5	5	7
5	Underground flow rate of mainline exploitation	Qn_dtml	0.2	0.2	0.33	0.33	1	3	3	3	5
6	Experimental groundwater intake flow	rate Qn–huttn	0.17	0.2	0.2	0.33	0.33	1	3	5	5
7	Underground flow of cave mining	Qn_hdong	0.14	0. 14	0.2	0.2	0.33	0.33	1	3	5
8	Socio–economic	0.14	0.14	0.2	0.2	0.33	0.2	0.33	1	3	9
	Economical	0.11	0.14	0.14	0.2	0.2	0.33	1	Total	2.83	4.46
	0.13		8.35	12.21	18.2	23.73	31.53	39.33	51	b	.

b) Determine the weight for each factor

The weight will be calculated based on the importance of factors. The values of weights are shown in Table 4.

Table 4. Matrix of Variations & Weights [B].

No.	Factor	KH	Surface water volume Surface water	Flow Subterranean runoff	Volume Rainfall	Flow through concentrated water supply works	Underground flow volume exploiting open circuit	Flow rate underground water suction experiment	Flow rate underground flow of cave exploitation	Social	Economy	Weight W [B]
1	Surface water flow	Qm	0.35	0.45	0.36	0.33	0.27	0.25	0.22	0.2	0.18	0.29
2	Rainfall	X	0.18	0.22	0.36	0.25	0.27	0.21	0.22	0.18	0.18	0.23
3	Underground runoff	Qn	0.12	0.07	0.12	0.25	0.16	0.21	0.16	0.18	0.14	0.16
4	Underground runoff Centralized water supply system	Qn_cntt	0.09	0.07	0.04	0.08	0.16	0.13	0.16	0.13	0.14	0.11
5	Outflow underground water flow	rate Qn_dtml	0.07	0.04	0.04	0.03	0.05	0.13	0.1	0.08	0.1	0.07
6	Experimental groundwater intake flow	rate Qn–huttn	0.06	0.04	0.02	0.03	0.02	0.04	0.1	0.13	0.1	0.06
7	Underground flow of cave mining	Qn_hdong	0.05	0.03	0.02	0.02	0.02	0.01	0.03	0.08	0.1	0.04
8	Social	0.04	0.03	0.02	0.02	0.02	0.01	0.01	_	0.03	0.06	0.03
9	Economic	0.04	0.02	0.02	0.01	0.01	0.01	0.01	0.01	0.02	0.02	_
	Total		1	1	1	1	1	1	1	1	Society	1

c) Check the fitness of the weights

The fitness of the weights is started with the determination ofthe weight sum vector and the consistency vector.

The weight vector is a matrix [C] calculated by [C] = [A]×[B].

Table 5. Weight vector [C] determined by factors.

No.	Factor	KH	[C]=[A]×[B]
1	Surface water discharge	Qm	3.01
2	Rainfall	X	2.43
3	Underground runoff	Qn	1.67
4	underground flow through the centralized water supply facility	Qn_cntt	1.15
5	Outflow groundwater exploitation of the highway	Qn_dtml	0.72
6	Experimental underground flow	rate Qn–huttn	0.58
7	underground flow ratecave mining	Qn_hdong	0.37
8	Social	Xh	0.24
9	Economic economic	0.15	Consistency

Vector [D] is calculated according to the formula = [C]/[B].

Table 6. The consistency vector [D] is determined according to the factors.

No.	Factor	KH	[D]=[C]/[B]
1	Surface water discharge	Qm	10.33
2	Rainfall	X	10.60
3	runoff	Qn	10.66
4	Undergroundunderground flow volume exploited through the centralized water supply works	Qn_cntt	10.32
5	Underground flow volume exploited on the main road	Qn_dtml	10.25
6	Experimental underground water flow volume	Qn–huttn	9.68
7	Underground flow volume exploiting caves Qn_hdong	Xh	9.22
8	Social	KT	9.23
9	Economic	9.50	Consistency

- Index CI = 0.122
- RI is a random index corresponding to 9 factors, look up the table RI = 1.45
- Consistency ratio CR = 0.08 ≤ 0.1

d) Rating scale for each indicator

Based on the opinions of experts, through the workshop and based on the data situation, applicability of the model and the criteria identified above, a 10–point scale is proposed for each indicator. Assessment results for communes with special difficulties in water resources is shown in Table 7. According to the results summaried in Table 7, the total score is analyzed to assess the sustainability of the solutions to exploit and use water sources as below:

- Very sustainable: E > 2.5 points: in which the criterion of water source must be very sustainable
- Sustainable: 1.5 < E ≤ 2.5 points: in which the criterion of water source must be sustainable
- Unsustainable: E ≤ 1.5 points

Table 7. Assessment results for communes with special difficulties in water resources based on the assessment criteria.

District	Commune	Area (km^2)	Water source							Society	Economy	E rain water	Surface water	Groun dwater	Proposed solutions
			X (mm)	Qm	Qn	Qn_ cntt	Qn_ dtml	Qn- huttn	Qn_ hdong	Xh	Kt				
Bac Yen	Hong Ngai	56.75	5	9	4	3	1	2	1	1.0	1.0	1.50	2.00	1.20	Exploiting springs Building reservoirs, hanging tanks
	Chim Van	72.35	5	9	3	2	1	2	1	1.0	1.0	1.50	2.00	1.00	
	Hua Nhan	61.46	4	6	3	2	1	2	1	1.0	1.0	1.06	1.50	1.00	Building reservoirs, hanging tanks
	Lang Cheu	55.5	5	9	3	2	1	2	1	1.0	1.0	1.50	2.00	1.00	Building reservoirs,

District	Commune	Area (km^2)	Water source							Society	Economy	E rain water	Surface water	Groun dwater	Proposed solutions
			X (mm)	Qm	Qn	Qn_ cntt	Qn_ dtml	Qn- huttn	Qn_ hdong	Xh	Kt				
															hanging tanks
Muong La	Chieng Muon	81.77	5	9	3	2	1	2	1	1.0	1.0	1.50	2.00	1.00	Building reservoirs, hanging tanks
	Chieng Lao	128.79	5	9	4	3	1	2	1	1.0	1.0	1.50	2.00	1.20	Exploiting springs + Building reservoirs, hanging tanks
	Hua Trai	98.68	5	9	3	2	1	2	1	1.0	1.0	1.50	2.00	1.00	Building reservoirs, hanging tanks
	Nam Gion	120.55	5	9	3	2	1	2	1	1.0	1.0	1.50	2.00	1.00	Exploiting springs + Building reservoirs, hanging tanks
	Pi Toong	50.06	5	9	4	3	1	2	1	1.0	1.0	1.50	2.00	1.20	Exploiting springs + Building reservoirs, hanging tanks
	Ta Bu	67.38	4	9	4	3	1	2	1	1.0	1.0	1.06	2.00	1.20	Building reservoirs, hanging tanks
Phu Yen	Huy Tan	21.15	5	9	4	3	1	2	1	1.0	1.0	1.50	2.00	1.20	Exploiting springs
Quynh Nhai	Muong Sai	60.45	5	9	4	3	1	2	1	1.0	1.0	1.50	2.00	1.20	Exploiting springs
sông Mã	Daa Mon	136	5	6	3	2	1	2	1	1.0	1.0	1.50	1.50	1.00	Building reservoirs, hanging tanks
	Nậm Ty	128.38	4	6	3	2	1	2	1	1.0	1.0	1.06	1.50	1.00	Building reservoirs, hanging tanks
Sop Cop	Sam Kha	134.03	5	6	4	3	2	2	1	1.0	1.0	1.50	1.50	1.32	Exploiting springs
Thuan Chau	Bo Muoi	62.21	4	6	3	2	1	2	1	1.0	1.0	1.06	1.50	1.00	Exploiting springs + Building reservoirs, hanging tanks
	Co Tong	29.87	4	6	3	2	1	2	1	1.0	1.0	1.06	1.50	1.00	Exploiting springs + Building reservoirs, hanging tanks
Yen Chau	Chieng Dong	71.73	4	6	3	2	1	2	1	1.0	1.0	1.06	1.50	1.00	Exploiting springs + Building reservoirs, hanging tanks
	Chieng Tương	68.75	5	6	3	2	1	2	1	1.0	1.0	1.50	1.50	1.00	Building reservoirs, hanging tanks
Van Ho	Long Luong	63.28	5	8	3	3	1	2	1	1.2	1.0	1.56	1.96	1.04	Building reservoirs, hanging tanks

4. Conclusion

It is no doubt that when there is not enough data to calculate for the alternative selection, especially for mountainous areas with special difficulties such as in Son La province, the AHP method proves to be useful. By comparing pairs of criteria based on their importance to water resources, society and economy, to establish solutions for sustainable exploitation and use to ensure water sources for domestic and agricultural use.

industry for water–deficient areas, then compare and evaluate each pair of options based on the priority of selection if each criterion is considered separately, and combine these evaluation angles, the results of comprehensive comparison are explicitly more convincing. The article applies for Son La province, based on a set of comparison criteria to illustrate the application of the solution. When there are more comparison criteria, detailed evaluation results of the criteria, it is possible to use specialized software, or group the criteria into more groups and solve the problem combined with the analytical Network (Analytical Network Process) to better reflect reality as well as save more computation time.

Author contribution statement: Developing research ideas: S.P.K., H.H.N., H.L.T.T, L.P.T.H.; Selection of research methods: L.P.T.H.L.; Data processing: T.N.V., T.N.T., Determination of AHP: L.P.T.H., T.N.V., T.N.T.; Writing draft articles: S.P.K., H.H.N., H.L.T.T., L.P.T.H.; Edited articles: S.P.K., H.H.N., H.L.T.T., L.P.T.H., T.N.T.

Acknowledgements: This study was carried out under the sponsorship of the provincial scientific research project under the Decision No. 1948/QD–UBND dated August 14, 2021. Besides, the authors would like to thank for the help. of communes is especially difficult in the process of surveying and conducting this research.

Competing interest statement: The authors warrant that this article is the work of the authors, has not been published anywhere, and has not been copied from previous studies; there is no conflict of interest in the author group.

References

1. Saaty, T.L. Decision making with the Analytic Hierarchy Process. *Int. J. Services.* **2008**, *1(1)*, 83–98.
2. Anagnostopoulos, K.P.; Vavatsikos, A.P. An AHP model for construction contractor prequalification. *Oper. Res.* **2006**, *6*, 333–346.
3. Martínez, E.; Escudey, M. Evaluación y decisión multicriterio: *Una perspectiva. Copade. Neuquen. Gov. Ar.* **1997**.
4. Saaty, T.L. Decision-Making with the AHP: Why is the Principal Eigenvector Necessary. *Eur. J. Oper. Res.* **2003**, 145(1), 85–91. https://doi.org/10.1016/S0377-2217(02)00227-8.
5. Saaty, T.L.; Vargas, L.G. Decision Making in Economic, Political, Social, and Technologycal Environments with the Analytic Hierarchy Process. RWS Publication, Pittsburgh, PA, USA, 1994.
6. Ishizaka, A.; Labib, A. Review of the main developments in the analytic hierarchy process. *Expert Syst. Appl*. **2011**, *38*, 14336–14345.
7. Shi, S.G.; Cao, J.C.; Feng, L.; Liang, W.Y.; Zhang, L.Q. Construction of a technique plan repository and evaluation system based on AHP group decision-making for emergency treatment and disposal in chemical pollution accidents. *J. Hazard. Mater.* **2014**, *276*, 200–206.
8. Dragincic, J.; Milica, V. AHP Based Group Decision Making Approach to Supplier Selection of Irrigation Equipment. *Water Res.* **2013**, *41*, 782–791.
9. Akaa, O.U.; Abu, A.; Spearpoint, M.; Giovinazzi, S. A group-AHP decision analysis for the selection of applied fire protection to steel structures. *Fire Saf. J.* **2016**, *86*, 95–105.
10. Lin, S.W.; Lu, M.T. Characterizing disagreement and inconsistency in experts' judgments in the analytic hierarchy process. *Manag. Decis*. **2012**, *50*, 1253–1265.
11. Zyoud, S.H.; Hafez, S.; Subhi, S.; Ayman, R.; Al-Wadi, F.; Hanusch, D.F. Utilizing analytic hierarchy process (AHP) for decision making in water loss management of intermittent water supply systems. Sanitation and Hygiene for Development. *J. Water* **2016**, *6(4)*, 534–546.

12. Daniel, B. Evaluation on groundwwater recharges capacity using the AHP method case study: the moldavian plain. Conference: Air and water components of the environment, 2019.
13. Truong, N.H. Application of Analysis Hirection (AHP) method in seclection of design options of hydraulic projects.
14. Quan, N.T. Using Analytic Hierarchy Process (AHP) to select construction method alternatives. Ha Noi University of Civil Engineering, 2015.
15. Lingjie Zhou. Evaluation model of regional water supply capacity based on AHPCRITIC method. Proceeding of the 2nd International Conference on Economics, Social Science, Arts, Education and Management Engineering, 2016.
16. Jesús Rubén, S.N.; Carmen Julia, N.G.; David Humberto, S.N.; Eduardo Herrera, P. Analytic Hierarchy Process (AHP) to Optimize the Service in a Water Supply Network. *J. Mate. Sci. Eng. B.* **2020**, *10(1–2)*, 10–17.
17. Arulbalaji, P.; Padmalal, D.; Sreelash, K. GIS and AHPTechniques Based Delineation of Groundwater Potential Zones: a case study from Southern Western Ghats, India. *Sci. Rep.* **2019**, *9*, 2082. https://doi.org/10.1038/s41598-019-38567-x.
18. Summary report of the topic. Research to identify water sources and solutions for domestic and agricultural water supply for water shortage areas in Son La province. Institute of Hydrology, Environment and Climate Change, 2022.
19. IHECC. Thematic report Determining the criteria for water sources, exploitation conditions, socio–cultural, environmental, economic, technical and technological, management and exploitation to ensure living water sources. activities for daily life and agriculture for areas lacking water in Son La province. Institute of Hydrology, Environment and Climate Change, 2022.

Table of content